

Single–crossover recombination and ancestral recombination trees

Dissertation zur Erlangung
des akademischen Grades

Doktor der Naturwissenschaften

vorgelegt an der Technischen Fakultät
der Universität Bielefeld

eingereicht von

Dipl.-Biomath. Ute von Wangenheim

Bielefeld im Juni 2011

Supervisors
Prof. Dr. Ellen Baake
Prof. Dr. Sven Rahmann

Gedruckt auf alterungsbeständigem Papier  ISO 9706.

Contents

1	Introduction	5
1.1	Theoretical population genetics	5
1.2	Recombination dynamics in mathematics	7
2	Biological fundamentals	13
2.1	Genetic diversity	13
2.2	Recombination	14
2.2.1	Meiosis	14
2.2.2	Mechanisms of recombination and crossover events	14
2.2.3	Crossover: occurrence and frequencies	17
3	Single-crossover recombination in discrete time: The model	21
3.1	The mathematical setup	22
3.2	Excursus: SCR in continuous time	25
3.3	SCR in discrete time	28
3.3.1	Two and three sites	30
3.3.2	Four sites	32
3.3.3	General case	32
3.4	Reduction to segments	36
3.5	The commutator and linearisation	41
3.6	Diagonalisation	48
4	Recombination and ancestral recombination trees: an explicit solution	55
4.1	The finite population counterpart: the Wright-Fisher model	56
4.2	Ancestral recombination process	59
4.2.1	The ancestral process	59
4.2.2	Segments and the segmentation process	60
4.2.3	Ancestral recombination trees	63
5	Outlook: The general recombination model	77
5.1	Introduction and Notation	77
5.2	The general recombination model in continuous time	79
5.2.1	Three Sites	82

5.2.2	Four Sites	84
5.2.3	Product structure	87
5.3	Trees in the general recombination model	90
5.4	Genetic algebras for the general recombination model	94
5.4.1	Linearisation	97
5.4.2	Haldane linearisation for the recombination dynamics	98
6	Summary and Discussion	105
	Bibliography	111

Chapter 1

Introduction

Recombination dynamics belongs to the research area of theoretical population genetics which forms an exciting interdisciplinary field, combining biological processes of inheritance with mathematical modeling.

1.1 Theoretical population genetics

Theoretical population genetics is concerned with investigating the genetic composition of populations and the mathematical study of how this changes with time due to evolutionary processes such as mutation, selection and recombination, or factors like random genetic drift, migration, environmental changes etc. The primary source of data used in population genetics is regarding genetic variation in populations with the aim to describe changes in this variation in terms of the fundamental rules of inheritance. These rules describe how the genetic material of the parental population is transmitted to the population formed by their offspring.

Recent advances in molecular biology, which have been mainly driven by faster and cheaper DNA sequencing technologies, have led to an increasing amount of data that can be used for population genetics studies. As an example, it is now common to analyse multiple genetic loci instead of only one or two loci as population genetics was restricted to approximately 25 years ago. This allows population genetics to reveal genome-wide patterns and locus-specific effects of evolution [65].

Population genetics uses mathematical models to achieve theoretical understandings of the evolutionary processes e.g. to infer the ancestral relationship of various species as well as to obtain information about the evolutionary history within one species. These models are used to study the factors that shape populations on an abstract level by taking into account the more relevant processes while ignoring the less relevant ones. Although mathematical models are necessarily idealised by concentrating on the most decisive factors, they nonetheless contribute to a greater understanding of the underlying dynamics and the interplay of the processes that affect populations. They

allow to study certain evolutionary factors separately and can thus provide new ideas about the mechanisms of these forces. Indeed, there are several examples that show that complex scenarios can be described by relatively simple models surprisingly well, see [65].

Further questions of theoretical population genetics address the estimation of mutation and recombination rates, predictions of the future system behaviour as well as the detection of evidence for population size fluctuations, migration, selectionary forces and various forms of geographical structures such like subdivision. In addition, population genetics is used for simulation studies and supports research of the genome structure such as mapping of disease genes, identifying regions affected by selection and regions with unusual mutation rates.

Population genetics models appear in various forms: in discrete or continuous time and in a deterministic or a stochastic manner. They also include a wide range of mathematical fields: probability theory, stochastic processes, theory of differential and difference equations and algebra.

Indeed, population genetics has even motivated a new area of mathematics, the theory of *Genetic Algebras*. Algebraic structures arise in genetics in a quite natural way due to the genetic laws of inheritance. In particular, they exhibit an interesting mathematical feature since these algebras are generally commutative but non-associative algebras [56, 69].

In this work, we investigate a model that only incorporates the evolutionary factor of recombination. Recombination happens during gamete formation in sexually reproducing organisms when maternal and paternal chromosomes exchange genetic material. Thus, recombination contributes significantly to genetic variation since it introduces new allele combinations into the population. In fact, recombination has such an impact on population genetics studies that it can be hardly ignored in population genetics models. It has already been shown in simulation studies around 30 years ago that recombination has a significant effect on the sampling properties of a neutral allele model [34]. However, the effects of recombination are complex and not completely resolved yet, see [34], and invite further research. Recombination is also said to be the fundamental phenomenon that distinguishes the population genetics of multiple loci from that of a single locus [12], the main reason due to the effect of scrambling evolutionary history, i.e. it allows linked loci on a chromosome to have *different* histories (i.e. genealogies). This influences statistical methods involved in population genetics since recombination reduces dependencies between loci, i.e. loosely linked loci can be viewed as independent replicates of the evolutionary process. For example, when considering the famous stochastic process *Coalescence* [43], the only way that variance (caused by the random nature of the trees that are simulated during this process) can be reduced is by incorporating recombination (and *not* by increasing the sample size) [58].

Furthermore, recombination finds application in certain optimisation problems based on *genetic algorithms* [61] and constitutes the main process in *directed evolution experiments* that are amongst others used for engineering improved proteins and enzymes.

For the inference of the optimal parameters of these processes, a mathematical description for recombination is of crucial importance [53].

Nevertheless, modeling recombination dynamics leads to a possibly very large set of nonlinear equations, due to the random mating of the partner individuals involved, that exhibit a complex structure.

1.2 Recombination dynamics in mathematics

The dynamics of the genetic composition of populations evolving under recombination has been a long-standing subject of research. The traditional models assume random mating, non-overlapping generations (meaning discrete time) and populations so large that stochastic fluctuations may be neglected and a law of large numbers (or infinite-population limit) applies so that the evolution of an infinitely large population is essentially deterministic. Even this highly idealised setting leads to models that are notoriously difficult to treat and solve, namely, to large systems of coupled, nonlinear difference equations. A good introduction and overview of mathematical models with recombination can be found in [11, 12].

Although recombination requires a population of diploid organisms, the process is usually formulated at the level of the populations haploid *gametes*, i.e. the evolution of a population is a description of the formation of gametes in the population [12]. The diploid individual then originates as a *zygote* formed by the fusion of two (male and female) gametes. Identifying a population by its gamete pool is justified by the principle of random mating that is described in detail by Jennings [36]: *random mating of zygotes gives the same results as random mating of the gametes which they produce* (from [36]).

The abstract process of recombination can be briefly described as follows: a diploid cell (obtained by the fusion of two haploid gametes and also referred to as *zygote*) undergoes meiosis, the cell division cycle necessary for sexual reproduction, that results in gametes as haploid products. These gametes may either carry the same genetic material as one of the parental gametes or they carry part of the maternal material and part of the paternal material - in this case, recombination has occurred.

Elucidating the underlying structure and finding solutions to the recombination equations has been a challenge to theoretical population geneticists for nearly a century. The first studies go back to Jennings [36] in 1917 and Robbins [57] in 1918. Building on [36], Robbins solved the dynamics for two diallelic¹ loci (also called sites from now on) and gave an explicit formula for the gamete frequencies as functions of time. To overcome the obstacles of nonlinearity, Robbins introduced a new function of the gamete frequencies to diagonalise the dynamics - an approach that became a common way to deal with the nonlinearities of recombination dynamics. Furthermore, he showed that

¹each locus has two possible alleles.

the population approaches a stationary distribution in which the alleles are associated at random (which is now common knowledge).

Geiringer [24] investigated the general recombination model for an arbitrary number of loci and for arbitrary ‘recombination distributions’ (meaning collections of probabilities for the various partitions of the sites that may occur during recombination) in 1944. She was the first to state the general form of the solution of the recombination equation (as a convex combination of all possible products of certain marginal frequencies derived from the initial population) and developed a method for the recursive evaluation of the corresponding coefficients. This simplifies the calculation of the type frequencies at any time compared to the direct evaluation through successive iteration of the dynamical system. She applied this idea to confirm the two site solution and to infer an explicit solution for the three site case [25]. Even though she also worked out the method for the general case in principle, its evaluation becomes quite involved for more than three sites.

Her work was followed by Bennett [7] in 1954. He introduced a multilinear transformation of the type frequencies to certain functions that he named *principal components*. They correspond to linear combinations of certain correlation functions (i.e. measures of linkage disequilibrium) that transform the dynamical system (exactly) into a linear one. The new variables decay independently and geometrically for all times, whence they decouple and diagonalise the dynamics. They therefore provide an elegant solution in principle, but the price to be paid is that the coefficients of the transformation must be constructed via recursions that involve the parameters of the recombination model. Bennett worked this method out for up to six sites, but did not give an explicit method for an arbitrary number of sites. This was later on completed by Dawson [14, 15], who showed that the transformation to diagonalise the dynamics is always of the form Bennett claimed and derived a general and explicit recursion for the coefficients of the principal components (at least for the diallelic case).

While all the work mentioned above assumes models in discrete time, E. and M. Baake proposed a recombination model in continuous time [3], considering the special case where recombination is restricted to single-crossovers, i.e. the case where maximum one crossover event can happen in the same generation. Even though the recombination equations exhibit the same nonlinear character as the ones in the previously mentioned models, the corresponding dynamics can be solved in closed form [3, 4]. Again, a crucial ingredient is a transformation to certain correlation functions (or linkage disequilibria) that linearise and diagonalise the system. Fortunately, in this case, the corresponding coefficients are independent of the recombination parameters and the transformation is available explicitly. This is an essential simplification to previous results on recombination dynamics and suggests an underlying linearity in the dynamics.

E. Baake and Herms [5] studied the finite population counterpart to the deterministic single-crossover model, i.e. the Moran model with single-crossover recombination. Simulation studies for four diallelic sites indicate that a population of approximately

10^5 can be considered as ‘infinite’, i.e. in this case the deterministic limit constitutes a very good approximation to the actual non-deterministic process. Further results on single-crossover recombination for finite and infinite populations are summarised in [6].

An alternative framework to study recombination dynamics for infinite populations is the representation via algebraic structures that was initiated by Etherington in 1939 [17]. A good review about algebras in genetics can be found in [56], while [69] offers a complete overview of this topic. Algebraic structures in population genetics arise due to the multiplicative nature of sexual reproduction. As an example, consider an arbitrary (but finite) number of gametes a_1, \dots, a_n in a random mating population. Random mating of two gametes a_i and a_j forms the zygote $a_i a_j$ and the resulting offspring gamete is obtained according to the following rule:

$$a_i a_j = \sum_{k=1}^n \gamma_{ijk} a_k,$$

where the coefficients γ_{ijk} fulfil

- $0 \leq \gamma_{ijk} \leq 1$.
- $\sum_{k=1}^n \gamma_{ijk} = 1$.
- $\gamma_{ijk} = \gamma_{jik}$.

Then, a_1, \dots, a_n can be considered as the basis of an algebra with the above multiplication rule where each element $p := \sum_{i=1}^n \alpha_i a_i$, $0 \leq \alpha_i \leq 1$, $\sum_{i=1}^n \alpha_i = 1$, of this algebra corresponds to an actual population, i.e. the coefficients α_i signify the relative frequencies of the gametes a_i in the population. Furthermore, the coefficients γ_{ijk} specify the laws of inheritance and multiplication of two populations corresponds to the production of the offspring population of gametes. The above algebra is called *genetic algebra* [56, 69].

Algebras which arise in genetics are generally *commutative* but *non-associative* as should be obvious from a purely biological perspective. If a population p mates randomly within its generation (which is usually assumed), then the successive generations are given by the sequences of *plenary powers* $p^{[n]} = p^{[n-1]} p^{[n-1]}$.

There exist several definitions of algebras that could have genetic significance (e.g. *algebras with genetic realisation*, and *baric algebras*, compare [56, 69]), but the ‘main’ definition of such an algebra, the *Genetic Algebra*, was first given by Schafer in 1949 [60] and later formulated in a more coherent way by Gonshor [26]. Most theoretical results that are important for population genetics are based on the assumption of a genetic algebra, while at the same time many genetic situations fit this definition. In particular, each gametic algebra is a genetic algebra after Gonshors definition, and thus the process we are interested in - the process of recombination on the basis of gametes - is a genetic algebra. To determine the successive generations in terms of an initial population remains complicated due to the quadratic evolutionary operator. In 1930 Haldane

described a procedure that became known as *Haldane linearisation*, compare [48, 52], which in some cases allows the representation of the quadratic operator as a linear one (on a higher dimensional space). Following this idea, Holgate [32] proved that this linearisation works for each genetic algebra, so that in particular the original vector space of each gametic algebra (with recombination) can be embedded into an higher-dimensional vector space where the dynamics can be represented linearly. Bennett's [7] and Dawson's [14, 15] linearisation procedure is essentially an example of Haldane linearisation outside the abstract framework of algebras.

In this work, a single-crossover recombination model in discrete-time is studied extensively for the first time. Single-crossover recombination (SCR) is a special, although biologically relevant, case that corresponds to the extreme characteristic of the biological phenomenon of interference (where the occurrence of a crossover event completely inhibits any other crossover events in the same generation). A solution for the corresponding model in continuous time has already been found in [3, 4]. However, the discrete-time case is quite different and important to consider since the overwhelming part of literature deals with non-overlapping generations. We seek to elaborate the underlying mathematical structure of the discrete-time process by providing a systematic, but still elementary, approach that exploits the inherent (multi)linear and combinatorial structure of the problem. Besides contributing to the understanding of how recombination affects populations, the final goal is to state the genetic composition of a population at any time based upon a given initial population. In addition, knowledge of the structure of the single-crossover model in discrete time turns out to be very helpful for the study of an extended model, the general recombination model, where the restriction to single-crossovers is omitted.

To begin with, we explain the biological foundations of recombination in Chapter 2. In Chapter 3, we first describe the discrete-time single-crossover model and the general framework. We then recapitulate the essentials of the continuous-time model, in particular the diagonalising transformation, and its solution. Returning to discrete time, we first analyse explicitly the cases of two, three, and four sites. For two and three sites, the dynamics is analogous to that in continuous time (and, in particular, available in closed form), but differs thereafter. This is because a certain linearity present in continuous time is now lost. The differences to the continuous-time dynamics and the resulting difficulties to solve the equations are then studied in detail. In particular, the transformation operators used in continuous time are not sufficient to both linearise *and* diagonalise the discrete-time dynamics. However, they lead to a *linearisation* which is worked out in the following. We show that the resulting linear system has a triangular structure that is then diagonalised in a recursive way.

In Chapter 4, we develop a new approach to infer an explicit solution of the single-crossover dynamics by viewing the recombination process from another perspective. In doing so, we use the underlying stochastic process (with reference to a finite population) to trace recombination backwards in time, i.e. by backtracking the ancestry of the various independent segments each type is composed of. This results in binary tree structures, the *ancestral recombination trees*, which can be used as a tool to formulate

an explicit solution.

Chapter 5 serves as an introduction to the general recombination model, where the restriction to single-crossovers is dropped. We formulate the recombination equation (in continuous time) together with its particular notation and examine the model with several examples. Furthermore, we consider the tree structure that corresponds to the solution of the general recombination model. Finally, we briefly indicate how to discuss this model in the frame of genetic algebras.

We conclude with a summary and discussion of our results in Chapter 6.

Chapter 2

Biological fundamentals

As mentioned in the introduction, population genetics seeks to understand the genetic structure of a population and how this changes from generation to generation due to several evolutionary forces (see below). The data used in population genetics is usually *polymorphism data*, where polymorphism refers to the simultaneous occurrence of two or more different forms (i.e. different nucleotides or alleles) at the same location in the genome (with reference to a population or a sample of a population). Explaining the biological foundations, we follow [47].

2.1 Genetic diversity

Guaranteeing genetic variability is of crucial importance for a population since this allows the members of the population to adapt to environmental changes. *Mutation* is the only factor that is able to introduce new sequence forms into the population, i.e. without mutations there would be no polymorphisms. Mutations are rare, e.g. in bacterial cells the mutation rate per nucleotide is around 10^{-9} per generation [47]. Mutation is counteracted by *selection*, the evolutionary factor that refers to the organisms environmental interactions, and affects the probability of survival and the number of progenies, respectively. Selection occurs whenever an individual and its progenies have a different chance of survival, relative to other individuals, due to sequence differences. Through this process, harmful mutations can be eliminated while the proportion of sequences carrying beneficial mutations can be increased within the population.

Furthermore, populations are affected by a random factor called *genetic drift*. In any finite population, the set of gametes passed to the next generation is typically not a copy of the set of the gametes of the parental generation but a random sample of these. Thus, due to stochastic fluctuations, two succeeding generations vary in their compositions. The smaller the population, the stronger is the impact of genetic drift, while genetic drift can be often ignored in very large populations.

Finally, *recombination* breaks up *linkage* between loci on the same chromosome and thus increases the amount of allele combinations.

2.2 Recombination

Recombination occurs in sexually reproducing organisms and refers to the reassortment and exchange of genetic material during the formation of the gametes (i.e. sperm and egg cells). This may then lead to new combinations of the genetic material (i.e. new *genotypes*) and therefore recombination increases the genetic diversity of a population, having a profound influence on genome diversity and evolution.

The cells of *diploid* organisms contain two *homologs* of each morphological type of chromosome. The two homologs constituting each pair of *homologous chromosomes* are descended from different parents, i.e. homologous chromosomes are typically not identical. Recombination occurs during *meiosis*, the type of cell division when a diploid *germ cell* gives rise to four gametes with a haploid set of chromosomes.

2.2.1 Meiosis

Meiosis includes two phases of cell division, *meiosis 1* and *meiosis 2*. Initially, the genetic material of the diploid (*premeiotic*) germ cell is replicated to give rise to chromosomes that consist of two identical *sister chromatids* that are attached at the *centromere*¹. In the early phase of meiosis 1, the pairs of homologous chromosomes pair with each other by a process called *synapsis* to form a *tetrad*, which is composed of four homologous chromatids (two maternal and two paternal). At this stage, recombination events occur, leading to the exchange of homologous nucleotide sequences between a maternal and a paternal chromatid. We will discuss this process in detail below. Afterwards, the pairs of homologous chromosomes (each consisting of two sister chromatids) are separated and randomly distributed to two daughter cells while the sister chromatids remain associated. Finally, in meiosis 2, the sister chromatids are also separated, which results in the formation of four haploid gametes as the outcome of meiosis. The process of meiosis is illustrated in Figure 2.1.

2.2.2 Mechanisms of recombination and crossover events

As mentioned above, during early meiosis 1, the homologous chromosome pairs are physically connected and recombination events are observed. Indeed, in nearly all organisms at least one recombination event is *required* to ensure proper cell division. Recombination is thus not only an important factor to increase genetic diversity but for survival of the cell as well [50]. Recombination forms an essential physical connection

¹the centromere is a constricted DNA region that associates itself with several proteins and is required for proper cell division.

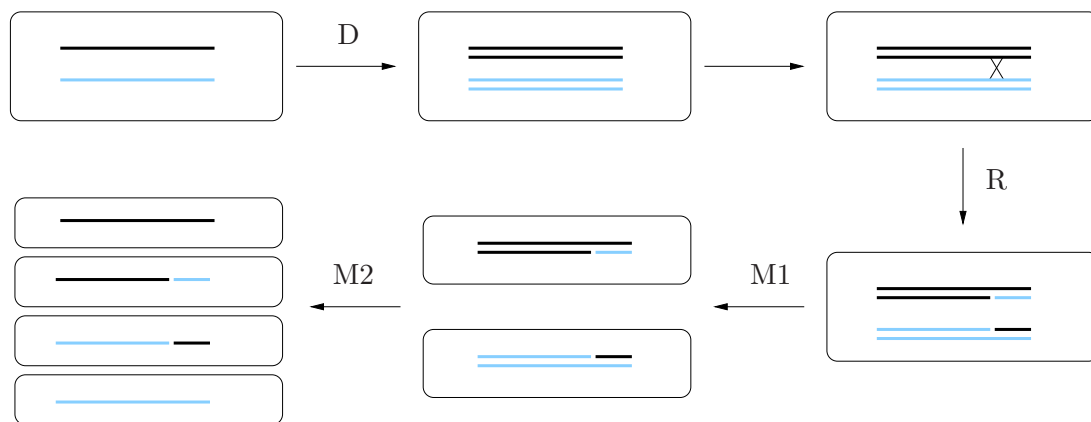


Figure 2.1: Illustration of meiotic cell division with one pair of homologous chromosomes in a diploid germ cell: Initially, the genetic material is duplicated (D). Afterwards, synapsis and recombination occur, resulting in recombined chromosomes (R). During meiosis 1, the homologous chromosomes are separated (M1), followed by a second cell division in meiosis 2 when the sister chromatids segregate to result in four haploid gametes (M2).

between homologous chromosomes, which is called *chiasma*². This subsequently allows chromosomes to align correctly on the meiosis 1 *spindle*³ and thus to accurately segregate to different daughter cells during the first cell division. Evidence of the importance of recombination for meiosis can be found in studies with *S. cerevisiae* mutants where the blocking of recombination also blocks proper segregation in meiosis 1 [42].

Recombination starts with a double-strand break induced by the Spo11 protein in the DNA of one of the homologous chromosomes. The ends of the broken DNA are then digested by exonucleases⁴ to produce single-stranded DNA. This allows one of the cut strands to disassociate from its complementary strand and particular *recombinase* enzymes to catalyse its pairing with the complementary strand of the intact homologous chromosome aiming for its repair⁵. This is the so-called strand invasion by which the invading strand displaces its homologous strand from the actual intact chromosome. The invading strand is then extended by DNA polymerase (using the complementary strand of its homologue as template) until the displaced single-strand pairs with the other single-strand from the (double-strand cut) homologous chromosome. After further DNA extension, where again the respective homologous complementary single-strand is used as template, the two ends from the double-strand break are ligated and

²cytological manifestation at the point of nucleotide exchange between two homologues due to meiotic recombination [50].

³bipolar array of microtubules that forms during meiosis to which chromosomes attach and by which chromosomes are segregated to daughter cells [50].

⁴enzymes that digest nucleotides from the end of a polynucleotide chain.

⁵The mechanism of recombination is indeed strongly related to DNA repair mechanisms in the cell.

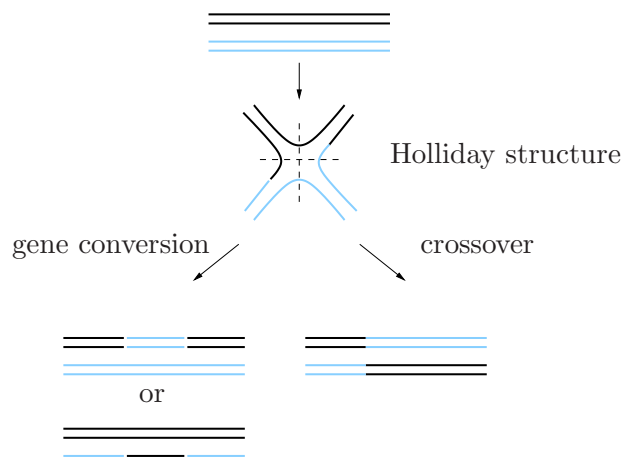


Figure 2.2: Resolution of the Holliday structure through either gene conversion (horizontal cut) or through a crossover (vertical cut). Here, each pair of strands displays the DNA double-strand structure.

the resulting structure is the famous *Holliday structure*⁶. The Holliday structure is then resolved by cleavage of the strands. The resolution of the Holliday structure can be done in two different ways (depending on which pair of strands in the complex is cut): this results in either a *crossover* event (recombined chromosomes due to a reciprocal nucleotide exchange) or in a *non-crossover* event, also known as *gene conversion*, where part of the nucleotide sequence of one chromosome is replaced by the sequence of its homologue (i.e. there is no exchange of sequences but replacement), see also Figure 2.2. Gene conversion is due to the fact that in a region located in the immediate vicinity of the initial break point, a *heteroduplex* is found: one strand of one chromosome is base-paired with the strand of the homologous chromosome, i.e. usually base-pair mismatches are obtained. Mismatches are usually repaired by specific repair mechanisms of the cell where one strand acts as template for the other strand to correct for these; as a result one sequence replaces the other in this area. Importantly, only crossover recombination products are ultimately manifested as chiasmata, so that - following the previous explanation - always one crossover event per pair of homologs is required, the so-called ‘obligatory chiasma’ [9].

Indeed, there also exist models that challenge the well-established Holliday model where crossovers and non-crossovers form as alternative outcomes of the resolution of the Holliday structure. An example is the ‘Early crossover decision model’ [9] claiming that the decision to generate a crossover or a non-crossover event is made shortly after the double-strand break, i.e. much earlier than the stage at which the Holliday structure is resolved. Afterwards, they claim two different pathways, one that generates non-crossover events and an alternative pathway (which involves the Holliday structure)

⁶named after Robin Holliday who first stated this structure in 1964 [33].

that generates crossover events.

Cytological data in mammals show a ratio of approximately 10:1 of non-crossovers to crossovers following a double-strand break, while the average ratio of non-crossovers to crossovers in yeast is said to be around 2:1 (this might also differ within different regions on the chromosomes) [41]. Despite the excess of non-crossovers compared to crossovers, most studies have focused on crossover events since gene conversion is generally much harder to spot (e.g. via evolutionary models), see [39, 66].

Similarly, we will be only concerned with crossover events, more precisely with so-called *single-crossover* events, recombination events where exactly one crossover occurs. Even though we use this restriction primarily for mathematical purposes, it is also biologically justified - at least for shorter DNA sequences - since crossovers are in general rare events. Additionally, the phenomenon of *interference* also explains why single-crossovers exhibit a relevant special case. In the following, with recombination, we will always refer to a real crossover event.

Interference

Interference accounts for the fact that the occurrence of one crossover event reduces the probability that another crossover will occur simultaneously in a nearby region. For closely adjacent regions, interference is usually complete (i.e. completely inhibits any further crossover) [40] and it is typically inversely correlated with distance. Thus, interference is crucial to the observation that the distribution of crossovers along chromosomes is strikingly nonrandom (see below) by introducing dependencies between levels of recombination in adjacent regions.

Although the molecular mechanisms of interference are still not completely understood, there exist several theories about this remarkable factor [9, 23, 40, 51]. One often proposed model is the ‘stress relief’ model [51]: this claims that the designation of a crossover involves structural changes on the chromosome that relieve mechanical stress to neighbouring regions. Thereby, the occurrence of further crossovers is inhibited while the effect of interference decreases to more distant regions. With regard to this model, the formation of the obligatory crossover is determined by ensuring sufficient initial stress. Furthermore, the overall view is that the mechanisms of crossover control operate at the level of whole chromosomes rather than on particular chromosome regions or nucleotide sequences [40].

2.2.3 Crossover: occurrence and frequencies

So far, we have seen that homologous chromosomes during meiosis (almost) always experience the obligatory crossover and additionally that the phenomenon of interference is observed, i.e. crossovers tend to be spaced. Furthermore, recombination events are more likely to occur in some regions of the genome than in others, i.e. they exhibit a striking nonrandom distribution [41]. How this distribution is formed and which factors

support (or suppress) recombination is an intensely debated issue. Most recombination events cluster within so-called recombination *hotspots*, small (around 1-2 kb) genomic intervals with high recombination activities which are surrounded by large stretches of non-recombining DNA. As an example, average spacing between clusters is about 65 kb in humans [41]. Estimates suggest that about 80 % of all crossover events occur in 10-20 % of the whole genomic material [13]. These hotspots are found in different genomic regions and share no obvious sequence similarities.

Crossover activity is usually expressed in *centimorgans* (cM)⁷ per megabase pair (Mb). The *genetic distance* of 1 cM between two loci corresponds to a 1 % frequency of recombinant progeny. In particular, genetic distance does not correspond to the physical distance due to the uneven distribution of crossovers. Recombination rates - even within the same species - vary highly depending on a wide range of factors which are not known or completely understood yet. The average crossover frequency in humans is about 1.1 cM/Mb, but there also exist hotspots with recombination activities of 0.3 cM/Mb and 370 cM/Mb, respectively [41]. For comparison, the average crossover rate in mice is around 0.5 cM/Mb (even though there exists a hot spot with an intense peak activity of 1300 cM/Mb), and for yeast the average is as high as 370 cM/Mb [41]. Further observations suggest that in most species females exhibit more crossovers than men, many hotspots show a high content of the bases Guanin and Cytosin and that smaller chromosomes have higher recombination rates than larger ones (at least in humans). In many mammals, the crossover rate is reduced near the centromeres and increased near the telomeres⁸. Furthermore, it has been proposed that the recombination rate is also positively correlated with gene density and nucleotide diversity [13].

To conclude, recombination is a fundamentally important process, not only because it is required for accurate chromosome segregation, but also because it plays a significant role in shaping the genetic history of populations. Due to this, when studying questions of genome evolution, it is necessary to incorporate the factor recombination into the respective methods. First of all, it is the only factor (together with the related factor gene conversion) that allows linked loci to have independent evolutionary histories [58]. Thus, it has an extensive influence on conclusions regarding population relations and the inference of other evolutionary parameters such as mutation rates and selection values [13]. Furthermore, indications suggest that recombination might be associated with mutational processes, and that selection might be more efficient in regions with high recombination activity [37].

Many studies are concerned with building so-called *recombination rate maps* of various genomes to capture the local recombination landscape of chromosomes, i.e. characterising hotspots and their corresponding crossover rates, see for example [13, 37, 45] and references therein. Increasing knowledge about recombination has also important implications for human genetics, e.g. the mapping of disease genes in connection with

⁷named after Thomas Hunt Morgan (1866-1945), who discovered genetic linkage.

⁸particular DNA region at the ends of each chromosome.

linkage studies⁹ [45].

As a matter of course, including recombination into mathematical tools in population genetics is unavoidable. However, primarily due to its nonlinear nature, recombination is difficult to employ mathematically and also results in computational difficulties [58].

⁹linkage studies use *linkage disequilibrium* (LD) as a measure of whether alleles at different loci on the same chromosome coexist in a population nonrandomly. Recombination breaks down LD since it decouples alleles.

Chapter 3

Single–crossover recombination in discrete time: The model

The recombination model we are considering in this work is the discrete-time counterpart of the one described by E. and M. Baake in [3]. The model describes the dynamics of the genetic composition of sexually reproducing populations that evolve with recombination acting as the only evolutionary force. As a special case, we only consider single-crossovers, which leads to what we call single-crossover recombination (SCR). In particular, we restrict ourselves to the deterministic limit of infinite population size, also known as infinite population limit (IPL), where the population is identified with a probability measure on type space that evolves deterministically. Thus, we neglect any stochastic fluctuations that are commonly referred to as *genetic drift*.

Furthermore, we make the following assumptions: Both sexes are assumed to be equal, i.e. they agree in the composition of all haplotypes as well as in all recombination parameters. With reference to Hardy, see [30], the single allele frequencies remain constant with time. We will describe the dynamics on the level of the gametes (haplotypes) with respect to the concept of random mating stating that the random union of zygotes is equivalent to the random union of all the gametes which these produce. Jennings [36] already showed in 1917 that it is indeed sufficient to only consider the gamete pool of an infinite large population instead of taking into account the diploid nature of sexually reproducing organisms. The process we are considering can then be idealised as follows, see also Figure 3.1: We assume a very large population (indeed, in our model an ‘infinite’ large population) of gametes. To recombine, two gametes are chosen randomly out of the population, and a crossover leads to the exchange of genetic material before (and after, respectively) the crossing point. Afterwards, the mixed gametes separate and replace their parents in the population.

Since we only consider single-crossovers, the new recombined gametes consist of exactly two segments: the leading segment of the first and the trailing segment of the second parent.

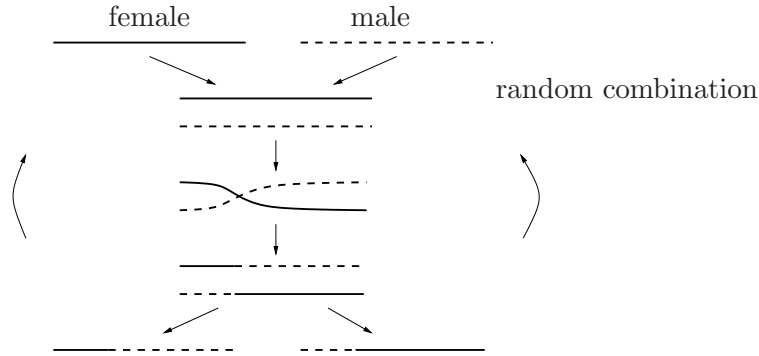


Figure 3.1: Schematic representation of the life cycle of a gamete population under recombination: Random mating of two gametes.

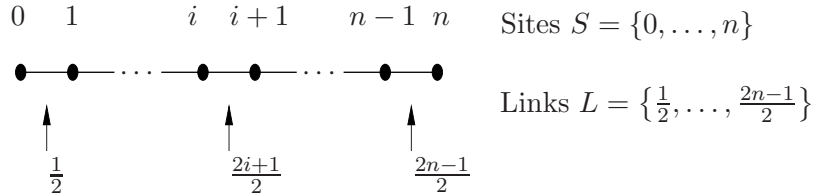


Figure 3.2: Illustration of a gamete with sites and links.

3.1 The mathematical setup

A gamete (of length $n + 1$, say) is represented as a linear arrangement of the $n + 1$ *sites* of the set $S = \{0, 1, \dots, n\}$. Sites are discrete positions on a gamete that may be interpreted as gene or nucleotide positions. A set X_i collects the possible elements (such as alleles or nucleotides) at site i . For convenience, we restrict ourselves to *finite* sets X_i , though much of the theory can be extended to the case that each X_i is a locally compact space, see [4], which can be of importance for applications in quantitative genetics [20]. What we call a *type* is then defined as a sequence $(x_0, x_1, \dots, x_n) \in X_0 \times X_1 \times \dots \times X_n =: X$, where X denotes the (finite) *type space*.

Recombination events take place at the so-called *links* between neighbouring sites, collected into the set $L = \{\frac{1}{2}, \frac{3}{2}, \dots, \frac{2n-1}{2}\}$, where link $\alpha = \frac{2i+1}{2}$ is the link between sites i and $i + 1$, see also Figure 3.2. Since we only consider single-crossovers here, each individual event yields an exchange of the sites either before or after the respective link between the two types involved. A recombination event at link $\frac{2i+1}{2}$ that involves $x = (x_0, \dots, x_n)$ and $y = (y_0, \dots, y_n)$ thus results in the types $(x_0, \dots, x_i, y_{i+1}, \dots, y_n)$ and $(y_0, \dots, y_i, x_{i+1}, \dots, x_n)$, with both pairs considered as *unordered*.

Since we assume an infinite population, we are not looking at the individual dynamics, but at the induced dynamics on the probability distribution on the type space X . The

population at time t , $t \in \mathbb{N}_0$, is then described by $p_t = (p_t(x))_{x \in X} \in \mathcal{P}(X)$, where $p_t(x)$ denotes the relative frequency of type $x \in X$ at time t , and $\mathcal{P}(X)$ is the set of probability measures on X . Let ρ_α , $\alpha \in L$, denote the probability for a crossover at link α in every time step. Consequently, we must have $\rho_\alpha \geq 0$ and $\sum_{\alpha \in L} \rho_\alpha \leq 1$, where $\rho_\alpha > 0$ is assumed from now on without loss of generality (when $\rho_\alpha = 0$, the set $X_{\alpha - \frac{1}{2}} \times X_{\alpha + \frac{1}{2}}$ can be considered as a space for an effective site that comprises $\alpha - \frac{1}{2}$ and $\alpha + \frac{1}{2}$).

Then, the time evolution of the relative frequencies $p_t(x)$ of types $x = (x_0, \dots, x_n)$ when starting from an initial population p_0 at time $t = 0$, is given by the following system of *recombination equations* for all $x \in X$:

$$\begin{aligned} p_{t+1}(x) &= \sum_{\alpha \in L} \rho_\alpha p_t(x_0, x_1, \dots, x_{[\alpha]}, *, *, \dots, *) p_t(*, *, \dots, *, x_{[\alpha]}, x_{[\alpha]+1}, \dots, x_n) \\ &\quad + \left(1 - \sum_{\alpha \in L} \rho_\alpha\right) p_t(x), \quad \text{with } t \in \mathbb{N}_0. \end{aligned} \tag{3.1}$$

Here, $[\alpha]$ ($\lceil \alpha \rceil$) denotes the largest integer below (the smallest above) α and the star $*$ at site i stands for X_i , and thus indicates marginalisation at site i . (3.1) explains how to obtain the frequency of any type $x = (x_0, \dots, x_n)$ at time $t + 1$ with regard to time t : Any type $x = (x_0, \dots, x_n)$ at time $t + 1$ can result from recombination at link $\alpha \in L$ of type $(x_0, x_1, \dots, x_{[\alpha]}, *, *, \dots, *)$ with type $(*, *, \dots, *, x_{[\alpha]}, x_{[\alpha]+1}, \dots, x_n)$ present at time t (compare Figure 3.3), and, furthermore, all types x of time t that are not involved in recombination, remain in the population. Since (3.1) describes a

$$\begin{array}{ccc} x_0, \dots, x_{[\alpha]}, *, \dots, * & \xrightarrow{\rho_\alpha} & x_0, \dots, x_{[\alpha]}, x_{[\alpha]}, \dots, x_n \\ *, \dots, *, x_{[\alpha]}, \dots, x_n & & *, \dots, *, *, \dots, * \end{array}$$

Figure 3.3: Recombination at link α resulting in type $x = (x_0, \dots, x_n)$.

large nonlinear coupled system of difference equations, the way to an explicit solution is rather difficult. An important step to solve (3.1) lies in its reformulation in a more compact way with the help of certain recombination operators.

Recombination operators

Let X be the type space considered in our model. To construct the recombination operators, we first need the canonical projection operator $\pi_i : X \rightarrow X_i$, defined by $x \mapsto \pi_i(x) = x_i$ as usual. Likewise, for any index set $J \subseteq S$, the projector π_J is defined as $\pi_J : X \rightarrow X_J := \prod_{i \in J} X_i$. We will frequently use

$$\pi_{<\alpha} := \pi_{\{0, \dots, [\alpha]\}} \quad \text{and} \quad \pi_{>\alpha} := \pi_{\{[\alpha], \dots, n\}}.$$

Since $\pi_{<\alpha}$ describes a projection on the sites before link α , while $\pi_{>\alpha}$ projects on the sites behind α , these can be understood as ‘*cut-and-forget*’ operators since they ‘cut out’ the leading and the trailing segment of a type x , respectively, and ‘forget’ about the rest. The projectors induce linear mappings from $\mathcal{P}(X)$ to $\mathcal{P}(X_J)$ by $p \mapsto \pi_J.p := p \circ \pi_J^{-1}$, where π_J^{-1} denotes the preimage under π_J and \circ indicates composition of mappings. The operation $.$ (not to be confused with a multiplication sign) is known as the pullback of π_J with respect to p . Consequently, $\pi_J.p$ is the marginal distribution of p with respect to the sites of J , i.e. $\pi_J.p(\pi_J(x)) = (p \circ \pi_J^{-1})(\pi_J(x)) = p(\{y \in X | \pi_J(y) = \pi_J(x)\})$ for any $x \in X$.

Recombinator

We can now define recombination via the the ‘cut-and-forget’ operators. If we consider recombination at link α , performed on the entire population, then the resulting population consists of randomly chosen leading segments relinked with randomly chosen trailing segments. This operation may be described through the (elementary) recombination operator (or *recombinator* for short) $R_\alpha: \mathcal{P}(X) \rightarrow \mathcal{P}(X)$, defined by $p \mapsto R_\alpha(p)$ with

$$R_\alpha(p) := (\pi_{<\alpha}.p) \otimes (\pi_{>\alpha}.p), \quad (3.2)$$

where \otimes denotes the product measure and reflects the independent combination of both marginals $\pi_{<\alpha}.p$ and $\pi_{>\alpha}.p$. The recombinators are in particular structural *non-linear* operators that do not depend on the recombination probabilities.

Properties of the recombinators

Before we rewrite the recombination equations in terms of the recombinator, let us recall some of their elementary properties. The proofs can be found in [3].

Proposition 3.1. *On $\mathcal{P}(X)$, the elementary recombinators are idempotents and commute with one another. We thus have $R_\alpha^2 = R_\alpha$ and $R_\alpha R_\beta = R_\beta R_\alpha$ for all $\alpha, \beta \in L$. \square*

This proposition permits the consistent definition of *composite recombinators*

$$R_G := \prod_{\alpha \in G} R_\alpha \quad (3.3)$$

for arbitrary subsets $G \subseteq L$. In particular, one has $R_\emptyset = 1$ and $R_{\{\alpha\}} = R_\alpha$. Here, the product is to be read as composition, and clearly, $R_G(p)$ is the product measure with respect to all links in G .

Proposition 3.2. *On $\mathcal{P}(X)$, the elementary recombinators are commuting idempotents. For $\alpha \leq \beta$, they satisfy*

$$\pi_{<\alpha}(R_\beta(p)) = \pi_{<\alpha}p \quad \text{and} \quad \pi_{>\alpha}(R_\beta(p)) = (\pi_{\{[\alpha], \dots, [\beta]\}}p) \otimes (\pi_{>\beta}p); \quad (3.4)$$

likewise, for $\alpha \geq \beta$,

$$\pi_{>\alpha}(R_\beta(p)) = \pi_{>\alpha}p \quad \text{and} \quad \pi_{<\alpha}(R_\beta(p)) = (\pi_{<\beta}p) \otimes (\pi_{\{[\beta], \dots, [\alpha]\}}p). \quad (3.5)$$

Furthermore, the composite recombinators satisfy

$$R_G R_H = R_{G \cup H} \quad (3.6)$$

for arbitrary $G, H \subseteq L$. \square

These properties can be understood intuitively as well: (3.4) says that recombination at or after link α does not affect the marginal frequencies at sites before α , whereas the marginal frequencies at the sites after α change into the product measure (and vice versa in (3.5)). Furthermore, repeated recombination at link α does not change the situation any further (recombinators are idempotents) and the formation of the product measure with respect to ≥ 2 links does not depend on the order in which the links are affected.

Employing recombinators, the equations (3.1) in discrete time with a given initial distribution p_0 can be compactly rewritten as

$$p_{t+1} = p_t + \sum_{\alpha \in L} \rho_\alpha (R_\alpha - \mathbb{1})(p_t) =: \Phi(p_t). \quad (3.7)$$

As indicated, the non-linear operator of the right-hand side of (3.7) is denoted by Φ from now on.

As mentioned in the introduction, part of this work is to study the discrete-time recombination dynamics in comparison with the analogous dynamics in continuous time. Thus, before continuing with the investigation of the discrete-time model, the main results from the continuous-time model should be summarised. This is needed to fully understand the complications involving discrete time.

3.2 Excursus: SCR in continuous time

We now consider the recombination dynamics with overlapping generations employing the same assumptions as in the discrete-time model. Making use of the recombinators introduced above, the dynamics (in the IPL) is described by a system of differential equations for the time evolution of the probability distribution (or measure), starting from an initial condition p_0 at $t = 0$. It reads [3]

$$\dot{p}_t = \sum_{\alpha \in L} \tilde{\rho}_\alpha (R_\alpha - \mathbb{1})(p_t), \quad (3.8)$$

where $\tilde{\rho}_\alpha$ is now the *rate* for a crossover at link α . Although (3.8) describes a coupled system of nonlinear differential equations, the closed solution for its Cauchy (or initial value) problem is available [3, 4]:

Theorem 3.3. *The solution of the recombination equation (3.8) with initial value p_0 can be given in closed form as*

$$p_t = \sum_{G \subseteq L} \tilde{a}_G(t) R_G(p_0), \quad (3.9)$$

with the coefficient functions

$$\tilde{a}_G(t) = \prod_{\alpha \in L \setminus G} \exp(-\tilde{\rho}_\alpha t) \prod_{\beta \in G} (1 - \exp(-\tilde{\rho}_\beta t)). \quad (3.10)$$

These are non-negative functions, which satisfy $\sum_{G \subseteq L} \tilde{a}_G(t) = 1$ for all $t \geq 0$. \square

The underlying stochastic process for finite populations and the proof for the infinite population limit can be found in [5]. With reference to the stochastic process (i.e. independent Poisson processes for all $\alpha \in L$, each with parameter $\tilde{\rho}_\alpha$ in each individual), the coefficient functions can be interpreted probabilistically. Given an individual sequence in the population, $\tilde{a}_G(t)$ is the probability that the set of links that have seen at least one crossover event until time t is precisely the set G . Note that the product structure of the $\tilde{a}_G(t)$ implies independence of links, a decisive feature of the single-crossover dynamics in continuous time, as we shall see later on. By (3.9), p_t is always a convex combination of the probability measures $R_G(p_0)$ with $G \subseteq L$. Consequently, given an initial condition p_0 , the entire dynamics takes place on the closed simplex (within $\mathcal{P}(X)$) that is given by $\text{conv}\{R_G(p_0) \mid G \subseteq L\}$, where $\text{conv}(A)$ denotes the convex hull of A .

It is surprising that a closed solution for the dynamics (3.8) can be given explicitly. Explicit solutions for large nonlinear systems of differential equations are rare - solutions to differential equations are usually reserved for linear ones. This suggests the existence of an underlying linear structure [4] for (3.8), which is indeed the case and well known from similar equations, compare [48]. In the context of the formulation with recombinators, it can be stated as follows, compare [3] for details.

Theorem 3.4. *Let $\{c_{G'}^{(L')}(t) \mid \emptyset \subseteq G' \subseteq L' \subseteq L\}$ be a family of non-negative functions with $c_G^{(L)}(t) = c_{G_1}^{(L_1)}(t) c_{G_2}^{(L_2)}(t)$, valid for any partition $L = L_1 \dot{\cup} L_2$ of the set L and all $t \geq 0$, where $G_i := G \cap L_i$. Assume further that these functions satisfy $\sum_{H \subseteq L'} c_H^{(L')}(t) = 1$ for any $L' \subseteq L$ and $t \geq 0$. If $v \in \mathcal{P}(X)$ and $H \subseteq L$, one has the identity*

$$R_H \left(\sum_{G \subseteq L} c_G^{(L)}(t) R_G(v) \right) = \sum_{G \subseteq L} c_G^{(L)}(t) R_{G \cup H}(v),$$

which is then satisfied for all $t \geq 0$. \square

Here, the upper index specifies the respective set of links. So far, Theorem 3.4 depends crucially on the product structure of the functions $c_G^{(L)}(t)$, but we will show later how this assumption can be relaxed. In any case, the coefficient functions $\tilde{a}_G(t)$ of (3.10)

satisfy the conditions of Theorem 3.4. The result then means that the recombinators act linearly along solutions (3.9) of the recombination equation (3.8). Denoting φ_t as the forward flow of (3.8), Theorem 3.4 thus has the following consequence.

Corollary 3.5. *On $\mathcal{P}(X)$, the forward flow of (3.8) commutes with all recombinators, which means that $R_G \circ \varphi_t = \varphi_t \circ R_G$ holds for all $t \geq 0$ and all $G \subseteq L$. \square*

The conventional approach to solve the recombination dynamics consists in transforming the type frequencies to certain functions which diagonalise the dynamics, see [7, 14, 15, 48] and references therein for more. From now on, we will call these functions *principal components* after Bennett [7]. For the single-crossover dynamics in continuous time, they have a particularly simple structure: they are given by certain correlation functions, or *linkage disequilibria* (LDE), which play an important role in biological applications, see for example [64] and references therein. They have a counterpart at the level of operators on $\mathcal{P}(X)$.

Namely, let us define *LDE operators* on $\mathcal{P}(X)$ as linear combinations of recombinators via

$$T_G := \sum_{H \supseteq G} (-1)^{|H-G|} R_H, \quad \text{with } G \subseteq L, \quad (3.11)$$

so that the inverse relation is given by

$$R_H = \sum_{G \supseteq H} T_G \quad (3.12)$$

due to the combinatorial Möbius inversion formula, compare [1]. Let us note for further use that, by equation (3.6) in Proposition 3.2, $T_G \circ R_G = T_G$. Note also that, for a probability measure p on X , $T_G(p)$ is a signed measure on X ; in particular, it need not be positive. The LDEs are given by certain *components* of the $T_G(p)$ — see [3, 5] for more. In the continuous-time single-crossover setting, it was shown in [3] that, if p_t is the solution (3.9), the $T_G(p_t)$ satisfy

$$\frac{d}{dt} T_G(p_t) = - \left(\sum_{\alpha \in L \setminus G} \tilde{\rho}_\alpha \right) T_G(p_t), \quad \text{for all } G \subseteq L, \quad (3.13)$$

which is a *decoupled* system of homogeneous linear differential equations, with the standard exponential solution. That is, the LDE operators both linearise and diagonalise the system, and the LDEs are thus, at the same time, principal components.

A straightforward calculation now reveals that the solution (3.9) can be rewritten as

$$p_t = \sum_{G \subseteq L} \tilde{a}_G(t) R_G(p_0) = \sum_{K \subseteq L} b_K(t) T_K(p_0) = \sum_{K \subseteq L} T_K(p_t), \quad (3.14)$$

where the new coefficient functions are given by

$$b_K(t) := \exp \left(- \sum_{\alpha \in L \setminus K} \tilde{\rho}_\alpha t \right).$$

This way, an explicit solution for p_t is obtained as a decomposition into exponential factors. At this point, it is important to notice the simple structure of the LDE operators, which do not depend on the crossover rates. Moreover, the transformation between recombinators and LDE operators is directly given by Möbius formula, see equations (3.11) and (3.12). This is a significant simplification in comparison with previous results, compare [7, 14, 15, 24], where the coefficients of the transformation generally depend on the crossover rates and must be determined recursively.

To summarise the results from the continuous-time recombination model: Even though the dynamics is described through a large nonlinear coupled system of differential equations, an explicit solution to the dynamics could be found. This surprising result is due to an underlying linearity in the system that can be explained with the independence of links. In turn, this results in the linear action of the (nonlinear) recombinators on solutions of the dynamics as well as in the commuting property of the forward flow of the system of differential equations with all recombinators. Furthermore, the special structure of the continuous-time model is reflected in the simplifying construction of the principal components that are in particular independent of the recombination parameters (in contrast to previous results on recombination dynamics).

Below, we shall see that the SCR dynamics in *continuous* time is indeed a special case, and that the above results cannot be transferred directly to the corresponding dynamics in *discrete* time. Nevertheless, part of the continuous-time structure prevails and offers a useful entry point for the solution of the discrete-time counterpart.

3.3 SCR in discrete time

After this short introduction to the SCR dynamics in continuous time, we now continue with investigating the discrete-time dynamics described by (3.7). The final goal is to state an explicit solution to the dynamics, namely for $p_t = \Phi^t(p_0)$ with $t \in \mathbb{N}_0$. Based on the result for the continuous-time model, the solution is expected to be of the form

$$p_t = \Phi^t(p_0) = \sum_{G \subseteq L} a_G(t) R_G(p_0), \quad (3.15)$$

with $a_G(0) = \delta_{G, \emptyset}$, $a_G(t) \geq 0$, for all $G \subseteq L$, and $\sum_{G \subseteq L} a_G(t) = 1$, describing the (unknown) coefficient functions arising from the dynamics. This representation of the solution was first stated by Geiringer [24]. In particular, the discrete-time dynamics takes place on the simplex $\text{conv}\{R_G(p_0) \mid G \subseteq L\}$ as well. We will prove in Theorem 3.7 that this ansatz is indeed right and constitutes the solution to the recombination dynamics (3.7).

The structure of the solution (3.15) can also be illustrated by the following consideration, see also Figure 3.4: Starting at time $t = 0$, the initial population $p_0 = R_\emptyset(p_0)$ has not experienced any recombination event so far. Then imagine *all* individuals of p_0 to recombine at link $\alpha \in L$. The emerging population is then given by $R_\alpha(p_0)$.

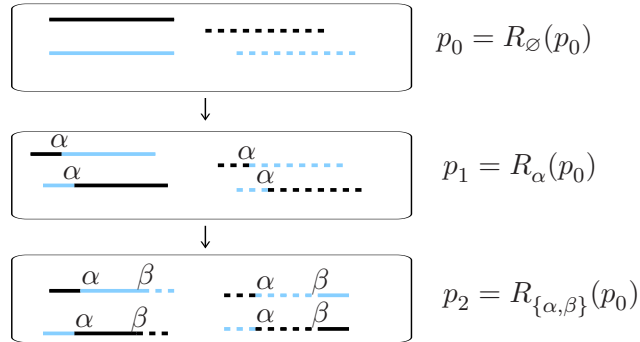


Figure 3.4: Illustration of the concept of recombined populations for four different gametes.

Furthermore, let recombination occur at another link $\beta \in L$ for all individuals, giving rise to the population $R_{\{\alpha, \beta\}}(p_0)$ etc. The $R_G(p_0)$, $G \subseteq L$, are the so-called *recombined* populations. Since, of course, recombination most likely will only happen to a fraction of the population as well as at different links, the actual population at time $t \in \mathbb{N}_0$ will be given as a mixture of the various recombined populations as stated by (3.15). In particular, the $a_G(t)$, $G \subseteq L$, give the corresponding proportions of the recombined populations and suggest the same probabilistic interpretation as in the continuous-time case: given an individual in the population p_t , $a_G(t)$, $G \subseteq L$, gives the probability that until time t *exactly* the links of G have been involved in recombination.

Remark 3.6. *We will define the underlying stochastic process to the IPL dynamics (3.7) in Section 4.1. With the help of another stochastic process, we will then eventually justify the stochastic interpretation of the coefficient functions, see Proposition 4.14.*

What we are left with is to determine the coefficient functions $a_G(t)$, $G \subseteq L$. The question is if we can make use of the tools developed for the solution of the analogous continuous-time dynamics, e.g. if we can adopt the transformation (3.11) to diagonalise the discrete-time dynamics.

In connection with this, we are particularly interested in whether a discrete-time equivalent to Corollary 3.5 exists, that is, whether all recombinators R_G commute with Φ . This is of importance since it would allow for a diagonalisation of the dynamics via the LDE operators (3.11). To see this, assume for a moment that $R_\alpha \circ \Phi = \Phi \circ R_\alpha$ for all $\alpha \in L$, and thus $R_G \circ \Phi = \Phi \circ R_G$ for all $G \subseteq L$. Noting that, when $\alpha \in G \subseteq H$, equation (3.6) from Proposition 3.2 implies that $(R_\alpha - \mathbb{1})R_H = R_{H \cup \{\alpha\}} - R_H = R_H - R_H = 0$,

we see that the assumption above would lead to

$$\begin{aligned}
T_G \circ \Phi &= \sum_{H \supseteq G} (-1)^{|H-G|} R_H \circ \Phi = \sum_{H \supseteq G} (-1)^{|H-G|} \Phi \circ R_H \\
&= \sum_{H \supseteq G} (-1)^{|H-G|} R_H + \sum_{H \supseteq G} (-1)^{|H-G|} \sum_{\alpha \in L} \rho_\alpha (R_\alpha - \mathbb{1}) R_H \\
&= T_G + \sum_{H \supseteq G} (-1)^{|H-G|} \sum_{\alpha \in L \setminus G} \rho_\alpha (R_\alpha - \mathbb{1}) R_H \\
&= \left(1 - \sum_{\alpha \in L \setminus G} \rho_\alpha\right) T_G + \sum_{\alpha \in L \setminus G} \rho_\alpha \sum_{\substack{H \supseteq G \\ \alpha \notin H}} \left((-1)^{|H-G|} R_{H \cup \{\alpha\}} + (-1)^{|H \cup \{\alpha\} - G|} R_{H \cup \{\alpha\}} \right) \\
&= \left(1 - \sum_{\alpha \in L \setminus G} \rho_\alpha\right) T_G,
\end{aligned}$$

so that, indeed, all $T_G(p_t)$ would decay geometrically. This wishful calculation is badly smashed by the nonlinear nature of the recombinators, and we are now concerned with true identities that repair the damage. To get an intuition for the dynamics in discrete time, let us first take a closer look at the discrete-time model with two, three, and four sites.

3.3.1 Two and three sites

For two sites, one simply has $S = \{0, 1\}$ and $L = \{\frac{1}{2}\}$, so that only one non-trivial recombinator exists, $R = R_{\frac{1}{2}}$, with corresponding recombination probability $\rho = \rho_{\frac{1}{2}}$. Consequently, the SCR equation simplifies to

$$p_{t+1} = \Phi(p_t) = \rho R(p_t) + (1 - \rho) p_t, \quad (3.16)$$

where p_t is a $|X|$ -dimensional probability vector. The solution is given by

$$p_t = a(t) p_0 + (1 - a(t)) R(p_0) \quad (3.17)$$

with $a(t) = a_\emptyset(t) = (1 - \rho)^t$. This formula is easily verified by induction [68]. Thus, in analogy with the SCR dynamics in continuous time, the solution is available in closed form, and the coefficient functions allow an analogous probabilistic interpretation. Furthermore, it is easily seen that the recombinators $R_\emptyset = \mathbb{1}$ and $R_{\frac{1}{2}} = R$ commute with Φ and therefore with Φ^t for all $t \in \mathbb{N}_0$. For two sites, the analogue of Corollary 3.5 thus holds in discrete time. As a consequence, the LDE operators from (3.11) decouple and linearise the system (3.16). At the level of the component LDEs, this is common knowledge in theoretical population genetics; compare [31, Chap. 3].

Similarly, the recombination equation (3.7) for three sites $S = \{0, 1, 2\}$ and links $L = \{\frac{1}{2}, \frac{3}{2}\}$ can be solved explicitly as well. An elementary calculation (applying

the iteration and comparing coefficients, see [68]) shows that the corresponding coefficient functions $a_G(t)$ follow the linear recursion

$$\begin{pmatrix} a_{\emptyset}(t+1) \\ a_{\frac{1}{2}}(t+1) \\ a_{\frac{3}{2}}(t+1) \\ a_{\{\frac{1}{2}, \frac{3}{2}\}}(t+1) \end{pmatrix} = \begin{pmatrix} 1 - \rho_{\frac{1}{2}} - \rho_{\frac{3}{2}} & 0 & 0 & 0 \\ \rho_{\frac{1}{2}} & 1 - \rho_{\frac{3}{2}} & 0 & 0 \\ \rho_{\frac{3}{2}} & 0 & 1 - \rho_{\frac{1}{2}} & 0 \\ 0 & \rho_{\frac{3}{2}} & \rho_{\frac{1}{2}} & 1 \end{pmatrix} \begin{pmatrix} a_{\emptyset}(t) \\ a_{\frac{1}{2}}(t) \\ a_{\frac{3}{2}}(t) \\ a_{\{\frac{1}{2}, \frac{3}{2}\}}(t) \end{pmatrix},$$

with solution

$$\begin{aligned} a_{\emptyset}(t) &= (1 - \rho_{\frac{1}{2}} - \rho_{\frac{3}{2}})^t, \\ a_{\frac{1}{2}}(t) &= (1 - \rho_{\frac{3}{2}})^t - (1 - \rho_{\frac{1}{2}} - \rho_{\frac{3}{2}})^t, \\ a_{\frac{3}{2}}(t) &= (1 - \rho_{\frac{1}{2}})^t - (1 - \rho_{\frac{1}{2}} - \rho_{\frac{3}{2}})^t, \\ a_{\{\frac{1}{2}, \frac{3}{2}\}}(t) &= 1 - (1 - \rho_{\frac{3}{2}})^t - (1 - \rho_{\frac{1}{2}})^t + (1 - \rho_{\frac{1}{2}} - \rho_{\frac{3}{2}})^t. \end{aligned} \tag{3.18}$$

If we compare this to the analogous coefficient functions $\tilde{a}_G(t)$, $G \subseteq \{\frac{1}{2}, \frac{3}{2}\}$, from the continuous-time dynamics, we observe a crucial difference. Recall that, in continuous time, single-crossovers imply *independence* of links, which is expressed in the product structure of the coefficient functions $\tilde{a}_G(t)$ (see (3.10)). As we find in (3.18), already for three sites, the coefficients of the discrete-time dynamics fail to show the product structure used in Theorem 3.4. The independence observed in continuous time is lost in discrete time, where a crossover event at one link forbids any other cut at other links in the same time step.

But even though Corollary 3.5, concerning the forward flow of (3.8), is a consequence of Theorem 3.4, which, in turn, is based upon the product structure of the coefficients, a short calculation reveals that $R_G \circ \Phi = \Phi \circ R_G$ still holds for the discrete-time model with three sites for all $G \subseteq \{\frac{1}{2}, \frac{3}{2}\}$. As a consequence, just as in the case of two sites, the T_G linearise *and* decouple the dynamics, which is well-known, see [7, 12] for more. In fact, we obtain:

$$\begin{aligned} T_{\emptyset}(\Phi(p)) &= (1 - \rho_{\frac{1}{2}} - \rho_{\frac{3}{2}})T_{\emptyset}(p), \\ T_{\frac{1}{2}}(\Phi(p)) &= (1 - \rho_{\frac{3}{2}})T_{\frac{1}{2}}(p), \\ T_{\frac{3}{2}}(\Phi(p)) &= (1 - \rho_{\frac{1}{2}})T_{\frac{3}{2}}(p), \\ T_{\{\frac{1}{2}, \frac{3}{2}\}}(\Phi(p)) &= T_{\{\frac{1}{2}, \frac{3}{2}\}}(p). \end{aligned}$$

To summarise: despite the loss of independence of links, an explicit solution of the discrete-time recombination dynamics is still available, and a linearisation and diagonalisation of the dynamics can be achieved with the methods developed for the continuous-time model, that is, a transformation to a solvable system via the T_G . However, things will become more complex if we go to four sites and beyond. In particular, there is

no equivalent to Corollary 3.5, i.e., in general, the recombinators *do not* commute with Φ , and we have to search for a new transformation that replaces (3.11), as will be explained next.

3.3.2 Four sites

The complication with four sites originates from the fact that $R_{\frac{3}{2}} \circ \Phi \neq \Phi \circ R_{\frac{3}{2}}$, so that the property described by Corollary 3.5 for continuous time is lost here. Consequently, the T_G fail the desired (diagonalisation) properties. In particular, one finds

$$T_{\emptyset}(\Phi(p)) = (1 - \rho_{\frac{1}{2}} - \rho_{\frac{3}{2}} - \rho_{\frac{5}{2}})T_{\emptyset}(p) - \rho_{\frac{1}{2}}\rho_{\frac{5}{2}}T_{\frac{3}{2}}(p),$$

so that an explicit solution of the model cannot be obtained as before. Furthermore, a simple but lengthy calculation shows that the coefficient functions $a_G(t)$ no longer follow a linear recursion for all $G \subseteq L$, see [68]. This raises the question why four sites are more difficult than three sites, even though independence of links has already been lost with three sites. To answer this, we look at the time evolution of the coefficient functions $a_G(t)$, $G \subseteq L$. For this purpose, let us return to the general model with an arbitrary number of sites.

3.3.3 General case

We now consider an arbitrary (but finite) set S with the corresponding link set L . For each $G \subseteq L$, we use the following abbreviations:

$$\begin{aligned} G_{<\alpha} &:= \{i \in G \mid i < \alpha\}, & G_{>\alpha} &:= \{i \in G \mid i > \alpha\}, \\ L_{\leq\alpha} &:= \{i \in L \mid i \leq \alpha\}, & L_{\geq\alpha} &:= \{i \in L \mid i \geq \alpha\}. \end{aligned}$$

We then obtain

Theorem 3.7. *For all $G \subseteq L$ and $t \in \mathbb{N}_0$, the coefficient functions $a_G(t)$ evolve according to*

$$a_G(t+1) = \left(1 - \sum_{\alpha \in L} \rho_{\alpha}\right) a_G(t) + \sum_{\alpha \in G} \rho_{\alpha} \left(\sum_{H \subseteq L_{\geq\alpha}} a_{G_{<\alpha} \cup H}(t) \right) \left(\sum_{K \subseteq L_{\leq\alpha}} a_{K \cup G_{>\alpha}}(t) \right), \quad (3.19)$$

with initial condition $a_G(0) = \delta_{G, \emptyset}$.

Proof. Geiringer [24] already explained in words how to derive this general recursion, and illustrated it with the four-site example; we give a proof via our operator formalism.

Using (3.15), the recombination equation for p_{t+1} reads

$$\begin{aligned} p_{t+1} &= \sum_{G \subseteq L} a_G(t+1) R_G(p_0) = \Phi(p_t) = \Phi\left(\sum_{G \subseteq L} a_G(t) R_G(p_0)\right) \\ &= \sum_{\alpha \in L} \rho_\alpha \left(\left(\pi_{<\alpha} \left(\sum_{H \subseteq L} a_H(t) R_H(p_0) \right) \right) \otimes \left(\pi_{>\alpha} \left(\sum_{K \subseteq L} a_K(t) R_K(p_0) \right) \right) \right) \\ &\quad + \left(1 - \sum_{\alpha \in L} \rho_\alpha \right) \left(\sum_{G \subseteq L} a_G(t) R_G(p_0) \right), \end{aligned}$$

where each product term in the first sum can be calculated as

$$\begin{aligned} &\left(\pi_{<\alpha} \left(\sum_{H \subseteq L} a_H(t) R_H(p_0) \right) \right) \otimes \left(\pi_{>\alpha} \left(\sum_{K \subseteq L} a_K(t) R_K(p_0) \right) \right) \\ &= \sum_{H, K \subseteq L} a_H(t) a_K(t) \left(\left(\pi_{<\alpha} R_H(p_0) \right) \otimes \left(\pi_{>\alpha} R_K(p_0) \right) \right) \\ &= \sum_{H, K \subseteq L} a_H(t) a_K(t) \left(\left(\pi_{<\alpha} R_{H_{<\alpha} \cup K_{>\alpha}}(p_0) \right) \otimes \left(\pi_{>\alpha} R_{H_{<\alpha} \cup K_{>\alpha}}(p_0) \right) \right) \\ &= \sum_{H, K \subseteq L} a_H(t) a_K(t) \left(R_\alpha \left(R_{H_{<\alpha} \cup K_{>\alpha}}(p_0) \right) \right), \end{aligned}$$

where we use the linearity of the projectors in the first step, and equations (3.4) and (3.5) from Proposition 3.2 in the second (more precisely, we use the left parts of equations (3.4) and (3.5), reading them both forward and backward). Insert this into the expression for p_{t+1} and rearrange the sums for a comparison of coefficients of R_G with $G \subseteq L$. Comparison of coefficients is justified by the observation that, for generic p_0 and generic site spaces, the vectors $R_G(p_0)$ with $G \subseteq L$ are the extremal vectors of the closed simplex $\text{conv}\{R_K(p_0) \mid K \subseteq L\}$. They are the vectors that (generically) cannot be expressed as non-trivial convex combination within the simplex, and hence the vertices of the latter (in cases with degeneracies, one reduces the simplex in the obvious way). If $G = \emptyset$, we only have $(1 - \sum_{\alpha \in L} \rho_\alpha) a_\emptyset(t)$ as coefficient for R_\emptyset . Otherwise, we get additional contributions for each $\alpha \in G$, namely, from those $H, K \subseteq L$ for which $H_{<\alpha} = G_{<\alpha}$ and $K_{>\alpha} = G_{>\alpha}$, while $H_{\geq\alpha}$ and $K_{\leq\alpha}$ can be any subset of $L_{\geq\alpha}$ and $L_{\leq\alpha}$, respectively. Hence, the term belonging to $R_G(p_0)$ reads

$$\sum_{\alpha \in G} \rho_\alpha \left(\sum_{H \subseteq L_{\geq\alpha}} \sum_{K \subseteq L_{\leq\alpha}} a_{G_{<\alpha} \cup H}(t) a_{K \cup G_{>\alpha}}(t) \right) + \left(1 - \sum_{\alpha \in L} \rho_\alpha \right) a_G(t),$$

and the assertion follows. \square

The iteration (3.19) can be understood intuitively as well: A type x resulting from recombination at link α is composed of two segments $x_{<\alpha}$ and $x_{>\alpha}$. These segments themselves may have been pieced together in previous recombination events already,

and the iteration explains the possible cuts these segments may carry along. The first term in the product stands for the type delivering the leading segment (which may bring along arbitrary cuts in the trailing segment), the second for the type delivering the trailing one (here any leading segment is allowed). The term $(1 - \sum_{\alpha \in L} \rho_\alpha) a_G(t)$ covers the case of no recombination.

This way, we also show that ansatz (3.15) is indeed right since it constitutes the (unique) solution to the discrete-time recombination dynamics (3.7).

Note that the above iteration is generally *nonlinear*, where the products stem from the fact that types recombine independently. This nonlinearity is the reason that an explicit solution cannot be given as before. A notable exception is provided by recombination events that occur at links where one of the involved segments cannot have been affected by previous crossovers, namely the links $\frac{1}{2}$ and $\frac{2n-1}{2}$. In this case, at least one of the factors in equation (3.19) becomes 1 (since, obviously, $G_{<\alpha} = \emptyset$ for $\alpha = \frac{1}{2}$ and $G_{>\alpha} = \emptyset$ for $\alpha = \frac{2n-1}{2}$) and the resulting linear and triangular recursion can be solved. Setting $\eta := 1 - \sum_{\alpha \in L} \rho_\alpha$, the coefficients for the corresponding link sets can be inferred directly (proof via simple induction) as

$$\begin{aligned} a_\emptyset(t) &= \eta^t, \\ a_{\frac{1}{2}}(t) &= (\eta + \rho_{\frac{1}{2}})^t - \eta^t, \\ a_{\frac{2n-1}{2}}(t) &= (\eta + \rho_{\frac{2n-1}{2}})^t - \eta^t, \quad \text{and} \\ a_{\{\frac{1}{2}, \frac{2n-1}{2}\}}(t) &= \eta^t - (\eta + \rho_{\frac{1}{2}})^t - (\eta + \rho_{\frac{2n-1}{2}})^t + (\eta + \rho_{\frac{1}{2}} + \rho_{\frac{2n-1}{2}})^t. \end{aligned} \tag{3.20}$$

This explains the availability of an explicit solution for the model with up to three sites, where we do not have links other than $\frac{1}{2}$ and/or $\frac{3}{2}$, so that all corresponding coefficients can be determined explicitly. Indeed, one recovers (3.18) with $n = 2$ and $\eta = 1 - \rho_{\frac{1}{2}} - \rho_{\frac{3}{2}}$. So far, we have observed that the product structure of the coefficient functions, known from continuous time, is lost in discrete time from three sites onwards; this reflects the dependence of links. In contrast, the linearity of the iteration is only lost from four sites onwards. The latter can be understood further by comparison of (3.19) with the differential equations for the coefficients of the continuous-time model. These read:

$$\frac{d}{dt} \tilde{a}_G(t) = - \left(\sum_{\alpha \in L \setminus G} \tilde{\rho}_\alpha \right) \tilde{a}_G(t) + \sum_{\alpha \in G} \tilde{\rho}_\alpha \tilde{a}_{G \setminus \{\alpha\}}(t), \tag{3.21}$$

that is, they are linear, with solution (3.10). Note that this linear dynamics emerges from a seemingly nonlinear one, namely the analogue of (3.19),

$$\frac{d}{dt} \tilde{a}_G(t) = - \left(\sum_{\alpha \in L} \tilde{\rho}_\alpha \right) \tilde{a}_G(t) + \sum_{\alpha \in G} \tilde{\rho}_\alpha \left(\sum_{H \subseteq L_{\geq \alpha}} \tilde{a}_{G_{<\alpha} \cup H}(t) \right) \left(\sum_{K \subseteq L_{\leq \alpha}} \tilde{a}_{K \cup G_{>\alpha}}(t) \right). \tag{3.22}$$

However, due to the product structure of the solution, the product term in the second

sum, when inserting (3.10), reduces to a single term,

$$\left(\sum_{H \subseteq L_{\geq \alpha}} \tilde{a}_{G_{< \alpha} \cup H}(t) \right) \left(\sum_{K \subseteq L_{\leq \alpha}} \tilde{a}_{K \cup G_{> \alpha}}(t) \right) = \tilde{a}_G(t) + \tilde{a}_{G \setminus \{\alpha\}}(t),$$

which turns (3.22) into (3.21).

What happens here is the following.

From four sites onwards (namely, beginning with $n = 3$ and a crossover at $\alpha = \frac{3}{2}$, and both in discrete and continuous time), it happens that leading and trailing segments meet that both possess at least one link that may possibly have seen a previous cut. When a crossover at α takes place, the new joint distribution of cuts before and after α is formed as the product measure of the marginal distributions of cuts in the leading and trailing segments (see (3.19) and (3.22)) — akin to the formation of product measures of marginal types by R_α . In continuous time, the links are all independent, hence the new combination leaves the joint distribution of cuts unchanged. Therefore, a set G of affected links (before and after α) is simply augmented by α if α is a ‘fresh’ cut; this results in the linearity of (3.21). In discrete time, however, the dependence between the links, in particular between those in the leading and trailing segment, means that the formation of the product measure changes the joint distribution of affected links, in addition to the new cut at α ; thus (3.19) remains nonlinear.

Since we aim at an explicit solution of the discrete-time recombination model, we need to find a way to overcome the obstacles of nonlinearity. Inspired by the results of the continuous-time model, we first search for a transformation that decouples and linearises the dynamics.

To this end, we first investigate the behaviour of the R_G and T_G in the discrete-time model since a deeper understanding of their actions will help us find a new transformation. We are still concerned with the LDE operators from the continuous-time model, because of their favourable structure and the existence of the inverse transformation (Möbius inversion). Moreover, as will become clear later, some of them still have the desired features and can be adopted directly for the discrete-time model. First, we need further notation.

Definition 3.8. *Two links $\alpha, \beta \in L$ are called adjacent if $|\alpha - \beta| = 1$. We say that a subset $\tilde{L} \subseteq L$ is contiguous if for any two links $\alpha, \beta \in \tilde{L}$ with $\alpha \leq \beta$, also all links between α and β belong to \tilde{L} (this includes the case $\tilde{L} = \emptyset$). A non-empty contiguous set of links is written as $\tilde{L} = \{\ell_{\min}, \dots, \ell_{\max}\}$.*

Whereas, according to Theorem 3.4, all recombinators act linearly on the solution of the continuous-time recombination equation, this is generally not true for the solution of the discrete-time model, though the following property still holds.

Lemma 3.9. *Let $\{c_G \mid G \subseteq L\}$ be a family of non-negative numbers with $\sum_{G \subseteq L} c_G = 1$. For an arbitrary $v \in \mathcal{P}(X)$ and for all $K \subseteq L$ with $L \setminus K$ contiguous, one has*

$$R_K \left(\sum_{G \subseteq L} c_G R_G(v) \right) = \sum_{G \subseteq L} c_G R_{G \cup K}(v).$$

Proof. When $K = \emptyset$, the claim is clear, because $R_\emptyset = \mathbb{1}$ and L itself is contiguous. Otherwise, we have $K = A \cup B$ with $A := \{\frac{1}{2}, \frac{3}{2}, \dots, \alpha\}$ and $B := \{\beta, \beta + 1, \dots, \frac{2n-1}{2}\}$ for some $\beta > \alpha$ (this includes the case $K = L$ via $\beta = \alpha + 1$). Since we work on $\mathcal{P}(X)$, we have $R_K = R_B R_A$ from Proposition 3.2. With the projection $\pi_i : \mathcal{P}(X) \rightarrow \mathcal{P}(X_i)$ onto a single site i , we obtain

$$\pi_i \left(\sum_{G \subseteq L} c_G R_G(v) \right) = \sum_{G \subseteq L} c_G \pi_i R_G(v) = \sum_{G \subseteq L} c_G \pi_i v = \pi_i v, \quad (3.23)$$

since π_i is a linear operator and $\pi_i R_G(v) = \pi_i v$ by Proposition 3.2. For the contiguous set A and $w := \sum_{G \subseteq L} c_G R_G(v)$, we obtain, with the help of (3.23) and a repeated application of Proposition 3.2,

$$\begin{aligned} R_A \left(\sum_{G \subseteq L} c_G R_G(v) \right) &= \pi_0 w \otimes \cdots \otimes \pi_{\lfloor \alpha \rfloor} w \otimes \pi_{> \alpha} w \\ &= \pi_0 v \otimes \cdots \otimes \pi_{\lfloor \alpha \rfloor} v \otimes \pi_{> \alpha} w = \sum_{G \subseteq L} c_G (\pi_0 v \otimes \cdots \otimes \pi_{\lfloor \alpha \rfloor} v \otimes \pi_{> \alpha} R_G(v)) \\ &= \sum_{G \subseteq L} c_G (\pi_0 R_G(v) \otimes \cdots \otimes \pi_{\lfloor \alpha \rfloor} R_G(v) \otimes \pi_{> \alpha} R_G(v)) = \sum_{G \subseteq L} c_G R_{A \cup G}(v). \end{aligned}$$

An analogous calculation reveals $R_B(\sum_{G \subseteq L} c_G R_{A \cup G}(v)) = \sum_{G \subseteq L} c_G R_{A \cup B \cup G}(v)$ for contiguous B . This proves the assertion. \square

Thus, only some particular recombinators act linearly on certain convex combinations, that notably include solutions of the recombination equation (3.7). We delay the intuitive explanation of Lemma 3.9 to the next section where we formally introduce the concept of segments that are produced by recombination.

3.4 Reduction to segments

In this section, we show a certain product structure of the recombinators and the LDE operators. This will turn out as the key for constructing an appropriate transformation. Recall that a crossover at link $\alpha \in L$ partitions S into $\{0, \dots, \lfloor \alpha \rfloor\}$ and $\{\lceil \alpha \rceil, \dots, n\}$ (i.e. what we were always referring to as leading and trailing segment, respectively). In general, recombination events at the links belonging to $G = \{\alpha_1, \dots, \alpha_{|G|}\} \subseteq L$, $\alpha_1 < \alpha_2 < \dots < \alpha_{|G|}$, induce the following *ordered* partition $\mathcal{S}_G = \{J_0^G, J_1^G, \dots, J_{|G|}^G\}$ of S (see Fig. 3.5):

$$J_0^G = \{0, \dots, \lfloor \alpha_1 \rfloor\}, J_1^G = \{\lceil \alpha_1 \rceil, \dots, \lfloor \alpha_2 \rfloor\}, \dots, J_{|G|}^G = \{\lceil \alpha_{|G|} \rceil, \dots, n\}. \quad (3.24)$$

Note that the partition is ordered due to the restriction to single crossovers. In connection with this, we have the tuple of links that correspond to the respective parts of the

partition \mathcal{S}_G (Fig. 3.5). Namely, for $G = \{\alpha_1, \dots, \alpha_{|G|}\} \subseteq L$, $\mathcal{L}_G := (I_0^G, I_1^G, \dots, I_{|G|}^G)$ with

$$I_0^G = \{\alpha \in L : \frac{1}{2} \leq \alpha < \alpha_1\}, \quad I_{|G|}^G = \{\alpha \in L : \alpha_{|G|} < \alpha \leq \frac{2n-1}{2}\}, \quad (3.25)$$

and $I_\ell^G = \{\alpha \in L : \alpha_\ell < \alpha < \alpha_{\ell+1}\}$ for $1 \leq \ell \leq |G| - 1$

specifies the links belonging to the respective parts of \mathcal{S}_G : the links associated with $J_k^G \in \mathcal{S}_G$, $0 \leq k \leq |G|$, are exactly those of $I_k^G \in \mathcal{L}_G$ (and vice versa).

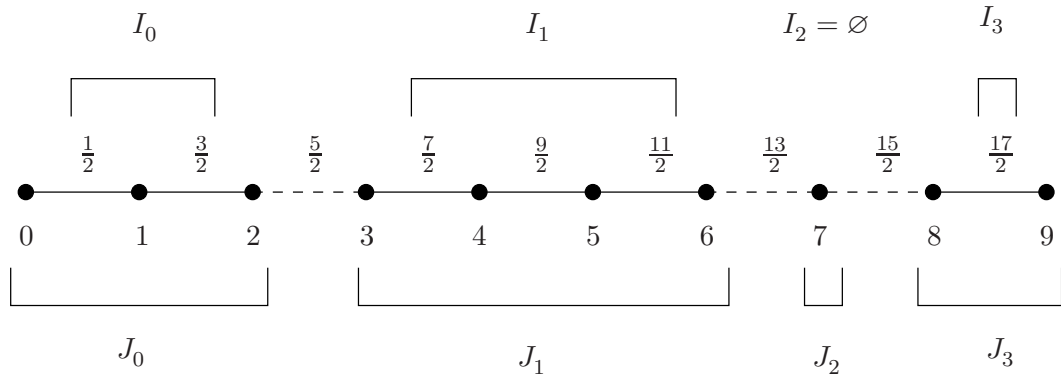


Figure 3.5: The full system with 10 sites (i.e., $S = \{0, \dots, 9\}$, $L = \{\frac{1}{2}, \dots, \frac{17}{2}\}$) cut at the links $G = \{\frac{5}{2}, \frac{13}{2}, \frac{15}{2}\}$ (broken lines). The resulting segments are characterised through $\mathcal{S}_G = \{J_0, \dots, J_3\}$ and $\mathcal{L}_G = (I_0, \dots, I_3)$ with $J_0 = \{0, 1, 2\}$, $J_1 = \{3, 4, 5, 6\}$, $J_2 = \{7\}$ and $J_3 = \{8, 9\}$ as well as $I_0 = \{\frac{1}{2}, \frac{3}{2}\}$, $I_1 = \{\frac{7}{2}, \frac{9}{2}, \frac{11}{2}\}$, $I_2 = \emptyset$ and $I_3 = \{\frac{17}{2}\}$ (the upper index G is suppressed here for clarity).

With this definition, $I_i^G = \emptyset$ is possible for each $0 \leq i \leq |G|$ and will be included (possibly multiply) in \mathcal{L}_G . Furthermore, $\mathcal{L}_\emptyset := (L)$, so that $I_0^\emptyset = L$. The upper index will be suppressed in cases where the corresponding set of links is obvious. Clearly, \mathcal{L}_G is not a partition of L , whereas \mathcal{S}_G is a partition of S . Thus, \mathcal{L}_G is a tuple and each segment is identified by a *contiguous* set of links. This way, recombination at the links in $G \subseteq L$ fragments the whole chromosome described through the sites S and the links L (what we will refer to as the ‘full system’ from now on) into several smaller *segments* that are characterised through the sites $J_k^{(G)}$ and the corresponding links $I_k^{(G)}$, $0 \leq k \leq |G|$.

Remark 3.10. *We can now interpret Lemma 3.9. Its intuitive content falls into place with the explanation of Theorem 3.7 with respect to all segments produced by R_K for $K \subseteq L$ with $L \setminus K$ contiguous. The linearity of the particular recombinators of Lemma 3.9 is due to the fact that R_K produces maximum one segment, namely the one with links $L \setminus K$ (and respective sites), that might be affected by previous recombination events. In contrast, all other segments consist of only a single site (and no link) and thus cannot bring along cuts from ‘the past’.*

We demonstrate below that it is sufficient to consider the segments produced by recombination separately, a property that reduces the problem of dealing with the re-

combination dynamics. Note first that repeated application of (3.4) and (3.5) leads to

$$\pi_{<\alpha}.R_G^{(L)}(p) = R_{G_{<\alpha}}^{(L_{<\alpha})}(\pi_{<\alpha}.p) \quad \text{and} \quad \pi_{>\alpha}.R_G^{(L)}(p) = R_{G_{>\alpha}}^{(L_{>\alpha})}(\pi_{>\alpha}.p), \quad (3.26)$$

where $R_G^{(L)}$ is our usual recombinator acting on $\mathcal{P}(X) = \mathcal{P}(X_0 \times \cdots \times X_n)$, and $R_{G_{<\alpha}}^{(L_{<\alpha})}$ denotes the respective recombinator on $\mathcal{P}(X_0 \times \cdots \times X_{[\alpha]})$, which acts on the segment specified through the sites $L_{<\alpha}$ and cuts the links $G_{<\alpha}$ (and analogously for $R_{G_{>\alpha}}^{(L_{>\alpha})}$). Likewise, recombinators $R_H^{(I)}$, $I \subseteq L$ and $H \subseteq I$, acting on any segment specified through the links I may be defined in the obvious way. For consistency, we define $R_\emptyset^{(\emptyset)} = \mathbb{1}$. From now on, the upper index specifies the corresponding segment the R_G (and, likewise, the T_G) are acting on. It will be suppressed in cases where the segment is obvious. We now explain the inherent product structure of the recombinators:

Proposition 3.11. *Let $G \subseteq L$. For each $\alpha \in G$ and $p \in \mathcal{P}(X)$, one has the identity*

$$R_G^{(L)}(p) = \left(R_{G_{<\alpha}}^{(L_{<\alpha})}(\pi_{<\alpha}.p) \right) \otimes \left(R_{G_{>\alpha}}^{(L_{>\alpha})}(\pi_{>\alpha}.p) \right).$$

Proof. For $\alpha \in G$, Proposition 3.2 implies :

$$\begin{aligned} R_G^{(L)}(p) &= R_\alpha^{(L)} \left(R_G^{(L)}(p) \right) = \left(\pi_{<\alpha}.R_G^{(L)}(p) \right) \otimes \left(\pi_{>\alpha}.R_G^{(L)}(p) \right) \\ &= \left(R_{G_{<\alpha}}^{(L_{<\alpha})}(\pi_{<\alpha}.p) \right) \otimes \left(R_{G_{>\alpha}}^{(L_{>\alpha})}(\pi_{>\alpha}.p) \right), \end{aligned}$$

where the last step follows from (3.26). □

This proposition carries over to the LDE operators:

Proposition 3.12. *On $\mathcal{P}(X)$, the LDE operators satisfy*

$$T_G^{(L)}(p) = \left(T_{G_{<\alpha}}^{(L_{<\alpha})}(\pi_{<\alpha}.p) \right) \otimes \left(T_{G_{>\alpha}}^{(L_{>\alpha})}(\pi_{>\alpha}.p) \right) \quad \text{for all } \alpha \in G,$$

where $T_{G_{<\alpha}}^{(L_{<\alpha})}$ and $T_{G_{>\alpha}}^{(L_{>\alpha})}$ now describe the operators acting on the simplices $\mathcal{P}(X_0 \times \cdots \times X_{[\alpha]})$ and $\mathcal{P}(X_{[\alpha]} \times \cdots \times X_n)$, respectively.

Proof. Let $\alpha \in G$. Using the product structure from Proposition 3.11 and splitting the sum into two disjoint parts, one obtains

$$\begin{aligned}
T_G^{(L)}(p) &= \sum_{H \supseteq G} (-1)^{|H-G|} R_H^{(L)}(p) \\
&= \sum_{H \supseteq G} (-1)^{|H-G|} \left(\left(R_{H_{<\alpha}}^{(L_{<\alpha})}(\pi_{<\alpha} p) \right) \otimes \left(R_{H_{>\alpha}}^{(L_{>\alpha})}(\pi_{>\alpha} p) \right) \right) \\
&= \sum_{L \setminus \{\alpha\} \supseteq H \supseteq G \setminus \{\alpha\}} (-1)^{|H-G \setminus \{\alpha\}|} \left(\left(R_{H_{<\alpha}}^{(L_{<\alpha})}(\pi_{<\alpha} p) \right) \otimes \left(R_{H_{>\alpha}}^{(L_{>\alpha})}(\pi_{>\alpha} p) \right) \right) \\
&= \sum_{L_{<\alpha} \supseteq H_{<\alpha} \supseteq G_{<\alpha}} (-1)^{|H_{<\alpha} - G_{<\alpha}|} \sum_{L_{>\alpha} \supseteq H_{>\alpha} \supseteq G_{>\alpha}} (-1)^{|H_{>\alpha} - G_{>\alpha}|} \\
&\quad \left(R_{H_{<\alpha}}^{(L_{<\alpha})}(\pi_{<\alpha} p) \otimes R_{H_{>\alpha}}^{(L_{>\alpha})}(\pi_{>\alpha} p) \right) \\
&= \left(\sum_{L_{<\alpha} \supseteq H_{<\alpha} \supseteq G_{<\alpha}} (-1)^{|H_{<\alpha} - G_{<\alpha}|} \left(R_{H_{<\alpha}}^{(L_{<\alpha})}(\pi_{<\alpha} p) \right) \right) \\
&\quad \otimes \left(\sum_{L_{>\alpha} \supseteq H_{>\alpha} \supseteq G_{>\alpha}} (-1)^{|H_{>\alpha} - G_{>\alpha}|} \left(R_{H_{>\alpha}}^{(L_{>\alpha})}(\pi_{>\alpha} p) \right) \right) \\
&= \left(T_{G_{<\alpha}}^{(L_{<\alpha})}(\pi_{<\alpha} p) \right) \otimes \left(T_{G_{>\alpha}}^{(L_{>\alpha})}(\pi_{>\alpha} p) \right),
\end{aligned}$$

which establishes the claim. \square

Using this argument iteratively on the respective segments, one easily obtains

$$T_G^{(L)}(p) = \left(T_{\emptyset}^{(I_0)}(\pi_{J_0} p) \right) \otimes \left(T_{\emptyset}^{(I_1)}(\pi_{J_1} p) \right) \otimes \cdots \otimes \left(T_{\emptyset}^{(I_{|G|})}(\pi_{J_{|G|}} p) \right), \quad (3.27)$$

where the upper index again specifies the corresponding segments associated with G , compare (3.25). Hence, the effect of T_G on the full system is given by that of T_{\emptyset} on the respective segments corresponding to G .

Our goal is now to study the effect of the R_G and T_G on Φ , the right-hand side of the recombination equation (3.15). This will show us in more detail when and why the LDE operators from the continuous-time model are not sufficient for solving the discrete-time model and, at the same time, will direct us to the new transformation.

If $\Phi^{(L)}$ denotes the right-hand side of the recombination equation on the full simplex $\mathcal{P}(X_0 \times \cdots \times X_n)$, then, for any contiguous $I = \{\alpha, \dots, \beta\} \subseteq L$, the right-hand side of the recombination equation on the subsimplex $\mathcal{P}(X_{[\alpha]} \times \cdots \times X_{[\beta]})$ will be denoted with $\Phi^{(I)}$. Again, we suppress the upper index when the simplex is obvious.

Proposition 3.13. *For the right-hand side of the recombination equation,*

$$\Phi^{(L)}(p) = \left(1 - \sum_{\alpha \in L} \rho_\alpha\right) p + \sum_{\alpha \in L} \rho_\alpha R_\alpha^{(L)}(p) = p + \sum_{\alpha \in L} \rho_\alpha (R_\alpha^{(L)} - \mathbb{1}^{(L)})(p),$$

one finds

$$R_\alpha^{(L)}(\Phi^{(L)}(p)) = \left(\Phi^{(L_{<\alpha})}(\pi_{<\alpha}.p)\right) \otimes \left(\Phi^{(L_{>\alpha})}(\pi_{>\alpha}.p)\right)$$

for every $\alpha \in L$ and $p \in \mathcal{P}(X)$.

Proof. Since $R_\alpha^{(L)}(\Phi^{(L)}(p)) = \left(\pi_{<\alpha}(\Phi^{(L)}(p))\right) \otimes \left(\pi_{>\alpha}(\Phi^{(L)}(p))\right)$, we obtain with the help of (3.26):

$$\begin{aligned} \pi_{<\alpha}(\Phi^{(L)}(p)) &= \pi_{<\alpha} \left(p + \sum_{\beta \in L} \rho_\beta (R_\beta^{(L)} - \mathbb{1}^{(L)})(p) \right) \\ &= \pi_{<\alpha}.p + \sum_{\beta < \alpha} \rho_\beta (R_\beta^{(L_{<\alpha})} - \mathbb{1}^{(L_{<\alpha})})(\pi_{<\alpha}.p) + \sum_{\beta \geq \alpha} \rho_\beta (R_\beta^{(L_{<\alpha})} - \mathbb{1}^{(L_{<\alpha})})(\pi_{<\alpha}.p) \\ &= \pi_{<\alpha}.p + \sum_{\beta < \alpha} \rho_\beta (R_\beta^{(L_{<\alpha})} - \mathbb{1}^{(L_{<\alpha})})(\pi_{<\alpha}.p) = \Phi^{(L_{<\alpha})}(\pi_{<\alpha}.p). \end{aligned}$$

Analogously, one obtains $\pi_{>\alpha}(\Phi^{(L)}(p)) = \Phi^{(L_{>\alpha})}(\pi_{>\alpha}.p)$, and the assertion follows. \square

More generally, this theorem implies inductively that

$$R_G^{(L)}(\Phi^{(L)}(p)) = \left(\Phi^{(I_0)}(\pi_{J_0}.p)\right) \otimes \left(\Phi^{(I_1)}(\pi_{J_1}.p)\right) \otimes \cdots \otimes \left(\Phi^{(I_{|G|})}(\pi_{J_{|G|}}.p)\right). \quad (3.28)$$

Finally, for the interaction between the $T_G^{(L)}$ and $\Phi^{(L)}$, we have the following result.

Proposition 3.14. *For the LDE operators (3.11) and all $G \subseteq L$, one has*

$$T_G^{(L)}(\Phi^{(L)}(p)) = \left(T_\emptyset^{(I_0)}(\Phi^{(I_0)}(\pi_{J_0}.p))\right) \otimes \cdots \otimes \left(T_\emptyset^{(I_{|G|})}(\Phi^{(I_{|G|})}(\pi_{J_{|G|}}.p))\right),$$

with J_i and I_i , $i = 0, \dots, |G|$, according to (3.24) and (3.25).

Proof. Using (3.28) and (3.27), one calculates

$$\begin{aligned} T_G^{(L)}(\Phi^{(L)}(p)) &= T_G^{(L)} \left(R_G^{(L)}(\Phi^{(L)}(p)) \right) = T_G^{(L)} \left(\left(\Phi^{(I_0)}(\pi_{J_0}.p)\right) \otimes \cdots \otimes \left(\Phi^{(I_{|G|})}(\pi_{J_{|G|}}.p)\right) \right) \\ &= \left(T_\emptyset^{(I_0)}(\Phi^{(I_0)}(\pi_{J_0}.p))\right) \otimes \cdots \otimes \left(T_\emptyset^{(I_{|G|})}(\Phi^{(I_{|G|})}(\pi_{J_{|G|}}.p))\right), \end{aligned}$$

which establishes the formula. \square

This result is of particular significance since it shows that, to determine the effect of the $T_G^{(L)}$ on Φ , it is sufficient to know the action of the T_\emptyset on the segments that correspond to G . Hence, we now need to determine $T_\emptyset \circ \Phi$. It will turn out that this relies crucially on the commutators of R_G with Φ , which will be the subject of the next section.

3.5 The commutator and linearisation

The more algebraic approach of [4], which was later generalised by Popa [55], suggests to further analyse the problem in terms of commuting versus non-commuting quantities. For $G \subseteq L$, the *commutator* is defined as

$$[R_G, \Phi] := R_G \circ \Phi - \Phi \circ R_G.$$

Recall that, in the continuous-time model, the linear action of the recombinators on the solution of the differential equations entails that the corresponding forward flow commutes with each recombinator (see Corollary 3.5). But this no longer holds for discrete time: $[R_G, \Phi] = 0$ is not true in general. We are interested in the commutators because — as we will see in a moment — they lead us to the evaluation of $T_\emptyset \circ \Phi$, and this in turn gives $T_G \circ \Phi$ (see Proposition 3.14).

Proposition 3.15. *On $\mathcal{P}(X)$, one has*

$$T_\emptyset \circ \Phi = \left(1 - \sum_{\alpha \in L} \rho_\alpha\right) T_\emptyset + \sum_{G \subseteq L} (-1)^{|G|} [R_G, \Phi].$$

Proof. Expressing the left-hand side as

$$T_\emptyset \circ \Phi = \sum_{G \subseteq L} (-1)^{|G|} (R_G \circ \Phi) = \sum_{G \subseteq L} (-1)^{|G|} (\Phi \circ R_G) + \sum_{G \subseteq L} (-1)^{|G|} [R_G, \Phi],$$

and using $\Phi = (1 - \sum_{\alpha \in L} \rho_\alpha) \mathbb{1} + \sum_{\alpha \in L} \rho_\alpha R_\alpha$, one calculates

$$\begin{aligned} \sum_{G \subseteq L} (-1)^{|G|} (\Phi \circ R_G) &= \sum_{\alpha \in L} \left(\sum_{G \subseteq L} (-1)^{|G|} \rho_\alpha R_\alpha R_G \right) + (1 - \sum_{\alpha \in L} \rho_\alpha) \sum_{G \subseteq L} (-1)^{|G|} R_G \\ &= (1 - \sum_{\alpha \in L} \rho_\alpha) T_\emptyset + \sum_{\alpha \in L} \sum_{\substack{G \subseteq L \\ \alpha \notin G}} \left((-1)^{|G|} \rho_\alpha R_\alpha R_G + (-1)^{|G \cup \{\alpha\}|} \rho_\alpha R_{G \cup \{\alpha\}} \right) \\ &= (1 - \sum_{\alpha \in L} \rho_\alpha) T_\emptyset + \sum_{\alpha \in L} \left(\sum_{\substack{G \subseteq L \\ \alpha \notin G}} (-1)^{|G|} \rho_\alpha (R_\alpha R_G - R_{G \cup \{\alpha\}}) \right) \\ &= (1 - \sum_{\alpha \in L} \rho_\alpha) T_\emptyset, \end{aligned}$$

which shows the claim. □

Proposition 3.15 shows that T_\emptyset only yields a diagonal component if *all* recombinators commute with Φ . We now need to determine the commutator $[R_G, \Phi]$. To this end, it is advantageous to introduce a new set of operators.

Definition 3.16. For $G \subseteq K \subseteq L$, we define the operators

$$\tilde{T}_{G,K} := \sum_{G \subseteq H \subseteq K} (-1)^{|H-G|} R_H. \quad (3.29)$$

Equivalently, for any $M \subseteq L \setminus G$, this means that

$$\tilde{T}_{G,G \dot{\cup} M} = \sum_{G \subseteq H \subseteq G \dot{\cup} M} (-1)^{|H-G|} R_H = \sum_{K \subseteq M} (-1)^{|K|} R_{G \dot{\cup} K}.$$

These operators act on the full simplex and can be interpreted in analogy to the original LDE operators (3.11), where the links in the complement of $G \dot{\cup} M$ (the disjoint union of G and M) are regarded as inseparable. If necessary, we will specify the system the operators are acting on by an upper index as before.

Lemma 3.17. On $\mathcal{P}(X)$, the operators (3.29) satisfy

$$\tilde{T}_{G,G} = R_G \quad \text{and} \quad \tilde{T}_{G,L} = T_G.$$

They have a product structure,

$$\tilde{T}_{G,G \dot{\cup} H}^{(L)}(p) = \left(\tilde{T}_{\emptyset, H \cap I_0^G}^{(I_0^G)}(\pi_{J_0^G}.p) \right) \otimes \left(\tilde{T}_{\emptyset, H \cap I_1^G}^{(I_1^G)}(\pi_{J_1^G}.p) \right) \otimes \cdots \otimes \left(\tilde{T}_{\emptyset, H \cap I_{|G|}^G}^{(I_{|G|}^G)}(\pi_{J_{|G|}^G}.p) \right), \quad (3.30)$$

for all $H \subseteq L \setminus G$. Moreover, one has

$$\tilde{T}_{G,G \dot{\cup} M} = \sum_{G \subseteq H \subseteq L \setminus M} T_H = \sum_{K \subseteq L \setminus (M \cup G)} T_{G \dot{\cup} K} \quad (3.31)$$

for all $G, M \subseteq L$ with $G \cap M = \emptyset$. Consequently, Möbius inversion returns T_G as

$$T_G = \sum_{G \subseteq H \subseteq L \setminus M} (-1)^{|H-G|} \tilde{T}_{H,H \dot{\cup} M}. \quad (3.32)$$

Proof. The first assertion is obvious; the second is analogous to (3.27) and follows along the same lines. Relation (3.31) is true since

$$\begin{aligned} \tilde{T}_{G,G \dot{\cup} M} &= \sum_{K \subseteq M} (-1)^{|K|} R_{G \dot{\cup} K} = \sum_{K \subseteq M} (-1)^{|K|} \sum_{H \supseteq G \dot{\cup} K} T_H = \sum_{H \supseteq G} \sum_{\substack{K \subseteq M \\ K \subseteq H}} (-1)^{|K|} T_H \\ &= \sum_{H \supseteq G} T_H \sum_{K \subseteq M \cap H} (-1)^{|K|} = \sum_{H \supseteq G} \delta_{M \cap H, \emptyset} T_H = \sum_{G \subseteq H \subseteq L \setminus M} T_H. \end{aligned}$$

In the second-last step, we used that, if H is a finite set, one has

$$\sum_{G \subseteq H} (-1)^{|G|} = \delta_{H, \emptyset}, \quad (3.33)$$

which is the key property of the Möbius function of ordered partitions [1]. \square

$$\frac{I_0^H}{\alpha_1} \mid \frac{I_1^H}{\alpha_2} \mid \frac{I_2^H}{\alpha_3} \mid \frac{I_3^H}{\alpha_4} \mid \frac{I_4^H}{\alpha_4}$$

Figure 3.6: Illustration of the segments, indicated here by their corresponding links, that evolve due to recombination at the links of $H = \{\alpha_1, \alpha_2, \alpha_3, \alpha_4\}$. In particular, the property of Lemma 3.19(4) should become obvious here: whether a set $G \subseteq L$ separates H is independent of its intersection with the first as well as the last segment I_0^H and $I_{|H|}^H$, respectively.

Before we turn to the commutator, we introduce a new function, the *separation function*, which will allow for a clear and compact notation.

Definition 3.18. For $G, H \subseteq L$ with $G \cap H = \emptyset$, we say that G separates H if, for all $\alpha, \beta \in H$ with $\alpha < \beta$, there is a $\gamma \in G$ with $\alpha < \gamma < \beta$. Hence, we define the separation function as

$$\text{sep}(G, H) = \begin{cases} 1, & \text{if } G \text{ separates } H, \\ 0, & \text{otherwise.} \end{cases}$$

In the particular cases $H = \emptyset$ and $H = \{\alpha\}$, $\alpha \in L$, we define $\text{sep}(G, H) = 1$ for all $G \subseteq L$, and it is understood that $\text{sep}(G, H) = 0$ whenever $G \cap H \neq \emptyset$.

First, let us summarise some elementary properties of the separation function.

Lemma 3.19. The separation function $\text{sep}(G, H)$ with $H \subseteq L \setminus G$ has the following properties:

1. $\text{sep}(G, H) = 0$, if H contains any adjacent links;
2. $\text{sep}(G, H) = 0$ implies $\text{sep}(G', H) = 0$ for all $G' \subseteq G$;
3. $\text{sep}(G, H) = 0$ whenever $L \setminus G$ is contiguous with $H \subseteq L \setminus G$ and $|H| \geq 2$;
4. $\text{sep}(G, H) = 1$ implies $I_i^H \cap G \neq \emptyset$ for all $i \in \{1, \dots, |H| - 1\}$. □

These four properties of the separation function can be easily figured out, compare also the illustration in Figure 3.6. Particularly note that Lemma 3.19(4) implies that $I_0^H \cap G = \emptyset$ and $I_{|H|}^H \cap G = \emptyset$ are possible for sets G that separate H , thus, these two segments differ crucially from the other segments that correspond to H .

Later, we need the following summation formula for the separation function.

Lemma 3.20. Let $H, K \subseteq L$ with $H \neq \emptyset$, $H \cap K = \emptyset$, and I_i^H defined as in (3.25). Then

$$\sum_{G \subseteq K} (-1)^{|G|} \text{sep}(G, H) = \text{sep}(K, H) (-1)^{|H|-1} \delta_{K \cap I_0^H, \emptyset} \delta_{K \cap I_{|H|}^H, \emptyset}.$$

Proof. For $\text{sep}(K, H) = 0$, the claim is clear by Lemma 3.19(2). We now define $A_i := K \cap I_i^H$ for all $i \in \{0, \dots, |H|\}$. Then, for $\text{sep}(K, H) = 1$, it follows from Lemma 3.19(4) that $A_j \neq \emptyset$ for all $1 \leq j \leq |H| - 1$. Likewise, since $G \subseteq K$, $\text{sep}(G, H) = 1$ if and only if $G \cap I_j^H \neq \emptyset$ for all $1 \leq j \leq |H| - 1$, with no condition emerging for $G \cap I_0^H$ or $G \cap I_{|H|}^H$. This gives

$$\sum_{G \subseteq K} (-1)^{|G|} \text{sep}(G, H) = \sum_{B_0 \subseteq A_0} (-1)^{|B_0|} \prod_{i=1}^{|H|-1} \left(\sum_{\substack{B_i \subseteq A_i \\ B_i \neq \emptyset}} (-1)^{|B_i|} \right) \sum_{B_{|H|} \subseteq A_{|H|}} (-1)^{|B_{|H|}|} = \prod_{j=0}^{|H|} F_j.$$

Here, for $j = 0$ and $j = |H|$, the factors F_j are given by $F_j := \sum_{B_j \subseteq A_j} (-1)^{|B_j|} = \delta_{A_j, \emptyset}$, where we have used (3.33). For $1 \leq j \leq |H| - 1$,

$$F_j := \sum_{\substack{B_j \subseteq A_j \\ B_j \neq \emptyset}} (-1)^{|B_j|} = -1 + \sum_{B_j \subseteq A_j} (-1)^{|B_j|} = -1 + \delta_{A_j, \emptyset} = -1,$$

where we have again used (3.33) in the second-last step, and $A_j \neq \emptyset$ in the last. \square

With this notation, let us take a closer look at $R_G^{(L)}(\Phi^{(L)}(p))$ for $G \subseteq L$. Evaluating (3.28) explicitly, using Definition 3.16, expanding and using the product structure (3.30) backwards gives

$$\begin{aligned} R_G^{(L)}(\Phi^{(L)}(p)) &= \left(\pi_{J_0} \cdot p + \sum_{\alpha_0 \in I_0} \rho_{\alpha_0} (R_{\alpha_0}^{(I_0)} - \mathbb{1}^{(I_0)}) (\pi_{J_0} \cdot p) \right) \otimes \cdots \otimes \\ &\quad \left(\pi_{J_{|G|}} \cdot p + \sum_{\alpha_{|G|} \in I_{|G|}} \rho_{\alpha_{|G|}} (R_{\alpha_{|G|}}^{(I_{|G|})} - \mathbb{1}^{(I_{|G|})}) (\pi_{J_{|G|}} \cdot p) \right) \\ &= \left(\mathbb{1}^{(I_0)} - \sum_{\alpha_0 \in I_0} \rho_{\alpha_0} \tilde{T}_{\emptyset, \alpha_0}^{(I_0)} \right) (\pi_{J_0} \cdot p) \otimes \cdots \otimes \left(\mathbb{1}^{(I_{|G|})} - \sum_{\alpha_{|G|} \in I_{|G|}} \rho_{\alpha_{|G|}} \tilde{T}_{\emptyset, \alpha_{|G|}}^{(I_{|G|})} \right) (\pi_{J_{|G|}} \cdot p) \\ &= \sum_{H \subseteq L \setminus G} (-1)^{|H|} \text{sep}(G, H) \rho_H \tilde{T}_{G, G \cup H}^{(L)}(p), \end{aligned}$$

where, in the last step, we have further set $\rho_H = \prod_{\alpha \in H} \rho_\alpha$ for all $H \subseteq L$ (in particular, $\rho_\emptyset = 1$) and used Lemma 3.19(4); note that the separation function is basically used as an indicator variable here. On the other hand, we obtain

$$\begin{aligned} \Phi \circ R_G &= \sum_{\alpha \in L \setminus G} \rho_\alpha R_\alpha R_G + \left(1 - \sum_{\alpha \in L \setminus G} \rho_\alpha \right) R_G = \tilde{T}_{G, G} - \sum_{\alpha \in L \setminus G} \rho_\alpha \tilde{T}_{G, G \cup \{\alpha\}} \\ &= \text{sep}(G, \emptyset) \tilde{T}_{G, G} - \sum_{\alpha \in L \setminus G} \text{sep}(G, \{\alpha\}) \rho_\alpha \tilde{T}_{G, G \cup \{\alpha\}}, \end{aligned}$$

which finally yields the commutator.

Theorem 3.21. *For all $G \subseteq L$, the commutator on $\mathcal{P}(X)$ is given by*

$$[R_G, \Phi] = \sum_{\substack{H \subseteq L \setminus G \\ |H| \geq 2}} (-1)^{|H|} \text{sep}(G, H) \rho_H \tilde{T}_{G, G \cup H}.$$

□

Please note that, by the properties of the separation function, many of the summands vanish. In particular, $[R_G, \Phi] = 0$ whenever $|L \setminus G| \leq 1$.

Corollary 3.22. *$[R_G, \Phi] = 0$ if $L \setminus G$ is contiguous.*

Proof. By Theorem 3.21, only terms with $|H| \geq 2$ need to be considered. For these, Lemma 3.19(3) tells us that $\text{sep}(G, H) = 0$ if $L \setminus G$ is contiguous and $H \subseteq L \setminus G$. Hence, $[R_G, \Phi] = 0$. □

Let us note in passing that the converse direction of Corollary 3.22 may fail if the site spaces are sufficiently trivial. Nevertheless, in the generic case, $[R_G, \Phi] = 0$ implies $\text{sep}(G, H) = 0$ for all $H \subseteq L \setminus G$ with $|H| \geq 2$, because the relevant terms then cannot cancel each other. We omit a more precise discussion of this point, because we do not need it later on.

Recalling that Φ^t is the discrete-time analogue of φ_t , we can consider Corollary 3.22 as what is left of Corollary 3.5 in discrete time. Hence, it becomes clear why the LDE operators (3.11) from the continuous-time model do not suffice to linearise *and* decouple the discrete-time dynamics.

We still aim at determining $T_\varnothing \circ \Phi$ according to Proposition 3.15. In doing so, we need to express the commutator $[R_G, \Phi]$ in terms of the T_G (which are related to the $\tilde{T}_{G, G \cup M}$ via (3.31)). This, and the consequences for general $T_G \circ \Phi$, $G \subseteq L$, are captured in the following theorem.

Theorem 3.23. *On $\mathcal{P}(X)$, the operators $T_G = T_G^{(L)}$ and $\Phi = \Phi^{(L)}$ satisfy*

$$T_G^{(L)} \circ \Phi^{(L)} = \sum_{K \supseteq G} z^{(L)}(G, K) T_K^{(L)} \quad (3.34)$$

for all $G \subseteq L$. The coefficients $z^{(L)}(\varnothing, K)$, $K \subseteq L$, are given by

$$z^{(L)}(\varnothing, \varnothing) = 1 - \sum_{\alpha \in L} \rho_\alpha \quad (3.35)$$

and, for $K \neq \varnothing$, by

$$z^{(L)}(\varnothing, K) = - \sum_{H \subseteq L \setminus K} \rho_H \text{sep}(K, H) (1 - \delta_{H \cap I_0^K, \varnothing}) (1 - \delta_{H \cap I_{|K|}^K, \varnothing}). \quad (3.36)$$

For $K \supseteq G \neq \varnothing$, the coefficients are recursively determined by

$$z^{(L)}(G, K) = z^{(I_0^G)}(\varnothing, K \cap I_0^G) \cdots z^{(I_{|G|}^G)}(\varnothing, K \cap I_{|G|}^G). \quad (3.37)$$

Proof. Let us first prove the case $G = \emptyset$. According to Proposition 3.15, we have $(1 - \sum_{\alpha \in L} \rho_\alpha) T_\emptyset \circ \Phi = T_\emptyset + \sum_{G' \subseteq L} (-1)^{|G'|} [R_{G'}, \Phi]$, where $(1 - \sum_{\alpha \in L} \rho_\alpha) = z^{(L)}(\emptyset, \emptyset)$ by definition. Let us thus evaluate the last term. In the first step, we insert the commutator from Theorem 3.21; we then use relation (3.31) and change the order of summation to arrive at

$$\begin{aligned} \sum_{G' \subseteq L} (-1)^{|G'|} [R_{G'}, \Phi] &= \sum_{G' \subseteq L} (-1)^{|G'|} \sum_{\substack{H \subseteq L \setminus G' \\ |H| \geq 2}} (-1)^{|H|} \text{sep}(G', H) \rho_H \tilde{T}_{G', G' \cup H} \\ &= \sum_{G' \subseteq L} (-1)^{|G'|} \sum_{\substack{H \subseteq L \setminus G' \\ |H| \geq 2}} (-1)^{|H|} \text{sep}(G', H) \rho_H \sum_{G' \subseteq K \subseteq L \setminus H} T_K \\ &= \sum_{K \subseteq L} T_K \sum_{\substack{H \subseteq L \setminus K \\ |H| \geq 2}} (-1)^{|H|} \rho_H \sum_{G' \subseteq K} (-1)^{|G'|} \text{sep}(G', H), \end{aligned} \quad (3.38)$$

which does not contain any term with T_\emptyset . We can now compare coefficients for T_K . Note first that, by (3.38), we only need to consider sets $H \subseteq L \setminus K$, that is, $H \cap K = \emptyset$. In this case, $\delta_{K \cap I_0^H, \emptyset} = 1 - \delta_{H \cap I_0^K, \emptyset}$ and $\delta_{K \cap I_{|H|}^H, \emptyset} = 1 - \delta_{H \cap I_{|K|}^K, \emptyset}$. This is true since $K \cap I_0^H = \emptyset$ ($\neq \emptyset$) implies that the smallest element in H is smaller (larger) than the smallest element in K , thus $H \cap I_0^K \neq \emptyset$ ($= \emptyset$) (and vice versa for $K \cap I_{|H|}^H$). Taking this together with Lemma 3.20, the coefficient of T_K in (3.38) turns into

$$\begin{aligned} \sum_{\substack{H \subseteq L \setminus K \\ |H| \geq 2}} (-1)^{|H|} \rho_H \sum_{G' \subseteq K} (-1)^{|G'|} \text{sep}(G', H) \\ &= - \sum_{\substack{H \subseteq L \setminus K \\ |H| \geq 2}} \rho_H \text{sep}(K, H) (1 - \delta_{H \cap I_0^K, \emptyset}) (1 - \delta_{H \cap I_{|K|}^K, \emptyset}) \\ &= - \sum_{H \subseteq L \setminus K} \rho_H \text{sep}(K, H) (1 - \delta_{H \cap I_0^K, \emptyset}) (1 - \delta_{H \cap I_{|K|}^K, \emptyset}). \end{aligned}$$

Note that, in the last step, the restriction on $|H|$ may be dropped since it is already implied by the factors involving the δ -functions (in case $|H| \leq 1$, at least one of the intersections $H \cap I_0^K$ and $H \cap I_{|K|}^K$ is empty). This proves the claim for $G = \emptyset$. For the case $G \neq \emptyset$, we follow Proposition 3.14 and write, for $p \in \mathcal{P}(X)$,

$$T_G^{(L)}(\Phi^{(L)}(p)) = \left(T_\emptyset^{(I_0)}(\Phi^{(I_0)}(\pi_{J_0}.p)) \right) \otimes \left(T_\emptyset^{(I_1)}(\Phi^{(I_1)}(\pi_{J_1}.p)) \right) \otimes \cdots \otimes \left(T_\emptyset^{(I_{|G|})}(\Phi^{(I_{|G|})}(\pi_{J_{|G|}}.p)) \right).$$

Applying the above result for $G = \emptyset$ to each factor, and using the product structure of Proposition 3.14 backwards, establishes the claim. \square

Corollary 3.24. *The coefficients $z(\emptyset, K)$ with $K \neq \emptyset$ can be expressed explicitly as*

$$z^{(L)}(\emptyset, K) = - \sum_{\alpha_0 \in I_0^K} \rho_{\alpha_0} \left(\prod_{i=1}^{|K|-1} (1 + \sum_{\alpha_i \in I_i^K} \rho_{\alpha_i}) \right) \sum_{\alpha_{|K|} \in I_{|K|}^K} \rho_{\alpha_{|K|}}. \quad (3.39)$$

Proof. Let us consider those H whose contribution to the sum in (3.36) is not annihilated by the separation function or the δ -functions. For $\text{sep}(K, H) = 1$ to hold, each $\alpha \in H$ must belong to a different $I_i^K \in \mathcal{L}_K$. Furthermore, H must contain one element each from I_0^K and $I_{|K|}^K$ (α_0 and $\alpha_{|K|}$, respectively) to keep the factors involving the δ -functions from vanishing. Thus, the sum in (3.36) may be factorised as claimed. \square

In particular, (3.39) entails

$$z^{(L)}(\emptyset, K) = 0 \quad \text{if } K \cap \left\{ \frac{1}{2}, \frac{2n-1}{2} \right\} \neq \emptyset. \quad (3.40)$$

Taking this together with (3.35), one obtains $z^{(L)}(\emptyset, K) = (1 - \sum_{\alpha \in L} \rho_{\alpha}) \delta_{K, \emptyset}$ for $K \subseteq L$ whenever $|L| \leq 2$, and hence, in these cases, $T_{\emptyset}^{(L)} \circ \Phi^{(L)} = (1 - \sum_{\alpha \in L} \rho_{\alpha}) T_{\emptyset}^{(L)}$ is already a diagonal component in line with the observation in Section 4. Furthermore, (3.37) from Theorem 3.23 and (3.40) entail that

$$z^{(L)}(G, K) = 0 \quad \text{whenever } K \cap \left(\bigcup_{0 \leq i \leq |G|} \{\min(I_i^G), \max(I_i^G)\} \right) \neq \emptyset. \quad (3.41)$$

Theorem 3.23 reveals the linear structure inherent in the action of T_G on Φ . In fact, the structure is even triangular (with respect to the partial ordering \subseteq) since $T_G^{(L)} \circ \Phi^{(L)}$ is a linear combination of the $T_K^{(L)}$, $K \supseteq G$. Thus, diagonalisation will boil down to recursive elimination. As a preparation, we make the following observation.

Corollary 3.25. *If $L \neq \emptyset$, one has the relation $z^{(L)}(G, L) = 0$ for all $\emptyset \subseteq G \subsetneq L$. Furthermore, $z^{(L)}(L, L) = 1$.*

Proof. When $\emptyset \subseteq G \subsetneq L$, the intersection in (3.41), with $K = L$, can never be empty, so that $z^{(L)}(G, L) = 0$ follows. If $G = L$, the property follows directly from (3.35) together with (3.37). \square

3.6 Diagonalisation

Motivated by the triangular structure of (3.34), we make the ansatz to define new operators U_G , $G \subseteq L$, as the following linear combination of the well-known T_G :

$$U_G = \sum_{H \supseteq G} c(G, H) T_H, \quad (3.42)$$

where the coefficients $c(G, H)$ are to be determined in such a way that they transform the recombination equation into a decoupled diagonal system, more precisely so that

$$U_G \circ \Phi = \lambda_G U_G, \quad G \subseteq L, \quad (3.43)$$

with eigenvalues λ_G that are still unknown as well. An example for this transformation can be found in Example 3.31. Note first that, with the help of (3.34), equations (3.42) and (3.43) may be rewritten as

$$\begin{aligned} U_G \circ \Phi &= c(G, G) (T_G \circ \Phi) + \sum_{N \supseteq G} c(G, N) (T_N \circ \Phi) \\ &= c(G, G) \left(z^{(L)}(G, G) T_G + \sum_{K \supseteq G} z^{(L)}(G, K) T_K \right) \\ &\quad + \sum_{N \supseteq G} c(G, N) \left(z^{(L)}(N, N) T_N + \sum_{M \supseteq N} z^{(L)}(N, M) T_M \right) \\ &\stackrel{!}{=} \lambda_G \left(c(G, G) T_G + \sum_{N \supseteq G} c(G, N) T_N \right) = \lambda_G U_G. \end{aligned} \quad (3.44)$$

Obviously, there is some freedom in the choice of the $c(G, G)$; we set $c(G, G) = 1$ for all $G \subseteq L$ (and we will see shortly that this is consistent). Equation (3.44) has the structure of an eigenvalue problem of a triangular matrix with coefficients $z^{(L)}(G, H)$, where the role of the unit vectors is taken by the T_H , and the $c(G, H)$, $H \supseteq G$, take the roles of the components of the eigenvector corresponding to λ_G (note that, by considering $c(G, H)$ for $H \supseteq G$ only, we have already exploited the triangular structure). Recall next that the eigenvalues of a triangular matrix are given by its diagonal entries, which are

$$\lambda_G = z^{(L)}(G, G) = \prod_{i=0}^{|G|} z^{(I_i^G)}(\emptyset, \emptyset) = \prod_{i=0}^{|G|} \left(1 - \sum_{\alpha_i \in I_i^G} \rho_{\alpha_i} \right) \quad (3.45)$$

by Theorem 3.23. In particular, $\lambda_\emptyset = z^{(L)}(\emptyset, \emptyset) = 1 - \sum_{\alpha \in L} \rho_\alpha \geq 0$. Indeed, the λ_G have already been identified by Bennett [7], Lyubich [48] and Dawson [14, 15] as the generalised eigenvalues of the linearised deterministic dynamics. We keep an interpretation of these coefficients and more about their important role in connection with the solution of the recombination model for Chapter 4. Let us first note the following:

Lemma 3.26. *For all $G, H \subseteq L$ with $G \subsetneq H$, one has $\lambda_G < \lambda_H$.*

Proof. Let $\emptyset \subsetneq G \subsetneq L$. Then, for $H = G \dot{\cup} \{\beta\}$, with $\beta \in I_i^G$ for an arbitrary $i \in \{0, \dots, |G|\}$, we see from (3.45) that $z^{(L)}(H, H) = \lambda_H$ and hence obtain

$$\begin{aligned} \lambda_H &= \left(\prod_{j=0}^{i-1} \left(1 - \sum_{\alpha_j \in I_j^G} \rho_{\alpha_j} \right) \right) \left(1 - \sum_{\substack{\alpha_i \in I_i^G \\ \alpha_i < \beta}} \rho_{\alpha_i} \right) \left(1 - \sum_{\substack{\alpha_i \in I_i^G \\ \alpha_i > \beta}} \rho_{\alpha_i} \right) \left(\prod_{j=i+1}^{|G|} \left(1 - \sum_{\alpha_j \in I_j^G} \rho_{\alpha_j} \right) \right) \\ &= \lambda_G \frac{\left(1 - \sum_{\substack{\alpha_i \in I_i^G \\ \alpha_i < \beta}} \rho_{\alpha_i} \right) \left(1 - \sum_{\substack{\alpha_i \in I_i^G \\ \alpha_i > \beta}} \rho_{\alpha_i} \right)}{\left(1 - \sum_{\alpha_i \in I_i^G} \rho_{\alpha_i} \right)} > \lambda_G, \end{aligned}$$

because all ρ_α are positive, as are all three terms in parentheses of the fraction, and $\rho_\beta > 0$ by assumption. Finally, the argument also works for $\lambda_\emptyset = 1 - \sum_{\alpha \in L} \rho_\alpha$, provided $1 - \sum_{\alpha \in L} \rho_\alpha > 0$. Since $\lambda_G > 0$ for all $G \neq \emptyset$, the claim trivially also holds for $1 - \sum_{\alpha \in L} \rho_\alpha = 0$. The assertion then follows inductively for any $H \supsetneq G$. \square

The coefficients $c(G, H)$ can now be calculated recursively as follows.

Theorem 3.27. *The coefficients $c(G, H)$ of (3.42) are determined by $c(G, G) = 1$ and*

$$c(G, H) = \frac{\sum_{H \supsetneq K \supsetneq G} c(G, K) z^{(L)}(K, H)}{\lambda_G - \lambda_H} \quad (3.46)$$

for $H \supsetneq G$. The coefficients of the inverse transformation of (3.42),

$$T_G = \sum_{H \supsetneq G} c^*(G, H) U_H, \quad \text{with } G \subseteq L, \quad (3.47)$$

are determined by

$$c^*(G, K) = - \sum_{K \supsetneq H \supsetneq G} c^*(G, H) c(H, K), \quad (3.48)$$

for $K \supsetneq G$ together with $c^*(G, G) = 1$.

Proof. Considering (3.44) with $c(G, G) = 1$, comparing coefficients for T_H , $H \supsetneq G$, and observing (3.45), one obtains

$$z^{(L)}(G, H) + c(G, H) \lambda_H + \sum_{H \supsetneq K \supsetneq G} c(G, K) z^{(L)}(K, H) \stackrel{!}{=} \lambda_G c(G, H),$$

and the recursion for $c(G, H)$ follows. It is always well-defined for all $H \supsetneq G$, since $\lambda_G < \lambda_H$ by Lemma 3.26. The recursion for the coefficients of the inverse transformation follows directly from

$$\begin{aligned} T_G &= \sum_{H \supsetneq G} c^*(G, H) U_H = \sum_{H \supsetneq G} c^*(G, H) \sum_{K \supsetneq H} c(H, K) T_K \\ &= \sum_{K \supsetneq G} T_K \sum_{K \supsetneq H \supsetneq G} c^*(G, H) c(H, K), \end{aligned}$$

which enforces $\sum_{K \supsetneq H \supsetneq G} c^*(G, H) c(H, K) = \delta_{K, G}$, as the T_K are distinct. \square

We now identify those T_G that already give diagonal components of the discrete-time system:

Theorem 3.28. *For all $G \subseteq L$ that satisfy $|I_i^G| \leq 2$ for all $i \in \{0, \dots, |G|\}$, one has*

$$T_G(\Phi(p)) = \lambda_G T_G(p)$$

for $p \in \mathcal{P}(X)$.

Proof. In this case, we have (3.41) for all $K \supseteq G$, hence $z(G, K) = \lambda_G \delta_{K,G}$, from which the assertion follows via Theorem 3.23. \square

Note that $|I_i^G| \leq 2$ for all $I_i^G \in \mathcal{L}_G$ simply implies that each segment consists of at most three sites, hence all segments can be reduced to the simple cases considered in Section 3.3. Then, for such G , $c(G, H) = c^*(G, H) = \delta_{G,H}$ for all $H \supseteq G$.

Remark 3.29. *With Theorem 3.28, one particularly finds for $p \in \mathcal{P}(X)$:*

$$\begin{aligned} T_L(\Phi(p)) &= T_L(p) \\ T_{L \setminus \{\alpha\}}(\Phi(p)) &= (1 - \rho_\alpha) T_{L \setminus \{\alpha\}}(p) \quad \text{for all } \alpha \in L. \\ T_{L \setminus \{\alpha, \beta\}}(\Phi(p)) &= \begin{cases} (1 - \rho_\alpha - \rho_\beta) T_{L \setminus \{\alpha, \beta\}}(p) & \text{for } \alpha, \beta \in L \text{ adjacent.} \\ (1 - \rho_\alpha)(1 - \rho_\beta) T_{L \setminus \{\alpha, \beta\}}(p) & \text{for } \alpha, \beta \in L \text{ not adjacent.} \end{cases} \end{aligned}$$

With the help of this transformation, we can finally specify the solution p_t of the recombination equation in terms of the initial condition p_0 . To this end, we first use the transformation (3.12) from the recombinators to the T_G operators, and then relation (3.47) to arrive at the U_H operators, which finally diagonalise the system according to (3.43). Finally, we use the appropriate inversions to return to the recombinators:

$$\begin{aligned} p_t &= \Phi^t(p_0) = R_\emptyset(\Phi^t(p_0)) = \sum_{G \subseteq L} T_G(\Phi^t(p_0)) = \sum_{G \subseteq L} \sum_{H \supseteq G} c^*(G, H) U_H(\Phi^t(p_0)) \\ &= \sum_{G \subseteq L} \sum_{H \supseteq G} c^*(G, H) \lambda_H^t U_H(p_0) = \sum_{G \subseteq L} \sum_{H \supseteq G} c^*(G, H) \lambda_H^t \sum_{M \supseteq H} c(H, M) T_M(p_0) \\ &= \sum_{G \subseteq L} \sum_{H \supseteq G} c^*(G, H) \lambda_H^t \sum_{M \supseteq H} c(H, M) \sum_{T \supseteq M} (-1)^{|T-M|} R_T(p_0). \end{aligned} \tag{3.49}$$

The coefficient functions can now be extracted as follows.

Theorem 3.30. *The coefficient functions $a_G(t)$ of the solution (3.15) of the recombination equation in discrete time may be expressed as*

$$a_G(t) = \sum_{M \subseteq G} (-1)^{|G-M|} \sum_{H \subseteq M} \sum_{K \subseteq H} c(H, M) \lambda_H^t c^*(K, H) \tag{3.50}$$

for all $G \subseteq L$. Here, $c(H, M)$ and $c^*(K, H)$ are the coefficients of Theorem 3.27. \square

Finally, we have arrived at a closed expression for the coefficient functions of our recombination model (3.7). Still, its corresponding coefficients $c(H, M)$ and $c^*(K, H)$ from (3.50) have to be determined in a recursive manner according to Theorem 3.27. Let us discuss the path to an explicit solution of the recombination dynamics model via the above chain of transformations with an example.

Example 3.31. To illustrate the construction, let us spell out the example of five sites. We have $S = \{0, 1, 2, 3, 4\}$ and $L = \{\frac{1}{2}, \frac{3}{2}, \frac{5}{2}, \frac{7}{2}\}$, the corresponding recombination probabilities ρ_α , $\alpha \in L$, $\lambda_\emptyset = 1 - \rho_{\frac{1}{2}} - \rho_{\frac{3}{2}} - \rho_{\frac{5}{2}} - \rho_{\frac{7}{2}}$, and a given initial population p_0 . Aiming at determining the coefficient functions $a_G(t)$ for all $G \subseteq L$, we can immediately write down $a_\emptyset(t) = \lambda_\emptyset^t$, $a_{\frac{1}{2}}(t) = (\lambda_\emptyset + \rho_{\frac{1}{2}})^t - \lambda_\emptyset^t$, $a_{\frac{7}{2}}(t) = (\lambda_\emptyset + \rho_{\frac{7}{2}})^t - \lambda_\emptyset^t$ and $a_{\{\frac{1}{2}, \frac{7}{2}\}}(t) = \lambda_\emptyset^t - (\lambda_\emptyset + \rho_{\frac{1}{2}})^t - (\lambda_\emptyset + \rho_{\frac{7}{2}})^t + (\lambda_\emptyset + \rho_{\frac{1}{2}} + \rho_{\frac{7}{2}})^t$, see (3.20).

If we wanted to determine the remaining coefficient functions $a_G(t)$ for a given time t , they could be calculated using the method of Geiringer [24] (i.e. Theorem 3.7). But since we aim at a closed solution for *all* t , we use the procedure developed above. To determine the coefficients of Theorem 3.30, we have to calculate the corresponding $c(G, H)$ and $c^*(G, H)$. Theorem 3.27 and 3.28 imply $U_L = T_L$, $U_{L \setminus \{\alpha\}} = T_{L \setminus \{\alpha\}}$ for all $\alpha \in L$, $U_{L \setminus \{\alpha, \beta\}} = T_{L \setminus \{\alpha, \beta\}}$ for all $\alpha, \beta \in L$, as well as $U_{\frac{3}{2}} = T_{\frac{3}{2}}$ and $U_{\frac{5}{2}} = T_{\frac{5}{2}}$. Hence, in these cases, the only non-vanishing coefficients are $c(L, L) = c(L \setminus \{\alpha\}, L \setminus \{\alpha\}) = c(L \setminus \{\alpha, \beta\}, L \setminus \{\alpha, \beta\}) = c(\{\frac{3}{2}\}, \{\frac{3}{2}\}) = c(\{\frac{5}{2}\}, \{\frac{5}{2}\}) = 1$ for all $\alpha, \beta \in L$. It remains to determine $U_{\frac{1}{2}}$, $U_{\frac{7}{2}}$ and U_\emptyset .

1. Constructing $U_{\frac{1}{2}}$:

The recursion starts with $c(\{\frac{1}{2}\}, \{\frac{1}{2}\}) = 1$. Following (3.41), $z^{(L)}(\{\frac{1}{2}\}, H) = 0$ for all $H \supsetneq \{\frac{1}{2}\}$ except for $H = \{\frac{1}{2}, \frac{5}{2}\}$, and thus the only non-zero $c(\{\frac{1}{2}\}, H)$, $H \supsetneq \{\frac{1}{2}\}$, is

$$c(\{\frac{1}{2}\}, \{\frac{1}{2}, \frac{5}{2}\}) = \frac{z(\{\frac{1}{2}\}, \{\frac{1}{2}, \frac{5}{2}\})}{\lambda_{\frac{1}{2}} - \lambda_{\{\frac{1}{2}, \frac{5}{2}\}}} = \frac{\rho_{\frac{3}{2}} \rho_{\frac{7}{2}}}{\rho_{\frac{5}{2}} + \rho_{\frac{3}{2}} \rho_{\frac{7}{2}}},$$

where we have used the recursion (3.46) together with $\lambda_{\frac{1}{2}} = 1 - \rho_{\frac{3}{2}} - \rho_{\frac{5}{2}} - \rho_{\frac{7}{2}}$ and $\lambda_{\{\frac{1}{2}, \frac{5}{2}\}} = (1 - \rho_{\frac{3}{2}})(1 - \rho_{\frac{7}{2}})$. So, for the transformation (3.42) we obtain

$$U_{\frac{1}{2}} = T_{\frac{1}{2}} + \frac{\rho_{\frac{3}{2}} \rho_{\frac{7}{2}}}{\rho_{\frac{5}{2}} + \rho_{\frac{3}{2}} \rho_{\frac{7}{2}}} T_{\{\frac{1}{2}, \frac{5}{2}\}},$$

so that $U_{\frac{1}{2}} \circ \Phi = (1 - \rho_{\frac{3}{2}} - \rho_{\frac{5}{2}} - \rho_{\frac{7}{2}}) U_{\frac{1}{2}}$. Analogously,

$$U_{\frac{7}{2}} = T_{\frac{7}{2}} + \frac{\rho_{\frac{1}{2}} \rho_{\frac{5}{2}}}{\rho_{\frac{3}{2}} + \rho_{\frac{1}{2}} \rho_{\frac{5}{2}}} T_{\{\frac{3}{2}, \frac{7}{2}\}}.$$

2. *Constructing U_\emptyset :*

By (3.41), the only non-vanishing coefficients are $c(\emptyset, \emptyset)$, $c(\emptyset, \{\frac{3}{2}\})$, $c(\emptyset, \{\frac{5}{2}\})$, and $c(\emptyset, \{\frac{3}{2}, \frac{5}{2}\})$. They are determined by the recursion (3.46) and lead to the following transformation (3.42):

$$U_\emptyset = T_\emptyset + \frac{\rho_{\frac{1}{2}}(\rho_{\frac{5}{2}} + \rho_{\frac{7}{2}})}{\rho_{\frac{3}{2}} + \rho_{\frac{1}{2}}(\rho_{\frac{5}{2}} + \rho_{\frac{7}{2}})} T_{\frac{3}{2}} + \frac{(\rho_{\frac{1}{2}} + \rho_{\frac{3}{2}})\rho_{\frac{7}{2}}}{\rho_{\frac{5}{2}} + (\rho_{\frac{1}{2}} + \rho_{\frac{3}{2}})\rho_{\frac{7}{2}}} T_{\frac{5}{2}} + \frac{\rho_{\frac{1}{2}}\rho_{\frac{7}{2}}}{\rho_{\frac{1}{2}}\rho_{\frac{7}{2}} + \rho_{\frac{3}{2}} + \rho_{\frac{5}{2}}} T_{\{\frac{3}{2}, \frac{5}{2}\}}.$$

Now that we know the $c(G, H)$, the coefficients $c^*(G, H)$ are calculated via (3.48). Finally, the remaining coefficient functions follow from Theorem 3.30:

$$\begin{aligned} a_{\frac{3}{2}}(t) &= \frac{\rho_{\frac{3}{2}}}{\rho_{\frac{1}{2}}(\rho_{\frac{5}{2}} + \rho_{\frac{7}{2}}) + \rho_{\frac{3}{2}}} (\lambda_{\frac{3}{2}}^t - \lambda_\emptyset^t), \\ a_{\frac{5}{2}}(t) &= \frac{\rho_{\frac{5}{2}}}{\rho_{\frac{7}{2}}(\rho_{\frac{1}{2}} + \rho_{\frac{3}{2}}) + \rho_{\frac{5}{2}}} (\lambda_{\frac{5}{2}}^t - \lambda_\emptyset^t), \\ a_{\{\frac{1}{2}, \frac{3}{2}\}}(t) &= \lambda_{\{\frac{1}{2}, \frac{3}{2}\}}^t - \lambda_{\frac{1}{2}}^t - \frac{\rho_{\frac{3}{2}}}{\rho_{\frac{1}{2}}(\rho_{\frac{5}{2}} + \rho_{\frac{7}{2}}) + \rho_{\frac{3}{2}}} (\lambda_{\frac{3}{2}}^t - \lambda_\emptyset^t), \\ a_{\{\frac{1}{2}, \frac{5}{2}\}}(t) &= \frac{\rho_{\frac{5}{2}}}{\rho_{\frac{3}{2}}\rho_{\frac{7}{2}} + \rho_{\frac{5}{2}}} (\lambda_{\{\frac{1}{2}, \frac{5}{2}\}}^t - \lambda_{\frac{1}{2}}^t) - \frac{\rho_{\frac{5}{2}}}{\rho_{\frac{7}{2}}(\rho_{\frac{1}{2}} + \rho_{\frac{3}{2}}) + \rho_{\frac{5}{2}}} (\lambda_{\frac{5}{2}}^t - \lambda_\emptyset^t), \\ a_{\{\frac{3}{2}, \frac{5}{2}\}}(t) &= \frac{\rho_{\frac{3}{2}} + \rho_{\frac{5}{2}}}{\rho_{\frac{1}{2}}\rho_{\frac{7}{2}} + \rho_{\frac{3}{2}} + \rho_{\frac{5}{2}}} \lambda_{\{\frac{3}{2}, \frac{5}{2}\}}^t - \frac{\rho_{\frac{3}{2}}}{\rho_{\frac{1}{2}}(\rho_{\frac{5}{2}} + \rho_{\frac{7}{2}}) + \rho_{\frac{3}{2}}} \lambda_{\frac{3}{2}}^t - \frac{\rho_{\frac{5}{2}}}{\rho_{\frac{7}{2}}(\rho_{\frac{1}{2}} + \rho_{\frac{3}{2}}) + \rho_{\frac{5}{2}}} \lambda_{\frac{5}{2}}^t \\ &\quad + \left(1 - \frac{(\rho_{\frac{1}{2}} + \rho_{\frac{3}{2}})\rho_{\frac{7}{2}}}{\rho_{\frac{7}{2}}(\rho_{\frac{1}{2}} + \rho_{\frac{3}{2}}) + \rho_{\frac{5}{2}}} - \frac{(\rho_{\frac{5}{2}} + \rho_{\frac{7}{2}})\rho_{\frac{1}{2}}}{\rho_{\frac{1}{2}}(\rho_{\frac{5}{2}} + \rho_{\frac{7}{2}}) + \rho_{\frac{3}{2}}} + \frac{\rho_{\frac{1}{2}}\rho_{\frac{7}{2}}}{\rho_{\frac{1}{2}}\rho_{\frac{7}{2}} + \rho_{\frac{3}{2}} + \rho_{\frac{5}{2}}}\right) \lambda_\emptyset^t, \\ a_{\{\frac{3}{2}, \frac{7}{2}\}}(t) &= \frac{\rho_{\frac{3}{2}}}{\rho_{\frac{1}{2}}\rho_{\frac{5}{2}} + \rho_{\frac{3}{2}}} (\lambda_{\{\frac{3}{2}, \frac{7}{2}\}}^t - \lambda_{\frac{3}{2}}^t) - \frac{\rho_{\frac{3}{2}}}{\rho_{\frac{1}{2}}(\rho_{\frac{5}{2}} + \rho_{\frac{7}{2}}) + \rho_{\frac{3}{2}}} (\lambda_{\frac{3}{2}}^t - \lambda_\emptyset^t), \\ a_{\{\frac{5}{2}, \frac{7}{2}\}}(t) &= \lambda_{\{\frac{5}{2}, \frac{7}{2}\}}^t - \lambda_{\frac{5}{2}}^t - \frac{\rho_{\frac{5}{2}}}{\rho_{\frac{7}{2}}(\rho_{\frac{1}{2}} + \rho_{\frac{3}{2}}) + \rho_{\frac{5}{2}}} (\lambda_{\frac{5}{2}}^t - \lambda_\emptyset^t), \\ a_{\{\frac{1}{2}, \frac{3}{2}, \frac{5}{2}\}}(t) &= \lambda_{\{\frac{1}{2}, \frac{3}{2}, \frac{5}{2}\}}^t - \lambda_{\{\frac{1}{2}, \frac{3}{2}\}}^t - \frac{\rho_{\frac{5}{2}}}{\rho_{\frac{5}{2}} + \rho_{\frac{3}{2}}\rho_{\frac{7}{2}}} (\lambda_{\{\frac{1}{2}, \frac{5}{2}\}}^t - \lambda_{\frac{1}{2}}^t) - \frac{\rho_{\frac{3}{2}} + \rho_{\frac{5}{2}}}{\rho_{\frac{3}{2}} + \rho_{\frac{5}{2}} + \rho_{\frac{1}{2}}\rho_{\frac{7}{2}}} \lambda_{\{\frac{3}{2}, \frac{5}{2}\}}^t \\ &\quad + \frac{\rho_{\frac{3}{2}}}{\rho_{\frac{1}{2}}(\rho_{\frac{5}{2}} + \rho_{\frac{7}{2}}) + \rho_{\frac{3}{2}}} \lambda_{\frac{3}{2}}^t + \frac{\rho_{\frac{5}{2}}}{\rho_{\frac{7}{2}}(\rho_{\frac{1}{2}} + \rho_{\frac{3}{2}}) + \rho_{\frac{5}{2}}} \lambda_{\frac{5}{2}}^t \\ &\quad - \left(1 - \frac{(\rho_{\frac{1}{2}} + \rho_{\frac{3}{2}})\rho_{\frac{7}{2}}}{\rho_{\frac{7}{2}}(\rho_{\frac{1}{2}} + \rho_{\frac{3}{2}}) + \rho_{\frac{5}{2}}} - \frac{(\rho_{\frac{5}{2}} + \rho_{\frac{7}{2}})\rho_{\frac{1}{2}}}{\rho_{\frac{1}{2}}(\rho_{\frac{5}{2}} + \rho_{\frac{7}{2}}) + \rho_{\frac{3}{2}}} + \frac{\rho_{\frac{1}{2}}\rho_{\frac{7}{2}}}{\rho_{\frac{1}{2}}\rho_{\frac{7}{2}} + \rho_{\frac{3}{2}} + \rho_{\frac{5}{2}}}\right) \lambda_\emptyset^t, \end{aligned}$$

$$\begin{aligned}
a_{\{\frac{1}{2}, \frac{3}{2}, \frac{7}{2}\}}(t) &= \lambda_{\{\frac{1}{2}, \frac{3}{2}, \frac{7}{2}\}}^t - \lambda_{\{\frac{1}{2}, \frac{3}{2}\}}^t - \lambda_{\{\frac{1}{2}, \frac{7}{2}\}}^t - \frac{\rho_{\frac{3}{2}}}{\rho_{\frac{3}{2}} + \rho_{\frac{1}{2}}\rho_{\frac{5}{2}}} \lambda_{\{\frac{3}{2}, \frac{7}{2}\}}^t + \lambda_{\frac{1}{2}}^t \\
&\quad + \frac{\rho_{\frac{3}{2}}}{\rho_{\frac{3}{2}} + \rho_{\frac{1}{2}}(\rho_{\frac{5}{2}} + \rho_{\frac{7}{2}})} \lambda_{\frac{3}{2}}^t + \frac{\rho_{\frac{3}{2}}}{\rho_{\frac{3}{2}} + \rho_{\frac{1}{2}}\rho_{\frac{5}{2}}} \lambda_{\frac{7}{2}}^t - \frac{\rho_{\frac{3}{2}}}{\rho_{\frac{3}{2}} + \rho_{\frac{1}{2}}(\rho_{\frac{5}{2}} + \rho_{\frac{7}{2}})} \lambda_{\emptyset}^t, \\
a_{\{\frac{1}{2}, \frac{5}{2}, \frac{7}{2}\}}(t) &= \lambda_{\{\frac{1}{2}, \frac{5}{2}, \frac{7}{2}\}}^t - \lambda_{\{\frac{5}{2}, \frac{7}{2}\}}^t - \lambda_{\{\frac{1}{2}, \frac{7}{2}\}}^t - \frac{\rho_{\frac{5}{2}}}{\rho_{\frac{5}{2}} + \rho_{\frac{3}{2}}\rho_{\frac{7}{2}}} \lambda_{\{\frac{1}{2}, \frac{5}{2}\}}^t + \lambda_{\frac{7}{2}}^t \\
&\quad + \frac{\rho_{\frac{5}{2}}}{\rho_{\frac{5}{2}} + \rho_{\frac{3}{2}}\rho_{\frac{7}{2}}} \lambda_{\frac{1}{2}}^t + \frac{\rho_{\frac{5}{2}}}{\rho_{\frac{5}{2}} + \rho_{\frac{7}{2}}(\rho_{\frac{1}{2}} + \rho_{\frac{3}{2}})} \lambda_{\frac{5}{2}}^t - \frac{\rho_{\frac{5}{2}}}{\rho_{\frac{5}{2}} + \rho_{\frac{7}{2}}(\rho_{\frac{1}{2}} + \rho_{\frac{3}{2}})} \lambda_{\emptyset}^t, \\
a_{\{\frac{3}{2}, \frac{5}{2}, \frac{7}{2}\}}(t) &= \lambda_{\{\frac{3}{2}, \frac{5}{2}, \frac{7}{2}\}}^t - \lambda_{\{\frac{5}{2}, \frac{7}{2}\}}^t - \frac{\rho_{\frac{3}{2}}}{\rho_{\frac{3}{2}} + \rho_{\frac{1}{2}}\rho_{\frac{5}{2}}} (\lambda_{\{\frac{3}{2}, \frac{7}{2}\}}^t - \lambda_{\frac{7}{2}}^t) - \frac{\rho_{\frac{3}{2}} + \rho_{\frac{5}{2}}}{\rho_{\frac{3}{2}} + \rho_{\frac{5}{2}} + \rho_{\frac{1}{2}}\rho_{\frac{7}{2}}} \lambda_{\{\frac{3}{2}, \frac{5}{2}\}}^t \\
&\quad + \frac{\rho_{\frac{3}{2}}}{\rho_{\frac{1}{2}}(\rho_{\frac{5}{2}} + \rho_{\frac{7}{2}}) + \rho_{\frac{3}{2}}} \lambda_{\frac{3}{2}}^t + \frac{\rho_{\frac{5}{2}}}{\rho_{\frac{7}{2}}(\rho_{\frac{1}{2}} + \rho_{\frac{3}{2}}) + \rho_{\frac{5}{2}}} \lambda_{\frac{5}{2}}^t \\
&\quad - \left(1 - \frac{(\rho_{\frac{1}{2}} + \rho_{\frac{3}{2}})\rho_{\frac{7}{2}}}{\rho_{\frac{7}{2}}(\rho_{\frac{1}{2}} + \rho_{\frac{3}{2}}) + \rho_{\frac{5}{2}}} - \frac{(\rho_{\frac{5}{2}} + \rho_{\frac{7}{2}})\rho_{\frac{1}{2}}}{\rho_{\frac{1}{2}}(\rho_{\frac{5}{2}} + \rho_{\frac{7}{2}}) + \rho_{\frac{3}{2}}} + \frac{\rho_{\frac{1}{2}}\rho_{\frac{7}{2}}}{\rho_{\frac{1}{2}}\rho_{\frac{7}{2}} + \rho_{\frac{3}{2}} + \rho_{\frac{5}{2}}}\right) \lambda_{\emptyset}^t,
\end{aligned}$$

and

$$\begin{aligned}
a_{\{\frac{1}{2}, \frac{3}{2}, \frac{5}{2}, \frac{7}{2}\}}(t) &= \lambda_{\{\frac{1}{2}, \frac{3}{2}, \frac{5}{2}, \frac{7}{2}\}}^t - \lambda_{\{\frac{1}{2}, \frac{3}{2}, \frac{5}{2}\}}^t - \lambda_{\{\frac{1}{2}, \frac{3}{2}, \frac{7}{2}\}}^t - \lambda_{\{\frac{1}{2}, \frac{5}{2}, \frac{7}{2}\}}^t - \lambda_{\{\frac{3}{2}, \frac{5}{2}, \frac{7}{2}\}}^t + \lambda_{\{\frac{1}{2}, \frac{3}{2}\}}^t \\
&\quad + \frac{\rho_{\frac{5}{2}}}{\rho_{\frac{5}{2}} + \rho_{\frac{3}{2}}\rho_{\frac{7}{2}}} \lambda_{\{\frac{1}{2}, \frac{5}{2}\}}^t + \lambda_{\{\frac{1}{2}, \frac{7}{2}\}}^t + \frac{\rho_{\frac{3}{2}} + \rho_{\frac{5}{2}}}{\rho_{\frac{3}{2}} + \rho_{\frac{5}{2}} + \rho_{\frac{1}{2}}\rho_{\frac{7}{2}}} \lambda_{\{\frac{3}{2}, \frac{5}{2}\}}^t \\
&\quad + \frac{\rho_{\frac{3}{2}}}{\rho_{\frac{3}{2}} + \rho_{\frac{1}{2}}\rho_{\frac{5}{2}}} \lambda_{\{\frac{3}{2}, \frac{7}{2}\}}^t + \lambda_{\{\frac{5}{2}, \frac{7}{2}\}}^t - \frac{\rho_{\frac{5}{2}}}{\rho_{\frac{5}{2}} + \rho_{\frac{3}{2}}\rho_{\frac{7}{2}}} \lambda_{\frac{1}{2}}^t - \frac{\rho_{\frac{3}{2}}}{\rho_{\frac{1}{2}}(\rho_{\frac{5}{2}} + \rho_{\frac{7}{2}}) + \rho_{\frac{3}{2}}} \lambda_{\frac{3}{2}}^t \\
&\quad - \frac{\rho_{\frac{5}{2}}}{\rho_{\frac{7}{2}}(\rho_{\frac{1}{2}} + \rho_{\frac{3}{2}}) + \rho_{\frac{5}{2}}} \lambda_{\frac{5}{2}}^t - \frac{\rho_{\frac{3}{2}}}{\rho_{\frac{3}{2}} + \rho_{\frac{1}{2}}\rho_{\frac{5}{2}}} \lambda_{\frac{7}{2}}^t \\
&\quad + \left(1 - \frac{(\rho_{\frac{5}{2}} + \rho_{\frac{7}{2}})\rho_{\frac{1}{2}}}{\rho_{\frac{1}{2}}(\rho_{\frac{5}{2}} + \rho_{\frac{7}{2}}) + \rho_{\frac{3}{2}}} - \frac{(\rho_{\frac{1}{2}} + \rho_{\frac{3}{2}})\rho_{\frac{7}{2}}}{\rho_{\frac{7}{2}}(\rho_{\frac{1}{2}} + \rho_{\frac{3}{2}}) + \rho_{\frac{5}{2}}} + \frac{\rho_{\frac{1}{2}}\rho_{\frac{7}{2}}}{\rho_{\frac{1}{2}}\rho_{\frac{7}{2}} + \rho_{\frac{3}{2}} + \rho_{\frac{5}{2}}}\right) \lambda_{\emptyset}^t,
\end{aligned}$$

where the λ_G are given by (3.45).

At the end, we are concerned with the asymptotic behaviour for large iteration numbers. In doing so, we first need the following property of the coefficients.

Lemma 3.32. *The coefficients $c(G, L)$ and $c^*(G, L)$ satisfy $c(G, L) = c^*(G, L) = \delta_{G, L}$ for arbitrary $\emptyset \subseteq G \subseteq L$.*

Proof. We have $c(G, G) = c^*(G, G) = 1$ for all G by Theorem 3.27. The claim for $c(G, L)$ now follows from the recursion (3.46) together with Corollary 3.25. Inserting this into recursion (3.48) establishes the relation for the $c^*(G, L)$. \square

Finally, let us consider what happens in the limit as $t \rightarrow \infty$.

Proposition 3.33. *The solution p_t of the recombination equation (3.7) with initial condition p_0 satisfies*

$$p_t \xrightarrow{t \rightarrow \infty} R_L(p_0) = \bigotimes_{i=0}^n (\pi_i p_0),$$

with exponentially fast convergence in the norm topology.

Proof. When expressing p_t in terms of U_H according to (3.49), we first observe $p_t = U_L(p_0) + \sum_{G \subsetneq L} \sum_{H \supseteq G} c^*(G, H) \lambda_H^t U_H(p_0)$, because $\lambda_L = 1$ and $c^*(G, L) = \delta_{G,L}$ by Lemma 3.32. Since $\bar{U}_L = R_L$, we obtain the following estimate in the variation norm

$$\begin{aligned} \|p_t - R_L(p_0)\| &= \left\| \sum_{G \subsetneq L} \sum_{H \supseteq G} c^*(G, H) \lambda_H^t U_H(p_0) \right\| \\ &\leq \sum_{H \subsetneq L} \lambda_H^t \left\| \sum_{G \subseteq H} c^*(G, H) U_H(p_0) \right\| \xrightarrow{t \rightarrow \infty} 0, \end{aligned}$$

which establishes the claim since $\lambda_H < 1$ for $H \neq L$. \square

As was to be expected, the solution of the recombination equation converges towards the independent combination of the alleles, that is towards *linkage equilibrium*. This is a well-known result that has been proved by many authors with their respective models of recombination, see for example [3, 11, 12, 25, 69].

Despite the construction of a solution to the recombination dynamics in an instructive way, we are still left with the question whether there might be a more direct approach to the solution, i.e. a solution that does not employ recursions like the one from Theorem 3.27. If we have a closer look at the explicit solution from Example 3.31, a systematic pattern does not seem to be directly perceptible. If we even go beyond five sites, the recursions become more and more involved, and the arising coefficient functions do not give any hint at what they are actually describing, i.e. what is actually happening within the dynamical system. After we have investigated the recombination model in detail, this result is thus not perfectly convincing. Therefore, provided with the knowledge about the recombination process from this chapter, we next set out to search for a closed expression for the coefficient functions $a_G(t)$ *without* the need of a transformation. In doing so, we will view the recombination process from another perspective.

Chapter 4

Recombination and ancestral recombination trees: an explicit solution

In this chapter, we develop a new approach to an explicit solution to the deterministic recombination dynamics (3.7). In doing so, we formulate the underlying *stochastic* process of the finite population counterpart of (3.7). This allows us to trace recombination backwards in time resulting in binary tree structures, the so-called *ancestral recombination trees*, which are then used as a tool to state an explicit solution to the dynamics.

The technique of looking backwards in time is extremely popular in population genetics these days. When investigating the evolution of a population that is formed by a complex process, the idea is to find an associated process (the *dual* process) with a preferably simpler structure than the original one. This dual process might then be used to infer information about the original evolutionary process. In population genetics, these dual processes are primarily backwards processes concerning the genealogy of a population. Arguably the most famous backwards approach is the *coalescence* originally introduced by Kingman [43] in 1982, where lineages of a sample of individuals from a present-day population are traced backwards in time. On a more abstract level, the usage of dual processes is strongly related to the study of *interactive particle systems*, for a good introduction refer to [16].

Unless otherwise stated, we will use all notation from Chapter 3 including those describing gametes, types and recombination probabilities.

4.1 The finite population counterpart: the Wright-Fisher model

When dealing with finite populations, the changes in the genetic structure of the population are due to a stochastic rather a deterministic process as we have formulated in the previous chapter. These variations due to the stochastic effect of sampling are commonly known as *genetic drift*. A well known and, owing to its simplicity, commonly used model in finite population genetics is the so-called *Wright-Fisher model* (Fisher [21], Wright [70]). Although several versions of the Wright-Fisher model exist (see [19] for a good overview), which incorporate different evolutionary forces, there are two basic characteristics common to all. The first is that the finite population size is assumed to be constant. The second is that the population evolves through non-overlapping generations whereby, at each time step, the entire population dies and is replaced by its offspring. The offspring are sampled from the parental generation with replacement and equal probability, i.e. Wright-Fisher models exhibit a ‘multinomial sampling characteristic’. They are commonly formulated as discrete-time Markov processes.

In our case, the dynamics of a finite population that evolves solely due to single-crossover recombination can be described by the following Wright-Fisher model, see also Figure 4.1.

Wright-Fisher model with single-crossover recombination

The model assumes each generation to be of constant size N . Each individual lives only one generation and dies after the offspring are produced. In each generation, each offspring individual chooses its parent(s) independently according to the following scheme:

- with probability $0 \leq 1 - \sum_{\alpha \in L} \rho_\alpha < 1$ a single parent is selected uniformly at random from the previous generation;
- with probability $\rho_\alpha > 0$, $\alpha \in L$, two parents are chosen uniformly and randomly to recombine at link α , this giving rise to the corresponding recombined offspring (with the leading segment from the first and the trailing segment from the second parent).

We denote the population at time t by

$Z_t = (Z_t(x))_{x \in X} \in E := \{\nu \text{ counting measure on } X \mid \|\nu\| = N\}$, where $\|\cdot\|$ denotes total variation norm and $Z_t(x)$ is the number of individuals of type x at time t . We will also need the corresponding normalised quantity $\hat{Z}_t := \frac{1}{N} Z_t$. It is clear that an individual that recombines at link $\alpha \in L$ in generation t draws its type from $R_\alpha(\hat{Z}_{t-1})$, and a non-recombining individual draws its type from $\hat{Z}_{t-1} = R_\varnothing(\hat{Z}_{t-1})$.

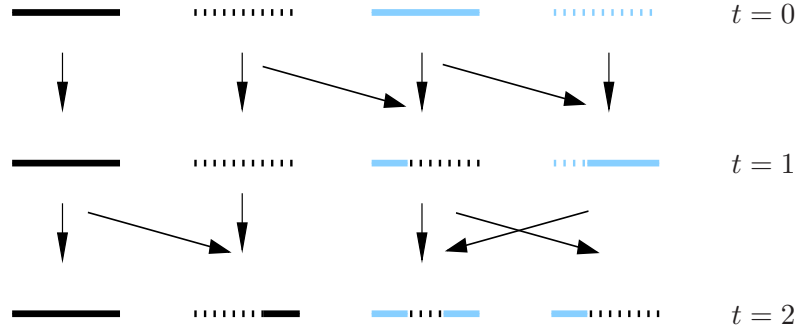


Figure 4.1: Wright-Fisher model with single-crossover recombination for $N = 4$.

The discrete-time Markov chain $\{\hat{Z}_t\}_{t \in \mathbb{N}_0}$ on $\mathcal{P}(X)$ may therefore be formulated as follows:

- In each generation t , let $N_\alpha(t)$, $\alpha \in L$, denote the random number of new individuals that are created from the previous generation with recombination at link $\alpha \in L$. Analogously, $N_\emptyset(t)$ is the number of individuals that are sampled without recombining. Clearly, they follow a multinomial distribution:

$$(N_\emptyset(t), N_{\frac{1}{2}}(t), \dots, N_{\frac{2n-1}{2}}(t)) \sim \mathcal{M}(N, 1 - \sum_{\alpha \in L} \rho_\alpha, \rho_{\frac{1}{2}}, \dots, \rho_{\frac{2n-1}{2}}), \quad \text{iid for all } t. \quad (4.1)$$

- In generation t , the subpopulation $Y_\beta(t)$ of individuals that experienced recombination at link $\beta \in L$ or no recombination (indicated by $\beta = \emptyset$) is given by

$$Y_\beta(t) \sim \mathcal{M}(N_\beta(t), R_\beta(\hat{Z}_{t-1})), \quad \beta \in L \text{ or } \beta = \emptyset. \quad (4.2)$$

- Finally, we obtain \hat{Z}_t via

$$\hat{Z}_t = \frac{1}{N} Y_\emptyset(t) + \frac{1}{N} \sum_{\alpha \in L} Y_\alpha(t). \quad (4.3)$$

Next, we show that the infinite population limit (IPL) from the above model, where we let $N \rightarrow \infty$ without rescaling any other parameters so that we lose the stochastic effects of sampling, indeed results in our deterministic model (3.7). First of all, we obviously have for all $t \in \mathbb{N}$

$$\frac{N_\alpha(t)}{N} \xrightarrow{N \rightarrow \infty} \rho_\alpha, \alpha \in L, \quad \text{and} \quad \frac{N_\emptyset(t)}{N} \xrightarrow{N \rightarrow \infty} 1 - \sum_{\alpha \in L} \rho_\alpha \quad \text{a.s.} \quad (4.4)$$

due to the strong law of large numbers. Furthermore, for $\beta \in L$ and $\beta = \emptyset$, $N_\beta(t) \rightarrow \infty$ for all $t \in \mathbb{N}$ as $N \rightarrow \infty$ a.s. and thus

$$\frac{Y_\beta(t)}{N_\beta(t)} \xrightarrow{N \rightarrow \infty} R_\beta(\hat{Z}_{t-1}) \quad \text{a.s.} \quad (4.5)$$

As a consequence of (4.3), (4.4) and (4.5), we have

$$\hat{Z}_t = \frac{N_\emptyset(t)}{N} \cdot \frac{Y_\emptyset(t)}{N_\emptyset(t)} + \sum_{\alpha \in L} \frac{N_\alpha(t)}{N} \cdot \frac{Y_\alpha(t)}{N_\alpha(t)} \xrightarrow{N \rightarrow \infty} \left(1 - \sum_{\alpha \in L} \rho_\alpha\right) \hat{Z}_{t-1} + \sum_{\alpha \in L} \rho_\alpha R_\alpha(\hat{Z}_{t-1}) \quad \text{a.s.} \quad (4.6)$$

This result already motivates the deterministic recombination dynamics from (3.7), and indeed we can prove that (3.7) describes the infinite population limit of the stochastic process:

Proposition 4.1 (Infinite Population Limit). *Let $\{\hat{Z}_t^{(N)}\}_{t \in \mathbb{N}_0}$, $N = 1, 2, \dots$, be the family of processes defined by (4.1), (4.2) and (4.3), with initial states such that $\lim_{N \rightarrow \infty} \hat{Z}_0^{(N)} = p_0$. Then, for every given $t \in \mathbb{N}_0$, one has*

$$\lim_{N \rightarrow \infty} \sup_{s \leq t} |\hat{Z}_s^{(N)} - p_s| = 0 \quad \text{a.s.}, \quad (4.7)$$

where $p_s = \Phi^s(p_0)$ denotes the solution of (3.7).

The corresponding situation in continuous time is covered by the very general law of large numbers by Ethier and Kurtz [18, Thm.11.2.1], but no such general result seems to be available in discrete time. Let us therefore include the few lines of proof here:

Proof. of Prop. 4.1 We can write $\hat{Z}_0^{(N)} = p_0 + \varepsilon_0$ and $\hat{Z}_t^{(N)} = \Phi(\hat{Z}_{t-1}^{(N)}) + \varepsilon_t$ for $t \in \mathbb{N}$, where $\{\varepsilon_t\}_{t \in \mathbb{N}_0}$ is a sequence of real-valued random variables. Due to (4.6), we can always choose N such that for any given $t \in \mathbb{N}_0$ and $\varepsilon > 0$, $|\varepsilon_s| \leq \varepsilon$ holds (almost surely) for all $s \leq t$. Since Φ is globally Lipschitz (it is differentiable and its domain, $\mathcal{P}(X)$, is compact), the claim then follows directly from a discrete version of the Gronwall lemma, compare [29]. \square

Remark 4.2. *We can also recompute the proof of Proposition 4.1 to make the assertion explicit:*

Using the same assumptions as in the above proof, we can define $e_t := |\hat{Z}_t^{(N)} - p_t|$ as the deviation between the stochastic process (defined via (4.1), (4.2) and (4.3)) and the deterministic process (3.7). Inductively, we then obtain

$$\begin{aligned} e_0 &= |\hat{Z}_0^{(N)} - p_0| \leq \varepsilon_0 \\ e_1 &= |\hat{Z}_1^{(N)} - p_1| = |\Phi(\hat{Z}_0^{(N)}) + \varepsilon_1 - \Phi(p_0)| \leq L|\varepsilon_0| + |\varepsilon_1| \\ e_2 &= |\hat{Z}_2^{(N)} - p_2| = |\Phi(\hat{Z}_1^{(N)}) + \varepsilon_2 - \Phi(p_1)| \leq L|\hat{Z}_1^{(N)} - p_1| + |\varepsilon_2| \leq L^2|\varepsilon_0| + L|\varepsilon_1| + |\varepsilon_2| \\ &\vdots \\ e_t &= \sum_{j=0}^t L^j |\varepsilon_j| \leq \sum_{j=0}^t L^j \varepsilon = \frac{1 - L^{t+1}}{1 - L} \cdot \varepsilon, \end{aligned}$$

where we use that Φ is Lipschitz with Lipschitz constant $L \neq 1$ (the case $L = 1$ obviously also yields the assertion) and the above explanations for that $\hat{Z}_t^{(N)} = \Phi(\hat{Z}_{t-1}^{(N)}) + \varepsilon_t$ for $t \in \mathbb{N}$ together with $|\varepsilon_s| \leq \varepsilon$ (almost surely) for all $s \leq t$.

Note that the convergence in (4.7) applies for any fixed $t \in \mathbb{N}_0$, but need *not* hold as $t \rightarrow \infty$. Indeed, the asymptotic behaviour of the stochastic system is fundamentally different from that of the deterministic one: Due to resampling, the Markov chain is absorbing (in fact, it experiences fixation of a single type with probability one in finite time). In contrast, the deterministic system never loses any type, and the complete product measure with respect to all links in L is obtained as the stationary distribution (linkage equilibrium), see Proposition 3.33.

After we have defined the underlying stochastic process to the deterministic dynamics, we will pursue the stochastic perspective in the following and look at recombination backward in time, which will lead us to the coefficient functions in closed form. This will be subject to the next section.

4.2 Ancestral recombination process

4.2.1 The ancestral process

In the *ancestral recombination process*, we follow the ancestry from a selected individual from the population that evolved according to the Wright-Fisher model as described by (4.1), (4.2) and (4.3). To this end, we start with an individual in the present population at time t and let time run backwards, as illustrated in Figure 4.2. Whenever a recombination event occurs, the genetic material of the individual has different ancestors and the genealogy bifurcates into two parts (i.e. leading and trailing segment of the respective ancestral material), and the ancestry of both parts is followed back from then on. Note that these parts only consist of (distinct) subsets of all sites, in particular they are joined with non-ancestral material which is of no significance for our process. As long as the (constant) population size N is finite, two parts that have been separated due to recombination may come together again in the same individual, i.e. the genealogy may coalesce. In population genetics, such a graph that takes into account coalescence as well as recombination events is called *ancestral recombination graph* as described in [28, 34]. In common literature [28, 34, 54, 46], the general sample size of individuals (or sequences) is considered to be greater than one. Usually for all these processes that involve coalescence, see e.g. Kingman [43], the population size is also considered to tend to infinity, but time as well as other parameters, such like mutation rates, are rescaled. Therefore, the ancestral process we are considering crucially differs from the commonly known processes. We consider the ancestry of the genetic material of a single individual to trace back the history of the segments it is composed of due to recombination. Indeed, we can ignore coalescence events when N tends towards infinity since we lose the resampling effect:

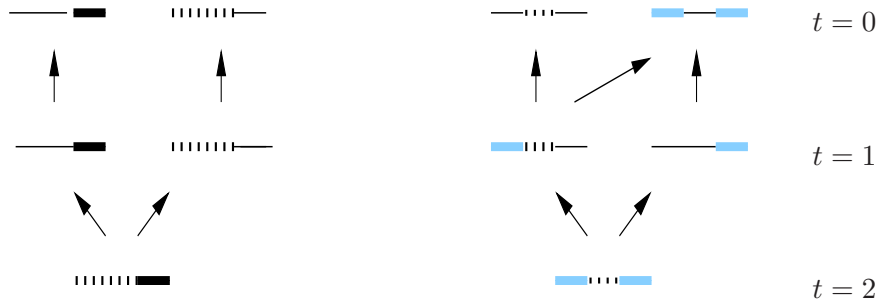


Figure 4.2: Ancestries for two individuals from a Wright-Fisher population. We trace back the ancestry of the segments present at $t = 2$; the thin black lines indicate non-ancestral material whose history is not relevant. The left graph refers to the second individual from Figure 4.1; here the two segments go back to two different ancestors. The right graph corresponds to the third individual from Figure 4.1. Here, two of its three segments have the same parent due to a coalescence event. In the infinite population limit, such a graph does not occur; rather all possible ancestries will be given as binary trees.

Fact 1. *In the ancestral process described above, the probability that no coalescence occurs in the genealogy of a given individual tends to 1 as $N \rightarrow \infty$.*

Proof. It is clear that only recombination events that take place within the ancestral material are relevant. As shown in Figure 4.2, at every such event, the leading and trailing parts of the respective ancestral material are separated into two randomly chosen parents; otherwise, the parental situation remains unchanged. Independently of N , the maximum number of segments an individual may be composed of is $|L| + 1$ (i.e. in case each link has been hit by recombination). Thus, the probability that all segments have different parents is greater or equal than

$$1 \cdot \left(1 - \frac{1}{N}\right) \cdot \left(1 - \frac{2}{N}\right) \cdot \dots \cdot \left(1 - \frac{|L|}{N}\right) \xrightarrow{N \rightarrow \infty} 1.$$

□

Therefore, each genealogy for one selected individual is given by a *full binary tree* (i.e. a tree, where each internal node has either none or exactly two children nodes) in the limit $N \rightarrow \infty$, see also Figure 4.2.

4.2.2 Segments and the segmentation process

As we have seen above, the segments an individual is composed of are gradually separated from each other in the ancestral process. This motivates to consider the following process of progressive segmentation (which will turn out to coincide with the ancestral

process in the limit $N \rightarrow \infty$): The complete segment that represents the entire chromosome is characterised by the full set of links $L = \{\frac{1}{2}, \dots, \frac{2n-1}{2}\}$ (and the corresponding sites $S = \{0, \dots, n\}$). If we follow back the ancestry of an individual that has experienced recombination at all links in $G = \{\alpha_1, \dots, \alpha_{|G|}\} \subseteq L$, $\alpha_1 < \alpha_2 < \dots < \alpha_{|G|}$, we obtain the genealogy of all the segments it is composed of. These are captured in the tuple

$$\mathcal{L}_G := \left(\left\{ \alpha : \frac{1}{2} \leq \alpha < \alpha_1 \right\}, \left\{ \alpha : \alpha_1 < \alpha < \alpha_2 \right\}, \dots, \left\{ \alpha : \alpha_{|G|} < \alpha \leq \frac{2n-1}{2} \right\} \right) = \mathcal{L}_G^{(L)},$$

just as we have already seen in Section 3.4, compare (3.25) and see also Figure 4.3. Again, we here use the upper index L to indicate that we consider the segments derived from the complete set L (but we will omit it if this is obvious). Different from the notation in Chapter 3, we only need the corresponding links to characterise the segments what makes the treatment in the frame used here less cumbersome.

This progressive segmentation can then be described by the following process:

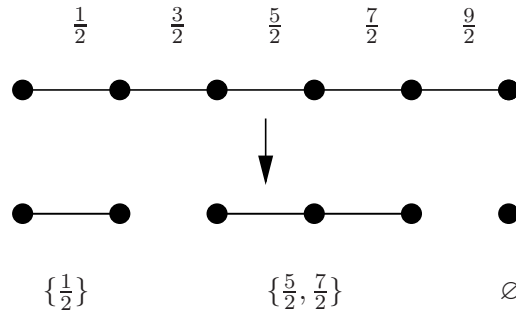


Figure 4.3: Example for $L = \{\frac{1}{2}, \dots, \frac{9}{2}\}$ and $G = \{\frac{3}{2}, \frac{9}{2}\}$: the three corresponding segments of $\mathcal{L}_G = (\{\frac{1}{2}\}, \{\frac{5}{2}, \frac{7}{2}\}, \emptyset)$.

Definition 4.3 (Segmentation process). *The segmentation process is the discrete-time Markov chain $\{F_t\}_{t \in \mathbb{N}_0}$, where F_t takes values in the power set of L according to the following rules. We start with $F_0 = \emptyset$. Then, if $F_t = G$, every segment $J \in \mathcal{L}_G$, independently of all other segments, either remains unchanged (probability $1 - \sum_{\alpha \in J} \rho_\alpha$), or is cut at a single link, namely at link $\alpha \in J$ with probability ρ_α . F_{t+1} is then the union of G and the set of all freshly cut links. That is,*

$$F_{t+1} = F_t \cup \left(\bigcup_{J \in \mathcal{L}_G} A_J \right), \quad \text{where } A_J = \begin{cases} \emptyset, & \text{with probability } 1 - \sum_{\alpha \in J} \rho_\alpha, \\ \{\alpha\}, & \text{with probability } \rho_\alpha, \text{ for all } \alpha \in J. \end{cases} \quad (4.8)$$

Note that, as in the Wright-Fisher model (and its deterministic limit), the links are not, in general, independent; however, the backward point of view adopted here reveals (conditional) independence of the segments. This will turn out as a key to the solution

(just as the independence of links was the crucial ingredient to the explicit solution of the continuous-time dynamics). One important property of the segmentation process, which reflects the conditional independence, is the probability that nothing happens in one time step (i.e. all currently present segments are not cut):

$$\mathbb{P}(F_{t+1} = G | F_t = G) = \prod_{J \in \mathcal{L}_G^{(L)}} (1 - \sum_{\alpha \in J} \rho_\alpha) = \lambda_G^{(L)}, \text{ for } G \subseteq L. \quad (4.9)$$

Thus, we rediscover the lambda coefficients from the diagonalisation process (3.45) from Section 3.6. As before, the upper index specifies the set of links the corresponding segments are derived from. Analogously, these coefficients are defined on any segment, i.e. on any contiguous set $I \subseteq L$, as $\lambda_H^{(I)} = \prod_{J \in \mathcal{L}_H^{(I)}} (1 - \sum_{\alpha \in J} \rho_\alpha)$, $H \subseteq I$. In particular,

$$\lambda_G^{(L)} = \prod_{I \in \mathcal{L}_G^{(L)}} \lambda_\emptyset^{(I)}. \quad (4.10)$$

We have constructed the segmentation process so that its time reversal is the process that gives rise to an individual pieced together from various segments due to recombination, i.e. for $F_t = G$, $G \subseteq L$, the outcome of the forward process is an individual that experienced recombination at the links of G . It is thus more than plausible that $a_G(t) = \mathbb{P}(F_t = G)$ for all $G \subseteq L$; this will be formally proved later on (see Proposition 4.14). This means, $a_G(t)$ is the sum over the probabilities of all possible paths of the segmentation process that lead to $F_t = G$. For $G = \emptyset$, $a_\emptyset(t) = \lambda_\emptyset^t$ follows directly from (3.19).

To further explain this, let us continue with an example.

Example 4.4. For four sites $S = \{0, 1, 2, 3\}$ with the corresponding links $L = \{\frac{1}{2}, \frac{3}{2}, \frac{5}{2}\}$, we consider the coefficient function $a_{\{\frac{1}{2}, \frac{3}{2}\}}(t)$, i.e. the probability that until time t exactly the links $\frac{1}{2}$ and $\frac{3}{2}$ have been involved in recombination. Solving (3.19) explicitly on the one hand (or with the help of Theorem 3.30 from Section 3.6), and considering the outcome of the segmentation process (4.8) on the other hand, one indeed obtains

$$\begin{aligned} a_{\{\frac{1}{2}, \frac{3}{2}\}}(t) &= \rho_{\frac{1}{2}} \rho_{\frac{3}{2}} \sum_{k=0}^{t-2} \lambda_\emptyset^k \sum_{i=0}^{t-2-k} \lambda_{\frac{1}{2}}^i \lambda_{\{\frac{1}{2}, \frac{3}{2}\}}^{t-2-k-i} + \rho_{\frac{1}{2}} \rho_{\frac{3}{2}} (1 - \rho_{\frac{5}{2}}) \sum_{k=0}^{t-2} \lambda_\emptyset^k \sum_{i=0}^{t-2-k} \lambda_{\frac{3}{2}}^i \lambda_{\{\frac{1}{2}, \frac{3}{2}\}}^{t-2-k-i} \\ &= \mathbb{P}(F_t = \{\frac{1}{2}, \frac{3}{2}\}). \end{aligned}$$

With reference to the segmentation process, this corresponds to summing explicitly over all paths of the trees of Figure 4.4. Here, the two sums reflect the order of the two separating events: The first term takes into account that link $\frac{1}{2}$ is the first to be cut, the second that link $\frac{3}{2}$ is cut first (time backwards). The respective lambda coefficients (4.9) ensure that nothing happens during the time between these separating events. All different time combinations are captured in the respective sums. In the case where $\frac{3}{2}$ is the first separation event, the additional factor $\lambda_\emptyset^{(\frac{5}{2})} = (1 - \rho_{\frac{5}{2}})$ is required to guarantee

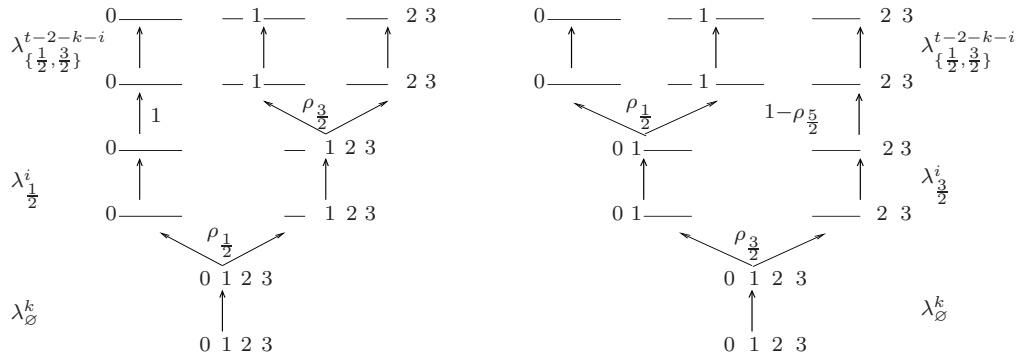


Figure 4.4: Two possible ways of the segmentation process resulting in $F_t = \{\frac{1}{2}, \frac{3}{2}\}$. The left panel refers to the first term of $\mathbb{P}(F_t = \{\frac{1}{2}, \frac{3}{2}\})$, the right one to the second. Here, this corresponds to the two possible histories of an individual present at time t that consists of three segments due to recombination at the links $\frac{1}{2}$ and $\frac{3}{2}$ and explains the structure of the coefficient function $a_{\{\frac{1}{2}, \frac{3}{2}\}}(t)$. The arrows point in backward direction of time in accordance with the ancestral recombination process.

that at the time of the second separation event (at link $\frac{1}{2}$), the segment described by link $\frac{5}{2}$ remains unchanged. The corresponding term for the other case is $\lambda_{\emptyset}^{(\emptyset)} = 1$.

Obviously, $\mathbb{P}(F_t = G)$ may be understood as a sum over tree topologies and branch lengths, i.e. we are concerned with all possible *ultrametric binary trees* that can be produced by the segmentation process, where each internal node corresponds to a separation event. We will show in the following that it is sufficient to deal with all *tree topologies* that belong to these ultrametric trees.

4.2.3 Ancestral recombination trees

We aim to state each coefficient function in terms of all corresponding binary tree topologies, i.e. we want to assign probabilities to each binary tree so that we can state each coefficient function as a sum of these probabilities. Let us anticipate that we will be able to evaluate the sum for each topology explicitly; for Example 4.4, this will result in

$$\begin{aligned} \mathbb{P}(F_t = \{\frac{1}{2}, \frac{3}{2}\}) &= \mathbb{P}(\text{Tree 1}) + \mathbb{P}(\text{Tree 2}) = \left((\lambda_{\{\frac{1}{2}, \frac{3}{2}\}}^t - \lambda_{\emptyset}^t) \frac{\rho_{\frac{1}{2}}}{\lambda_{\{\frac{1}{2}, \frac{3}{2}\}} - \lambda_{\emptyset}} - (\lambda_{\frac{1}{2}}^t - \lambda_{\emptyset}^t) \right) \\ &\quad + \left((\lambda_{\{\frac{1}{2}, \frac{3}{2}\}}^t - \lambda_{\emptyset}^t) \frac{\rho_{\frac{3}{2}}}{\lambda_{\{\frac{1}{2}, \frac{3}{2}\}} - \lambda_{\emptyset}} - (\lambda_{\frac{3}{2}}^t - \lambda_{\emptyset}^t) \frac{\rho_{\frac{3}{2}}}{\lambda_{\frac{3}{2}} - \lambda_{\emptyset}} \right), \end{aligned}$$

where Tree 1 refers to the tree topology of the left and Tree 2 to the topology of the right tree of Figure 4.4.

Let us now state a suitable definition for our tree topologies.

Definition 4.5 (Tree topology). For $\emptyset \neq G \subseteq L$, a (binary) tree topology is defined as $T := (G, m)$, where G signifies the set of internal nodes, and in particular $\gamma \in G$ designates the root of the tree. The function m is given by

$$\begin{aligned} m : G &\longrightarrow G \cup \{r\} \\ \alpha &\mapsto m(\alpha), \end{aligned}$$

with $m(\alpha)$ denoting the (unique) ancestor of the internal node $\alpha \in G$. Since obviously γ has no ancestor, we define the function m for γ as $m(\gamma) = r$.

Thus, $T = (G, m)$ has the internal nodes $\alpha \in G$ and the corresponding internal edges $E = \{(m(\alpha), \alpha) | \alpha \in G, m(\alpha) \neq r\}$. For later use, we also introduce the additional external edge (r, γ) that leads to the root γ . Note that we have not included the (external) leaves (and corresponding external edges) in our definition - what is rather unusual- since they will never be required explicitly. Thus, in particular for $G = \emptyset$, the only tree topology is the empty tree (with no nodes).

Example 4.6. For $G = \{\alpha_1, \dots, \alpha_5\} \subseteq L$, we consider the following tree topology $T = (G, m)$ with m given as $m(\alpha_1) = \alpha_2$, $m(\alpha_2) = r$, $m(\alpha_3) = \alpha_4$, $m(\alpha_4) = \alpha_2$, $m(\alpha_5) = \alpha_4$. The corresponding tree is shown in Figure 4.5.

It is commonly known from combinatorics that the number of full binary trees with n internal nodes is given by the n -th Catalan number C_n , with $C_n = \frac{(2n)!}{n!(n+1)!}$. Hence, for any $G \subseteq L$, we are dealing with $C_{|G|}$ different tree topologies.

We will need the following partial order on T .

Definition 4.7 (Partial order on $T = (G, m)$). A partial order \preceq on a tree topology $T = (G, m)$, $G \subseteq L$, with $\gamma \in G$ denoting the root of T , is defined as

$$\alpha \preceq \beta \iff \alpha \text{ is on the path from } \gamma \text{ to } \beta \text{ i.e. } \alpha = m^i(\beta) \text{ for some } i \in \{0, \dots, |G|\}.$$

Obviously, γ is the minimal element of G with respect to \preceq . Each edge of a particular tree topology can be associated with a certain segment. Hence, we define for $T = (G, m)$ and each $\alpha \in G$, $\alpha \neq \gamma$:

$$I_\alpha(T) := A \in \mathcal{L}_{\{\beta: \beta \preceq \alpha\}} \text{ s.t. } \alpha \in A.$$

Thus, $I_\alpha(T)$ identifies the contiguous subset of links that is associated with the internal edge $(m(\alpha), \alpha)$ such that, at this stage, $I_\alpha(T)$ is independent of all other links and describes the segment that will be next cut at link α (given the topology T). For the root γ , we particularly define $I_\gamma(T) := L$. An example for this is given in Figure 4.5. Note that, with the specification of $I_\gamma(T) := L = I_\gamma$ (independently of T), all $I_\alpha(T)$, $\alpha \neq \gamma$, are uniquely determined via T . From now on we will suppress the dependency of $I_\alpha(T)$ on the tree topology T for reasons of simplicity and write I_α instead of $I_\alpha(T)$. Next, we will define *subtrees*.

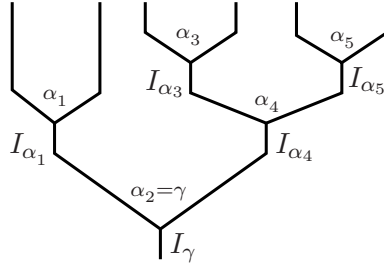


Figure 4.5: Tree topology $T = (G, m)$ for $G = \{\alpha_1, \dots, \alpha_5\}$ from Example 4.6. Each (internal) edge in the tree is identified with a certain segment. Here, we have $I_{\alpha_1} = L_{<\gamma}$, $I_{\alpha_2} = L$, $I_{\alpha_3} = \{\gamma + 1, \dots, \alpha_3, \dots, \alpha_4 - 1\}$, $I_{\alpha_4} = L_{>\gamma}$ and $I_{\alpha_5} = L_{>\alpha_4}$.

Definition 4.8 (Subtrees). *Given $T = (G, m)$, $\emptyset \neq G \subseteq L$, then for any $H \subseteq L$ a subtree of T is defined via $T_\alpha(H) = (G_\alpha(H), m^{(G_\alpha(H))})$ for every $\alpha \in G$, where*

$$G_\alpha(H) := \{\beta \in G \mid \alpha \preceq \beta \text{ and } h \not\preceq \beta \quad \forall h \in H \text{ with } \alpha \not\preceq h\}$$

and $m^{(G_\alpha(H))}$ is the restriction of m to $G_\alpha(H)$. We again define $m^{(G_\alpha(H))}(\alpha) = r$ as before for the root of the respective subtree.

Obviously, $G_\alpha(H)$ depends on the topology T (due to the partial ordering), but again we omit to indicate this for reasons of simplicity. The set of links associated with the edge that leads to any node β of a subtree $T_\alpha(H)$ is $I_\beta(T_\alpha(H)) = I_\beta(T)$.

Example 4.9. Let us consider the tree topology $T = (G, m)$ from Example 4.6. We then obtain for $H = \{\alpha_1, \alpha_2, \alpha_5\}$ subtrees $T_{\alpha_i}(H)$, $i = 1, \dots, 5$, with the following internal nodes: $G_{\alpha_1}(H) = \{\alpha_1\}$, $G_{\alpha_2}(H) = \{\alpha_2, \alpha_3, \alpha_4\}$, $G_{\alpha_3}(H) = \{\alpha_3\}$, $G_{\alpha_4}(H) = \{\alpha_3, \alpha_4\}$ and $G_{\alpha_5}(H) = \{\alpha_5\}$. The corresponding subtrees are shown in Figure 4.6.

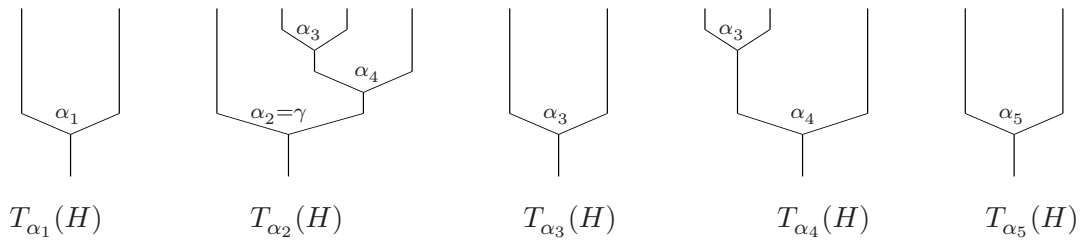


Figure 4.6: Subtrees for the tree topology from Example 4.6 with $H = \{\alpha_1, \alpha_2, \alpha_5\}$.

Before we come to the final theorems, we first need the following elementary, but useful variant of the geometric series:

Lemma 4.10. *For $a \neq b$, one has*

$$\sum_{i=0}^n a^i b^{n-i} = \frac{b^{n+1} - a^{n+1}}{b - a}.$$

Proof. A simple calculation reveals:

$$\sum_{i=0}^n a^i b^{n-i} = b^n \left(1 + \frac{a}{b} + \dots + \left(\frac{a}{b}\right)^n\right) = b^n \frac{1 - \left(\frac{a}{b}\right)^{n+1}}{1 - \frac{a}{b}} = \frac{b^{n+1} - a^{n+1}}{b - a}.$$

□

After we have introduced all notation that is necessary to understand the structure of the solution, we can now finally state the probability for each tree topology as follows:

Theorem 4.11. *The probability for the tree topology $T = (G, m)$, $G \subseteq L$, under the segmentation process from Definition 4.3 is given as $\mathbb{P}_t(T) = (\lambda_{\emptyset}^{(L)})^t$ for $G = \emptyset$, and, for $G \neq \emptyset$, as*

$$\mathbb{P}_t(T) = \sum_{\gamma \in H \subseteq G} (-1)^{|H|-1} [(\lambda_{G_{\gamma}(H)}^{(L)})^t - (\lambda_{\emptyset}^{(L)})^t] f(T, H), \quad (4.11)$$

where, for $H \subseteq G$,

$$f(T, H) := \prod_{\alpha \in G} g(T_{\alpha}(H)) \quad (4.12)$$

with

$$g(T) = \frac{\rho_{\gamma}}{\lambda_G - \lambda_{\emptyset}} \quad \text{for all } T = (G, m), G \neq \emptyset, \text{ with root } \gamma \in G,$$

so that in particular

$$g(T_{\alpha}(H)) := \frac{\rho_{\alpha}}{\lambda_{G_{\alpha}(H)}^{(I_{\alpha})} - \lambda_{\emptyset}^{(I_{\alpha})}}. \quad (4.13)$$

The segmentation process from Definition 4.3 is a Markov chain that can be viewed in the forward as well as in the backward direction (in analogy with the Kolmogorov forward - and backward equations for continuous-time Markov chains, see [2]): In the forward direction, the growth of the corresponding ultrametric tree is at the tree top. Here, the external branches are extended in case a segment is not affected by a separation event and split up, respectively, when a separation event occurs. Conversely, in the backward direction, the tree grows at its base, i.e. the branch leading to the root is extended and the two corresponding subtrees merge, respectively. The independence of the segments turns out to be advantageous when formulating the process in the forward direction as in Definition 4.3. In contrast, in the backward direction, one only has to deal with two objects, namely the left and the right subtree that emerge via the first segmentation event (and are joined when looking back), instead of a possibly large number of smaller segments at the top. This will be the advantageous point of view for the proof.

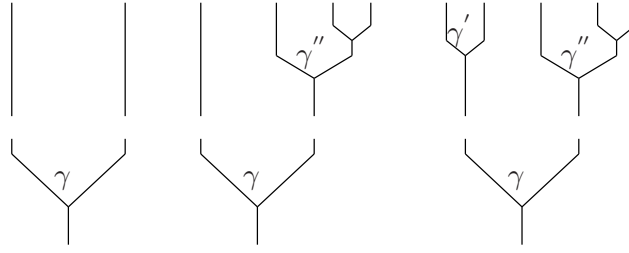


Figure 4.7: Joining together the left and the right subtree with respect to the root γ . Three different cases arise depending on whether the left and/or right subtree are empty trees. These cases are treated separately in the proof.

Proof. of Theorem 4.11. We will prove the claim via induction by - proceeding from top to base of a tree - progressively merging pairs of subtrees. In doing so, we firstly need some properties that refer to this particular tree decomposition. Let us consider a tree topology $T = (G, m)$, $\emptyset \neq G \subseteq L$, for any set of links L . The root of T is denoted with $\gamma \in G$. In case γ has two children nodes, then these are denoted with γ' (on $L_{<\gamma}$) and γ'' (on $L_{>\gamma}$). We then define the left subtree T' of T as $T' = (G_{<\gamma}, m^{(G_{<\gamma})})$ and analogously the right subtree T'' as $T'' = (G_{>\gamma}, m^{(G_{>\gamma})})$, both obviously with less nodes than T . For convenience we will denote $L_{<\gamma}$ ($L_{>\gamma}$) with L' (L'') as well as the respective nodes with $G' = G_{<\gamma}$ ($G'' = G_{>\gamma}$). In case γ has none or only one offspring node, we have to consider the empty tree as left and/or right subtree. Consequently, the offspring nodes of root γ are specified through the preimage of γ from the function m , i.e. $m^{-1}(\gamma) \in \{\{\emptyset\}, \{\gamma'\}, \{\gamma''\}, \{\gamma', \gamma''\}\}$. T can then be obtained by joining these subtrees together at root γ , see also Figure 4.7. With respect to the segmentation process, this refers to the event when the complete segment L is first cut at link γ , taking into account that this might happen at any time $j \in \{1, \dots, t\}$, i.e. L is preserved for $i = j - 1 \in \{0, \dots, t - 1\}$ times while the respective topologies T' and T'' last for the remaining $t - 1 - i$ time steps.

It is thus clear that

$$\mathbb{P}_t(T) = \sum_{i=0}^{t-1} (\lambda_{\emptyset}^{(L)})^i \rho_{\gamma} \mathbb{P}_{t-1-i}(T') \mathbb{P}_{t-1-i}(T''). \quad (4.14)$$

For all $L = L' \cup L'' \cup \{\gamma\}$ and all $G' \subseteq L'$, $G'' \subseteq L''$, we find due to the product structure of the lambda coefficients, compare (4.10),

$$\lambda_{G'}^{(L')} \cdot \lambda_{G''}^{(L'')} = \lambda_{G' \cup G'' \cup \{\gamma\}}^{(L)}. \quad (4.15)$$

Furthermore, Lemma 4.10 together with (4.13) implies

$$\begin{aligned} \rho_\alpha \sum_{i=0}^{t-1} (\lambda_\emptyset^{(I_\alpha)})^i (\lambda_{G_\alpha(H)}^{(I_\alpha)})^{t-i-1} &= \frac{\rho_\alpha}{\lambda_{G_\alpha(H)}^{(I_\alpha)} - \lambda_\emptyset^{(I_\alpha)}} \cdot ((\lambda_{G_\alpha(H)}^{(I_\alpha)})^t - (\lambda_\emptyset^{(I_\alpha)})^t) \\ &= g(T_\alpha(H)) ((\lambda_{G_\alpha(H)}^{(I_\alpha)})^t - (\lambda_\emptyset^{(I_\alpha)})^t) \end{aligned} \quad (4.16)$$

for all $\emptyset \neq G \subseteq L$ and $H \subseteq L$. For all $m^{-1}(\gamma) \subseteq H \subseteq G$ one finds

$$G_\gamma((H \cup \{\gamma\}) \setminus C) = \{\gamma\} \cup \bigcup_{\eta \in C} G_\eta(H) \quad \text{for } C \subseteq m^{-1}(\gamma). \quad (4.17)$$

An important property for the nodes of a subtree is the following: For all $H \subseteq G$ with $H' := G' \cap H$ and $H'' := G'' \cap H$ one has

$$\begin{aligned} G_\alpha(H) &= G_\alpha(H') = G'_\alpha(H') \quad \text{for all } \alpha \in G' \text{ and} \\ G_\alpha(H) &= G_\alpha(H'') = G''_\alpha(H'') \quad \text{for all } \alpha \in G'', \end{aligned} \quad (4.18)$$

so that consequently

$$\begin{aligned} T_\alpha(H) &= T'_\alpha(H') \quad \text{for all } \alpha \in G' \text{ and} \\ T_\alpha(H) &= T''_\alpha(H'') \quad \text{for all } \alpha \in G''. \end{aligned}$$

For all those H , this then leads to the following product rule for the function $f(T, H)$ from (4.12):

$$\begin{aligned} f(T, H) &= g(T_\gamma(H)) \cdot \prod_{\alpha \in G'} g(T_\alpha(H)) \prod_{\alpha \in G''} g(T_\alpha(H)) \\ &= g(T_\gamma(H)) \cdot \prod_{\alpha \in G'} g(T'_\alpha(H')) \prod_{\alpha \in G''} g(T''_\alpha(H'')) = g(T_\gamma(H)) f(T', H') f(T'', H''). \end{aligned} \quad (4.19)$$

Note that in case $G' = \emptyset$ or $G'' = \emptyset$, the corresponding empty product is defined as 1 as usual.

We now continue with the proof via induction over $|G|$. In case $G = \emptyset$, the claim holds trivially. For $G \subseteq L$ such that $|G| = 1$, i.e. $G = \{\gamma\}$, the left as well as the right subtree are empty trees. Using first (4.14), then the result for $G' = G'' = \emptyset$, then (4.15), and finally (4.16), we obtain

$$\begin{aligned} \mathbb{P}_t(T) &= \sum_{i=0}^{t-1} (\lambda_\emptyset^{(L)})^i \rho_\gamma \mathbb{P}_{t-1-i}(T') \mathbb{P}_{t-1-i}(T'') = \sum_{i=0}^{t-1} (\lambda_\emptyset^{(L)})^i \rho_\gamma (\lambda_\emptyset^{(L')})^{t-1-i} (\lambda_\emptyset^{(L'')})^{t-1-i} \\ &= \sum_{i=0}^{t-1} (\lambda_\emptyset^{(L)})^i \rho_\gamma (\lambda_\gamma^{(L)})^{t-1-i} = g(T_\gamma(\{\gamma\})) \left((\lambda_\gamma^{(L)})^t - (\lambda_\emptyset^{(L)})^t \right). \end{aligned}$$

We then assume the claim to hold for all tree topologies $T = (G, m)$ for all possible set of links \tilde{L} and $G \subseteq \tilde{L}$ with $|G| \leq k$ for some $k \in \mathbb{N}$. Thus, we next turn to $G = \{\alpha_1, \dots, \alpha_{k+1}\}$, $G \subseteq L$, and fixed $T = (G, m)$.

T with root α_1

We consider the case that T has the root $\gamma = \alpha_1$ such that the left subtree T' is an empty tree while T'' has the root $\gamma'' \in G''$, i.e. $m^{-1}(\gamma) = \{\gamma''\}$. We then find

$$\begin{aligned}
\mathbb{P}_t(T) &= \sum_{i=0}^{t-1} (\lambda_{\emptyset}^{(L)})^i \rho_{\gamma} \mathbb{P}_{t-1-i}(T') \mathbb{P}_{t-1-i}(T'') \\
&= \sum_{i=0}^{t-1} (\lambda_{\emptyset}^{(L)})^i \rho_{\gamma} (\lambda_{\emptyset}^{(L')})^{t-1-i} \sum_{\gamma'' \in H'' \subseteq G''} (-1)^{|H''|-1} \left((\lambda_{G''_{\gamma''}(H'')}^{(L'')})^{t-1-i} - (\lambda_{\emptyset}^{(L'')})^{t-1-i} \right) f(T'', H'') \\
&= \sum_{i=0}^{t-1} \lambda_{\emptyset}^i \rho_{\gamma} \sum_{\gamma'' \in H'' \subseteq G''} (-1)^{|H''|-1} \left(\lambda_{G_{\gamma}((H'' \cup \{\gamma\}) \setminus \{\gamma''\})}^{t-1-i} - \lambda_{G_{\gamma}(H'' \cup \{\gamma\})}^{t-1-i} \right) f(T'', H'') \\
&= \sum_{\gamma'' \in H'' \subseteq G''} (-1)^{|H''|-1} g(T_{\gamma}((H'' \cup \{\gamma\}) \setminus \{\gamma''\})) (\lambda_{G_{\gamma}((H'' \cup \{\gamma\}) \setminus \{\gamma''\})}^t - \lambda_{\emptyset}^t) f(T'', H'') \\
&\quad - \sum_{\gamma'' \in H'' \subseteq G''} (-1)^{|H''|-1} g(T_{\gamma}(H'' \cup \{\gamma\})) (\lambda_{G_{\gamma}(H'' \cup \{\gamma\})}^t - \lambda_{\emptyset}^t) f(T'', H'') \\
&= \sum_{\gamma'' \in H'' \subseteq G''} (-1)^{|H''|-1} (\lambda_{G_{\gamma}((H'' \cup \{\gamma\}) \setminus \{\gamma''\})}^t - \lambda_{\emptyset}^t) f(T, (H'' \cup \{\gamma\}) \setminus \{\gamma''\}) \\
&\quad - \sum_{\gamma'' \in H'' \subseteq G''} (-1)^{|H''|-1} (\lambda_{G_{\gamma}(H'' \cup \{\gamma\})}^t - \lambda_{\emptyset}^t) f(T, H'' \cup \{\gamma\}) \\
&= \sum_{\gamma \in H \subseteq G \setminus \gamma''} (-1)^{|H|-1} (\lambda_{G_{\gamma}(H)}^t - \lambda_{\emptyset}^t) f(T, H) - \sum_{\{\gamma, \gamma''\} \subseteq H \subseteq G} (-1)^{|H|} (\lambda_{G_{\gamma}(H)}^t - \lambda_{\emptyset}^t) f(T, H) \\
&= \sum_{\gamma \in H \subseteq G} (-1)^{|H|-1} (\lambda_{G_{\gamma}(H)}^t - \lambda_{\emptyset}^t) f(T, H).
\end{aligned}$$

Here, we have first used (4.14), then the induction hypothesis, and then the product structure of the lambda coefficients (4.15) together with the property (4.17) combined with (4.18). Next, we involve (4.16) (separately on each term in the brackets), use property (4.19) and finally change the summation variable. All topologies with root $\gamma = \alpha_{|G|}$ can be treated analogously.

T with root $\notin \{\alpha_1, \alpha_{|G|}\}$

For a topology $T = (G, m)$ with root $\gamma = \alpha_i$, $i = 2, \dots, |G| - 1$, we have to consider the left subtree T' with root γ' as well as the right subtree T'' with root γ'' , i.e. $m^{-1}(\gamma) = \{\gamma', \gamma''\}$. Proceeding exactly as in the previous case, we obtain

$$\begin{aligned}
\mathbb{P}_t(T) &= \sum_{i=0}^{t-1} (\lambda_{\emptyset}^{(L)})^i \rho_{\gamma} \mathbb{P}_{t-1-i}(T') \mathbb{P}_{t-1-i}(T'') \\
&= \sum_{i=0}^{t-1} (\lambda_{\emptyset}^{(L)})^i \rho_{\gamma} \sum_{\gamma' \in H' \subseteq G'} (-1)^{|H'|-1} \left((\lambda_{G'_{\gamma'}(H')}^{(L')})^{t-1-i} - (\lambda_{\emptyset}^{(L')})^{t-1-i} \right) f(T', H') \\
&\quad \times \sum_{\gamma'' \in H'' \subseteq G''} (-1)^{|H''|-1} \left((\lambda_{G''_{\gamma''}(H'')}^{(L'')})^{t-1-i} - (\lambda_{\emptyset}^{(L'')})^{t-1-i} \right) f(T'', H'') \\
&= \sum_{i=0}^{t-1} (\lambda_{\emptyset}^{(L)})^i \rho_{\gamma} \sum_{\gamma' \in H' \subseteq G'} \sum_{\gamma'' \in H'' \subseteq G''} (-1)^{|H'|+|H''|} \left(\lambda_{G_{\gamma}((H' \cup H'' \cup \{\gamma\}) \setminus \{\gamma', \gamma''\})}^{t-1-i} \right. \\
&\quad \left. - \lambda_{G_{\gamma}((H' \cup H'' \cup \{\gamma\}) \setminus \{\gamma''\})}^{t-1-i} - \lambda_{G_{\gamma}((H' \cup H'' \cup \{\gamma\}) \setminus \{\gamma'\})}^{t-1-i} + \lambda_{G_{\gamma}(H' \cup H'' \cup \{\gamma\})}^{t-1-i} \right) f(T', H') f(T'', H'') \\
&= \sum_{\gamma' \in H' \subseteq G'} \sum_{\gamma'' \in H'' \subseteq G''} (-1)^{|H'|+|H''|} \times \\
&\quad \left(g(T_{\gamma}((H' \cup H'' \cup \{\gamma\}) \setminus \{\gamma', \gamma''\})) (\lambda_{G_{\gamma}(H' \cup H'' \cup \{\gamma\}) \setminus \{\gamma', \gamma''\}}^t - \lambda_{\emptyset}^t) \right. \\
&\quad - g(T_{\gamma}((H' \cup H'' \cup \{\gamma\}) \setminus \{\gamma''\})) (\lambda_{G_{\gamma}(H' \cup H'' \cup \{\gamma\}) \setminus \{\gamma''\}}^t - \lambda_{\emptyset}^t) \\
&\quad - g(T_{\gamma}((H' \cup H'' \cup \{\gamma\}) \setminus \{\gamma'\})) (\lambda_{G_{\gamma}(H' \cup H'' \cup \{\gamma\}) \setminus \{\gamma'\}}^t - \lambda_{\emptyset}^t) \\
&\quad \left. + g(T_{\gamma}(H' \cup H'' \cup \{\gamma\})) (\lambda_{G_{\gamma}(H' \cup H'' \cup \{\gamma\})}^t - \lambda_{\emptyset}^t) \right) f(T', H') f(T'', H'') \\
&= \sum_{\gamma \in H \subseteq G \setminus \{\gamma', \gamma''\}} (-1)^{|H|-1} (\lambda_{G_{\gamma}(H)}^t - \lambda_{\emptyset}^t) f(T, H) \\
&\quad - \sum_{\{\gamma, \gamma'\} \subseteq H \subseteq G \setminus \{\gamma''\}} (-1)^{|H|} (\lambda_{G_{\gamma}(H)}^t - \lambda_{\emptyset}^t) f(T, H) \\
&\quad - \sum_{\{\gamma, \gamma''\} \subseteq H \subseteq G \setminus \{\gamma'\}} (-1)^{|H|} (\lambda_{G_{\gamma}(H)}^t - \lambda_{\emptyset}^t) f(T, H) \\
&\quad + \sum_{\{\gamma, \gamma', \gamma''\} \subseteq H \subseteq G} (-1)^{|H|-1} (\lambda_{G_{\gamma}(H)}^t - \lambda_{\emptyset}^t) f(T, H) \\
&= \sum_{\gamma \in H \subseteq G} (-1)^{|H|-1} (\lambda_{G_{\gamma}(H)}^t - \lambda_{\emptyset}^t) f(T, H).
\end{aligned}$$

(4.20)

□

We have now stated an explicit formula for the probability of a certain tree topology T , $\mathbb{P}_t(T)$. To further show its special structure, we can explain the probability (4.11) via *subtree decomposition*:

Definition 4.12 (Subtree decomposition). *Given a tree topology $T = (G, m)$ with root $\gamma \in G$, $\emptyset \neq G \subseteq L$, then each $\gamma \in H \subseteq G$ describes a decomposition of T into (non-empty) subtrees $T_\alpha(H) = (G_\alpha(H), m^{(G_\alpha(H))})$, $\alpha \in H$, each with root $\alpha \in H$ and internal nodes $G_\alpha(H)$.*

Obviously, there exist $2^{|G|-1}$ different decomposition of a topology T into subtrees, the simplest being the one for $H = \{\gamma\}$ such that $T_\gamma(\{\gamma\}) = T$, the finest the one for $H = G$ where each internal node $\alpha \in G$ is root of a subtree. Another example for subtree decomposition is shown in Figure 4.8. Using subtree decomposition, we can also state (4.12) differently:

Remark 4.13. *For any tree topology $T = (G, m)$, $\emptyset \neq G \subseteq L$, we can state (4.12) as*

$$f(T, H) = \prod_{\alpha \in H} \prod_{\beta \in G_\alpha(H)} g(T_\beta(H)). \quad (4.21)$$

Thus, as we can see from (4.11), to state the probability for a tree topology T , we have to sum over all possible subtree decompositions of T , and furthermore, the structure of the function $f(T, H)$ (4.21) implies that all these subtrees are conditionally independent.

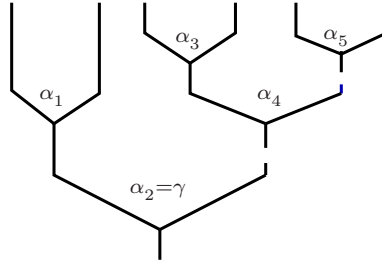


Figure 4.8: Decomposition of a tree topology into three subtrees via $H = \{\gamma, \alpha_4, \alpha_5\}$ such that $G_\gamma(H) = \{\alpha_1, \gamma\}$, $G_{\alpha_4}(H) = \{\alpha_3, \alpha_4\}$ and $G_{\alpha_5}(H) = \{\alpha_5\}$.

Subtree decomposition also explains the four arising sums in (4.20) of the above proof, i.e.

$$\begin{aligned} \mathbb{P}_t(T) = & \sum_{\gamma \in H \subseteq G \setminus \{\gamma', \gamma''\}} (-1)^{|H|-1} (\lambda_{G_\gamma(H)}^t - \lambda_\emptyset^t) f(T, H) - \sum_{\{\gamma, \gamma'\} \subseteq H \subseteq G \setminus \{\gamma''\}} (-1)^{|H|} (\lambda_{G_\gamma(H)}^t - \lambda_\emptyset^t) f(T, H) \\ & - \sum_{\{\gamma, \gamma''\} \subseteq H \subseteq G \setminus \{\gamma'\}} (-1)^{|H|} (\lambda_{G_\gamma(H)}^t - \lambda_\emptyset^t) f(T, H) + \sum_{\{\gamma, \gamma', \gamma''\} \subseteq H \subseteq G} (-1)^{|H|-1} (\lambda_{G_\gamma(H)}^t - \lambda_\emptyset^t) f(T, H). \end{aligned} \quad (4.22)$$

Here, the (non-empty) left subtree T' and the (non-empty) right subtree T'' with respect to the root γ of $T = (G, m)$ are joined together at γ . The induction ansatz implies that we consider all $2^{|G'| - 1}$ subtree decompositions of T' as well as all $2^{|G''| - 1}$ subtree decompositions of T'' . Consequently, there exist four possibilities to incorporate $\{\gamma\} = G \setminus (G' \cup G'')$ into each subtree decomposition (with respect to T' and T'') to finally obtain all possible $2^{|G| - 1}$ subtree decompositions of the tree T (see Figure 4.9):

- the subtree of the subtree decomposition of T' that contains γ' and the subtree of the subtree decomposition of T'' that contains γ'' are joined together via γ to form one subtree as part of the subtree decomposition of T (see Figure 4.9 a)); this corresponds to the first sum of (4.22).
- the subtree of the subtree decomposition of T'' that contains γ'' is joined together with γ while the subtree of the subtree decomposition of T' that contains γ' remains a separate part of the subtree decomposition of T (see Figure 4.9 b)); this corresponds to the second sum of (4.22).
- the subtree of the subtree decomposition of T' that contains γ' is joined together with γ while the subtree of the subtree decomposition of T'' that contains γ'' remains a separate part of the subtree decomposition of T (see Figure 4.9 c)); this corresponds to the third sum of (4.22).
- the subtrees of the decompositions of T' and T'' , respectively, remain unchanged and γ becomes the only node of a separate subtree of the subtree decomposition of T (see Figure 4.9 d)); this corresponds to the fourth sum of (4.22).

These four cases, or more precisely, the set of nodes that belong to the subtree that contains the root γ , correspond to the four different cases of (4.17) (assuming that $m^{-1}(\gamma) = \{\gamma', \gamma''\}$). Analogously, the two arising sums in the proof for $\gamma = \alpha_1$ (and $\gamma = \alpha_{|G|}$, respectively) can be explained in the obvious way.

After stating explicitly the probability for a certain tree topology, we furthermore know that $\mathbb{P}(F_t = G) = \sum_{T: T=(G, m)} \mathbb{P}_t(T)$, $G \subseteq L$, holds for the segmentation process. Next, we finally show that the solution of the recombination equation can indeed be stated as the sum over all possible tree probabilities:

Proposition 4.14. *For the coefficient functions of the recombination equation, one finds*

$$a_G(t) = \mathbb{P}(F_t = G), \quad \text{for all } G \subseteq L.$$

Before turning to the proof, we first need to express the coefficient functions on segments (as we have done it for recombinators etc. in Section 3.4), i.e. for $G \subseteq L$, $\alpha \in G$, we obtain

$$\sum_{H \subseteq L_{\geq \alpha}} a_{G < \alpha \cup H}^{(L)}(t) = a_{G < \alpha}^{(L < \alpha)}(t), \quad (4.23)$$

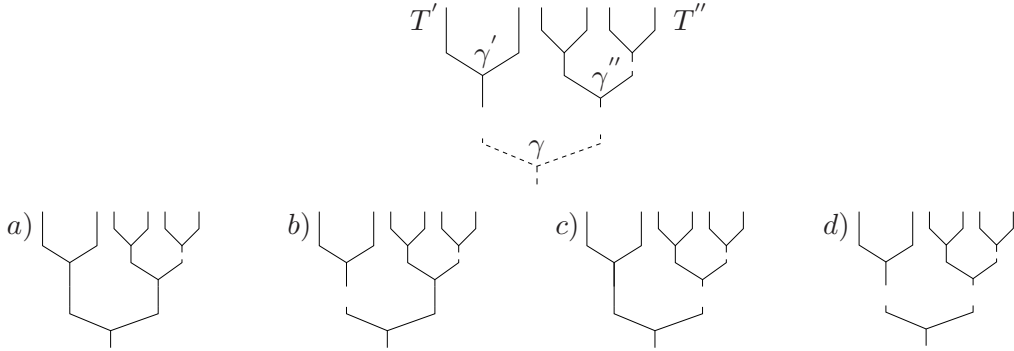


Figure 4.9: The non-empty trees T' and T'' are joined together at root γ to give rise to the tree T . With reference to the respective subtree decompositions of T' and T'' , there exist four possibilities to incorporate γ to form a subtree decomposition of T ; these are explained in the text.

where $a_{G < \alpha}^{(L < \alpha)}(t)$ denotes the respective coefficient function of the recombination dynamics on $\mathcal{P}(X_0 \times \cdots \times X_{[\alpha]})$ (and analogously for the segment $L_{> \alpha}$). For consistency, $a_{\emptyset}^{(\emptyset)}(t) := 1$. This is again a direct consequence of Proposition 3.2. We can then rewrite the iteration of the coefficient functions (3.7) as

$$a_G^{(L)}(t+1) = \lambda_{\emptyset}^{(L)} a_G^{(L)}(t) + \sum_{\alpha \in G} \rho_{\alpha} a_{G < \alpha}^{(L < \alpha)}(t) a_{G > \alpha}^{(L > \alpha)}(t). \quad (4.24)$$

Analogously, the segmentation process can be defined on particular segments, as usual we denote this by an upper index in brackets.

Proof. of Proposition 4.14

To prove the assertion, we show that $\mathbb{P}(F_t^{(L)} = G)$, $G \subseteq L$, indeed fulfils iteration (4.24). For $G = \emptyset$, the claim is obvious. For $G \neq \emptyset$, we fix one tree topology $T = (G, m)$. T then has root $\gamma \in G$ and the corresponding left subtree T' on $L_{< \gamma}$ and right subtree T'' on $L_{> \gamma}$. We then find:

$$\begin{aligned} \mathbb{P}_{t+1}(T) &= \sum_{i=0}^t \lambda_{\emptyset}^i \rho_{\gamma} \mathbb{P}_{t-i}(T') \mathbb{P}_{t-i}(T'') \\ &= \lambda_{\emptyset} \sum_{i=0}^{t-1} \lambda_{\emptyset}^i \rho_{\gamma} \mathbb{P}_{t-1-i}(T') \mathbb{P}_{t-1-i}(T'') + \rho_{\gamma} \mathbb{P}_t(T') \mathbb{P}_t(T'') = \lambda_{\emptyset} \mathbb{P}_t(T) + \rho_{\gamma} \mathbb{P}_t(T') \mathbb{P}_t(T''), \end{aligned}$$

where we again use (4.14) in the first and in the last step. Since this holds for all tree topologies T with corresponding left and right subtrees T' and T'' as well as

corresponding root $\gamma \in G$, we sum over all tree topologies (both sides) and obtain

$$\begin{aligned}
\mathbb{P}(F_{t+1}^{(L)} = G) &= \sum_{T:T=(G,m)} \mathbb{P}_{t+1}(T) = \lambda_{\emptyset} \sum_{T:T=(G,m)} \mathbb{P}_t(T) + \sum_{\substack{T:T=(G,m) \\ T'=(G_{<\gamma},m^{(L<\gamma)}), \\ T''=(G_{>\gamma},m^{(L>\gamma)})}} \rho_{\gamma} \mathbb{P}_t(T') \mathbb{P}_t(T'') \\
&= \lambda_{\emptyset} \sum_{T:T=(G,m)} \mathbb{P}_t(T) + \sum_{\gamma \in G} \rho_{\gamma} \sum_{T':T'=(G_{<\gamma},m^{(G<\gamma)})} \mathbb{P}_t(T') \sum_{T'':T''=(G_{>\gamma},m^{(G>\gamma)})} \mathbb{P}_t(T'') \\
&= \lambda_{\emptyset} \mathbb{P}(F_t^{(L)} = G) + \sum_{\gamma \in G} \rho_{\gamma} \mathbb{P}(F_t^{(L<\gamma)} = G_{<\gamma}) \mathbb{P}(F_t^{(L>\gamma)} = G_{>\gamma}).
\end{aligned}$$

This obviously corresponds to the iteration (4.24), and since the initial value at time 0, $\mathbb{P}(F_0^{(L)} = G) = \sum_{T:T=(G,m)} \mathbb{P}_0(T) = \delta_{G,\emptyset}$ - compare Theorem 4.11 - is also fulfilled, this proves the assertion. \square

Proposition 4.14 finally explains the stochastic interpretation of the coefficient functions from Section 3.3. Since the segmentation process keeps only track of the links that have been cut until time t with reference to a single ancestry, the fact that $a_G(t) = \mathbb{P}(F_t = G)$ justifies to interpret $a_G(t)$ as the probability that the links that have been involved in recombination in a single individual until time t are exactly those of G .

The final result then follows directly from Proposition 4.14:

Corollary 4.15. *The discrete-time recombination equation (3.7) has the solution*

$$p_t = \sum_{G \subseteq L} a_G(t) R_G(p_0),$$

where

$$a_G(t) = \sum_{T:T=(G,m)} \mathbb{P}_t(T) \quad (4.25)$$

for all $G \subseteq L$ and with $\mathbb{P}_t(T)$ as given in Theorem 4.11. \square

Thus, we have found an explicit representation for the solution of the recombination dynamics. What we are still left with is to enumerate all possible tree topologies for a given $G \subseteq L$, i.e. all $C_{|G|}$ different full binary trees.

Since trees - and in particular binary trees - are widely used structures that find a lot of applications especially in computer science, there exist many efficient algorithms to enumerate and generate them. Several of these algorithms also concentrate on full binary trees since there exists a well-known 1-to-1-correspondence between all full (often also called *strict* or *regular*) binary trees with n internal nodes and all general binary trees with in total n nodes [71]. The general idea to enumerate all binary trees is to represent each tree topology as a sequence of integers (or even as a single integer number) through a bijection, and to develop an efficient algorithm to generate all

appropriate (tree-representing) sequences and via them finally all possible binary trees. The general procedure to represent a tree topology with n nodes by a sequence of integers is the following described in [49]: each node is assigned a certain integer (e.g. for our trees, the index of the corresponding link) and by traversing the nodes in a specific order, uniquely determined n -tuples are obtained (some methods might even require the use of two traverses [49]). Commonly used orders for such a traversal are for example preorder traversal and inorder traversal, refer to [22]. For some methods, these sequences are then converted into integers, which is usually referred to as *ranking* while the reverse operation is called *unranking*. Indeed, there also exist methods that map directly from trees to integers, see for example [62]. However, the choice of the most efficient and appropriate method depends on the respective aspects that are essential to the application. For example, the mapping to a single integer, which is usually from the set of binary trees to $\{1, \dots, C_n\}$, is of particular use if the trees should follow a specific lexicographic order.

The first important work in this field was done by Knott [44] who encoded n -node binary trees by certain permutations of $\{1, \dots, n\}$, the *tree permutations*. Furthermore, he defined the (bijective) ranking function $rank(T)$ to assign each binary tree a number in the set $\{1, \dots, C_n\}$. The inverse of this function $rank^{-1}(i, n)$ then returns the tree permutation corresponding to the tree T with $rank(T) = i$. Using this method, the function can be used to generate all n -node binary trees. Zaks [71] represents full binary trees with n internal nodes by 0-1 sequences of length $2n$. He states conditions for these sequences to be *feasible*, i.e. to let them have the property that there exists a unique full binary tree that is represented by this sequence. Moreover, he proposes an algorithm that produces all C_n feasible sequences and thus leads to the generation of all full binary trees.

Particularly interesting - since the procedure shows similarities with our segmentation process - is the approach of Johnsen [38]. Johnsen generates full binary trees recursively, starting with the full binary tree with only one internal node, by adding two descending leaves to one of the trailing leaves of the current tree, a process he denotes with *grafting*. As a result, he describes each tree that was obtained by this procedure by its unique *grafting sequence*. Finally, he states a set of $k - 1$ inequalities whose integer solutions define all possible grafting sequences for full binary trees with k internal nodes. This allows the generation of all corresponding full binary trees.

Chapter 5

Outlook: The general recombination model

5.1 Introduction and Notation

So far, we restricted our recombination model to the particular case of single-crossovers. Even though this assumption is biologically justified in particular for shorter sequences (due to interference), the next step would be to formulate a recombination model that allows for *any* crossover event. While single-crossover recombination always leads to an *ordered* partition of sites, this no longer holds for general recombination events (see for example Figure 5.1). In connection with this, one of the main consequences of multiple crossovers is that it is no longer sufficient to explain recombination events via the links. Instead, we now have to describe recombination via induced partitions of sites. From the biological point of view (based on the assumption that exactly two parental gametes are involved in recombination), only partitions of the sites into two blocks (where one parent contributes one set of the sites, and the second parent the complementary set) have to be taken into account. In some cases (if only for the reason of mathematical completeness), it might be useful to include even more general processes of recombination that involve more than two parents. Despite its rather contrived construction, this may have applications for example in models that seek to explain cultural inheritance, compare [10]. For mathematical purposes, these models have been already discussed by Dawson [14, 15] and Baake [4]. However, to exclude the biologically meaningless cases, the corresponding recombination rates/probabilities



Figure 5.1: Effect of a double crossover between two types. In particular, the partition of sites is not ordered anymore.

can be set to zero.

In this chapter, a short introduction into the general recombination model and a first impression about the dynamics as well as the arising similarities and differences with previous results will be given. In doing so, we follow the same procedure as with the single-crossover model(s) in Chapter 3. These should serve as a starting point and motivation for further investigation of the general recombination model.

For the description of the general recombination model, we will need additional notation for partitions, where we primary follow the notation in [1]. As mentioned above, we only need the sites of $S = \{0, 1, \dots, n\}$ for modelling since the convenient ability to use links is no longer sufficient.

A *partition* \mathcal{A} of S is denoted by $\mathcal{A} = \{A_1, \dots, A_{|\mathcal{A}|}\}$ or for short $\mathcal{A} = (A_1|A_2|\dots|A_{|\mathcal{A}|})$, where the A_i are the *blocks* or *parts* of the partition \mathcal{A} . $|\mathcal{A}|$ denotes the number of blocks. All possible partitions are collected into the set $\Sigma(S) := \{(01\dots n), (0|12\dots n), \dots, (0|1|2|\dots|n)\}$, where in particular $I = (01\dots n)$ denotes the trivial partition that only consist of a single block while $\mathcal{S} = (0|1|2|\dots|n)$ denotes the partition where each block contains exactly one single element. For convenience, if the set of sites is clear, we will use the notation $\Sigma(S) = \Sigma$.

Furthermore, there is a (well-known) natural ordering of partitions which is defined as follows: for two partitions $\mathcal{A}, \mathcal{B} \in \Sigma$, $\mathcal{A} \preceq \mathcal{B}$ means that every block of \mathcal{A} is wholly contained in a block of \mathcal{B} . Then, \mathcal{A} is called a *refinement* of \mathcal{B} (or, \mathcal{B} is a *coarsening* of \mathcal{A}), and \preceq is the *refinement relation*. Obviously, $I \in \Sigma$ is the unique coarsest partition, whereas $\mathcal{S} \in \Sigma$ is the unique finest partition. For two partitions $\mathcal{A}, \mathcal{B} \in \Sigma$, the *finest joint coarsening* is denoted by $\mathcal{A} \vee \mathcal{B}$ and the *coarsest joint refinement* by $\mathcal{A} \wedge \mathcal{B}$.

Furthermore, a partition \mathcal{A} of S induces a partition \mathcal{U} on each subset $U \subseteq S$: for all $A \in \mathcal{A}$, either $A \cap U = \emptyset$ or $A \cap U \in \mathcal{U}$. This relation will be denoted by $\mathcal{U} = \mathcal{A} \overrightarrow{\cap} U$, see also [15] where this notation is used. Studying the general recombination model, induced partitions will be of significant importance.

Example 5.1. Let $S = \{0, 1, 2, 3, 4\}$, $\mathcal{A} = (023|14)$ and $\mathcal{B} = (03|12|4)$ and $U = \{0, 1, 2\}$. Then, $\mathcal{A} \wedge \mathcal{B} = (03|1|2|4)$, $\mathcal{A} \vee \mathcal{B} = (01234)$, $\mathcal{A} \overrightarrow{\cap} U = (02|1)$ and $\mathcal{B} \overrightarrow{\cap} U = (0|12)$.

The union of induced partitions on all parts of a partition of S is again a partition of S , indeed the following holds, compare [15]:

Corollary 5.2. Let $\mathcal{A} = (A_1|\dots|A_k)$ and $\mathcal{B}_1, \dots, \mathcal{B}_k$ be partitions of S . Then

$$\bigcup_{i=1}^k (\mathcal{B}_i \overrightarrow{\cap} A_i) = \mathcal{C}, \quad (5.1)$$

where \mathcal{C} is again a partition of S with $\mathcal{C} \preceq \mathcal{A}$. Furthermore, for a partition \mathcal{B} of S with $\mathcal{B} \preceq \mathcal{A}$, one finds

$$\bigcup_{i=1}^k (\mathcal{B} \overrightarrow{\cap} A_i) = \mathcal{B}.$$

□

As long as not stated otherwise, we take over all notation from Chapter 3 and 4. First of all, we have to redefine the recombinators in terms of partitions.

The recombinator

In analogy to the definition of the recombination operator via the links as in (3.2), we here define the recombinator for any partition $\mathcal{A} = (A_1|A_2|\dots|A_{|\mathcal{A}|}) \in \Sigma$ and for all $\omega \in \mathcal{P}(X)$ as

$$\bar{R}_{\mathcal{A}}(\omega) = \bigotimes_{i=1}^{|\mathcal{A}|} (\pi_{A_i} \cdot \omega) . \quad (5.2)$$

Analogous to the composite recombinators defined via set of links as in (3.6), we here find

$$\bar{R}_{\mathcal{A}} \circ \bar{R}_{\mathcal{B}} = \bar{R}_{\mathcal{A} \wedge \mathcal{B}} = \bar{R}_{\mathcal{B}} \circ \bar{R}_{\mathcal{A}} \text{ for arbitrary } \mathcal{A}, \mathcal{B} \in \Sigma ,$$

which obviously includes $\bar{R}_{\mathcal{A}}^2 = \bar{R}_{\mathcal{A}}$. We can now state a generalisation of Proposition 3.2 from Section 3.1, where the proof follows along the same lines:

Proposition 5.3. *Let $U \subseteq S$ and $\mathcal{A} \in \Sigma$ be any partition of S . Then, on $\mathcal{P}(X)$ the recombinators satisfy*

$$\pi_U \cdot \bar{R}_{\mathcal{A}}(p) = \pi_U \cdot \bar{R}_{\mathcal{B}}(p) \text{ for all } \mathcal{B} \in \Sigma \text{ with } \mathcal{B} \vec{\cap} U = \mathcal{A} \vec{\cap} U .$$

□

The intuitive content of Proposition 5.3 is the same as for the analogue in Proposition 3.2. When projecting on the sites of U , the partition of the sites of the complementary set $S \setminus U$ is of no relevance.

5.2 The general recombination model in continuous time

Let us start with the general recombination model in the IPL in *continuous* time since this will make clear that the continuous-time single-crossover model discussed in Section 3.2 is indeed a particular special case. We will show that the ‘nice’ properties observed in continuous time get lost as soon as we allow for any partition of sites (i.e. not only ordered partitions), and that the advantage of continuous time over discrete time - as in the single-crossover case - vanishes.

Let $\bar{\rho}_{\mathcal{A}} \geq 0$ denote the rate for a recombination event that corresponds to the partition $\mathcal{A} \in \Sigma$. We set $\bar{\rho}_I = 0$ since the partition I corresponds to an ‘empty’ recombination event (see (5.3)).

The general recombination equation then reads in analogy to (3.8):

$$\dot{p}_t = \sum_{I \neq \mathcal{A} \in \Sigma} \bar{\rho}_{\mathcal{A}}(\bar{R}_{\mathcal{A}} - \mathbb{1})(p_t), \quad (5.3)$$

starting from an initial distribution $p_0 \in \mathcal{P}(X)$, where as before $\mathbb{1} = \bar{R}_I$ denotes the recombinator that belongs to the trivial partition $I = (01 \dots n) \in \Sigma$. If we only refer to biological plausible cases, we set $\bar{\rho}_{\mathcal{A}} = 0$ for all $\mathcal{A} \in \Sigma$ with $|\mathcal{A}| \neq 2$. Obviously, we recover the single-crossover model (3.8) if we also set rates for unordered partitions $\mathcal{A} \in \Sigma$ to zero. As for the single-crossover model (in discrete as well as in continuous time), we expect the solution to be of the form

$$p_t = \sum_{\mathcal{A} \in \Sigma} \bar{a}_{\mathcal{A}}(t) \bar{R}_{\mathcal{A}}(p_0) \quad (5.4)$$

with $\bar{a}_{\mathcal{A}}(0) = \delta_{\mathcal{A}, I}$, where again the $\bar{a}_{\mathcal{A}}(t)$ are the deciding coefficient functions. In the following, we will show that this ansatz is indeed right and infer the corresponding differential equations for the coefficient functions. To this end, we first aim to determine $\bar{R}_{\mathcal{A}}(p_t)$ for any partition $\mathcal{A} = \{A_1, \dots, A_k\} \in \Sigma$ and thus calculate

$$\begin{aligned} \bar{R}_{\mathcal{A}}(p_t) &= \bar{R}_{\mathcal{A}}\left(\sum_{\mathcal{B} \in \Sigma} \bar{a}_{\mathcal{B}}(t) \bar{R}_{\mathcal{B}}(p_0)\right) = \pi_{A_1} \cdot p_t \otimes \dots \otimes \pi_{A_k} \cdot p_t \\ &= \pi_{A_1} \cdot \left(\sum_{\mathcal{B}_1 \in \Sigma} \bar{a}_{\mathcal{B}_1}(t) \bar{R}_{\mathcal{B}_1}(p_0)\right) \otimes \dots \otimes \pi_{A_k} \cdot \left(\sum_{\mathcal{B}_k \in \Sigma} \bar{a}_{\mathcal{B}_k}(t) \bar{R}_{\mathcal{B}_k}(p_0)\right) \\ &= \left(\sum_{\mathcal{B}_1 \in \Sigma} \bar{a}_{\mathcal{B}_1}(t) \pi_{A_1} \cdot \bar{R}_{\mathcal{B}_1}(p_0)\right) \otimes \dots \otimes \left(\sum_{\mathcal{B}_k \in \Sigma} \bar{a}_{\mathcal{B}_k}(t) \pi_{A_k} \cdot \bar{R}_{\mathcal{B}_k}(p_0)\right) \\ &= \sum_{\mathcal{B}_1, \dots, \mathcal{B}_k} \bar{a}_{\mathcal{B}_1}(t) \cdot \dots \cdot \bar{a}_{\mathcal{B}_k}(t) \left(\pi_{A_1} \cdot \bar{R}_{\mathcal{B}_1}(p_0) \otimes \dots \otimes \pi_{A_k} \cdot \bar{R}_{\mathcal{B}_k}(p_0)\right) \\ &= \sum_{\mathcal{B}_1, \dots, \mathcal{B}_k} \bar{a}_{\mathcal{B}_1}(t) \cdot \dots \cdot \bar{a}_{\mathcal{B}_k}(t) \left(\pi_{A_1} \cdot \bar{R}_{(\mathcal{B}_1 \vec{\cap} A_1) \cup (\mathcal{B}_2 \vec{\cap} A_2) \cup \dots \cup (\mathcal{B}_k \vec{\cap} A_k)}(p_0) \otimes \dots \otimes \right. \\ &\quad \left. \pi_{A_k} \cdot \bar{R}_{(\mathcal{B}_1 \vec{\cap} A_1) \cup (\mathcal{B}_2 \vec{\cap} A_2) \cup \dots \cup (\mathcal{B}_k \vec{\cap} A_k)}(p_0)\right) \\ &= \sum_{\mathcal{B}_1, \dots, \mathcal{B}_k} \bar{a}_{\mathcal{B}_1}(t) \cdot \dots \cdot \bar{a}_{\mathcal{B}_k}(t) \left(\bar{R}_{\mathcal{A}}(\bar{R}_{(\mathcal{B}_1 \vec{\cap} A_1) \cup (\mathcal{B}_2 \vec{\cap} A_2) \cup \dots \cup (\mathcal{B}_k \vec{\cap} A_k)})(p_0)\right) \\ &= \sum_{\mathcal{B}_1, \dots, \mathcal{B}_k} \bar{a}_{\mathcal{B}_1}(t) \cdot \dots \cdot \bar{a}_{\mathcal{B}_k}(t) \bar{R}_{(\mathcal{B}_1 \vec{\cap} A_1) \cup (\mathcal{B}_2 \vec{\cap} A_2) \cup \dots \cup (\mathcal{B}_k \vec{\cap} A_k)}(p_0). \end{aligned} \quad (5.5)$$

In the first five steps, we only use the ansatz for the solution p_t from (5.4), the definition of the recombinators as well as the linearity of the projectors. We then use assertion (5.1) of Corollary 5.2 together with Proposition 5.3 since for $\mathcal{C} := (\mathcal{B}_1 \vec{\cap} A_1) \cup (\mathcal{B}_2 \vec{\cap} A_2) \cup \dots \cup (\mathcal{B}_k \vec{\cap} A_k) \in \Sigma$ holds that $\mathcal{C} \vec{\cap} A_i = \mathcal{B}_i \vec{\cap} A_i$ for all $i \in \{1, \dots, k\}$. Afterwards, the definition of the recombinator is used, before employing $\mathcal{A} \wedge \mathcal{C} = \mathcal{C}$ since $\mathcal{C} \preceq \mathcal{A}$. This allows to state the induced differential equations for the coefficients of the solution (5.4):

Proposition 5.4. *The differential equations for the coefficients of the solution (5.4) are*

$$\dot{a}_{\mathcal{C}}(t) = \sum_{\mathcal{A} \succeq \mathcal{C}} \bar{\rho}_{\mathcal{A}} \left(\prod_{A \in \mathcal{A}} \sum_{\substack{\mathcal{Z} \in \Sigma: \\ \mathcal{Z} \vec{\cap} A = \mathcal{C} \vec{\cap} A}} \bar{a}_{\mathcal{Z}}(t) \right) - \sum_{\mathcal{A} \in \Sigma} \bar{\rho}_{\mathcal{A}} \bar{a}_{\mathcal{C}}(t) \quad (5.6)$$

for each $\mathcal{C} \in \Sigma$.

Proof. Having the ansatz $p_t = \sum_{\mathcal{B} \in \Sigma} \bar{a}_{\mathcal{B}}(t) \bar{R}_{\mathcal{B}}(p_0)$ for the solution of the recombination equation, one infers

$$\dot{p}_t = \sum_{\mathcal{A} \in \Sigma} \bar{\rho}_{\mathcal{A}} (\bar{R}_{\mathcal{A}} - \mathbb{1})(p_t) = \sum_{\mathcal{A} \in \Sigma} \bar{\rho}_{\mathcal{A}} (\bar{R}_{\mathcal{A}} - \mathbb{1}) \left(\sum_{\mathcal{B} \in \Sigma} \bar{a}_{\mathcal{B}}(t) \bar{R}_{\mathcal{B}}(p_0) \right) = \sum_{\mathcal{C} \in \Sigma} \dot{a}_{\mathcal{C}}(t) \bar{R}_{\mathcal{C}}(p_0). \quad (5.7)$$

The proof follows along the same lines as the proof of Theorem 3.7 from Section 3.3. We compare coefficients for $\bar{R}_{\mathcal{C}}(p_0)$ for a fixed $\mathcal{C} \in \Sigma$, where comparison of coefficients is justified for the same reason as stated in the proof of Theorem 3.7. The effect of any $\bar{R}_{\mathcal{A}}$ on p_t , $\mathcal{A} = (A_1 | \dots | A_k) \in \Sigma$, is given in (5.5), where we only find a contribution to $\bar{R}_{\mathcal{C}}(p_0)$ if $\mathcal{C} \preceq \mathcal{A}$, i.e. for those $\mathcal{B}_1, \dots, \mathcal{B}_k$ with $\mathcal{B}_1 \vec{\cap} A_1 = \mathcal{C} \vec{\cap} A_1, \dots, \mathcal{B}_k \vec{\cap} A_k = \mathcal{C} \vec{\cap} A_k$. Additionally, $\mathbb{1}(p_t)$ contributes to $\bar{R}_{\mathcal{C}}(p_0)$ only for $\mathcal{B} = \mathcal{C}$ in (5.7). Taking this together, (5.6) is obtained. \square

For completion, we show that the coefficient functions from (5.4) indeed form a probability vector:

Lemma 5.5. *Let $\underline{a}(t) = (\bar{a}_{(01\dots n)}(t), \dots, \bar{a}_{(0|1|\dots|n)}(t))$ denote the vector containing all coefficient functions. Then the induced differential equations $\dot{\underline{a}}_{\mathcal{C}}(t) = F_{\mathcal{C}}(\underline{a}(t)) - \sum_{\mathcal{A} \in \Sigma} \bar{\rho}_{\mathcal{A}} \bar{a}_{\mathcal{C}}(t)$, where $F_{\mathcal{C}}(\underline{a}(t)) := \sum_{\mathcal{A} \succeq \mathcal{C}} \bar{\rho}_{\mathcal{A}} \prod_{A \in \mathcal{A}} \sum_{\substack{\mathcal{Z} \in \Sigma: \\ \mathcal{Z} \vec{\cap} A = \mathcal{C} \vec{\cap} A}} \bar{a}_{\mathcal{Z}}(t)$, have a probability vector $\underline{a}(t)$ as solution.*

Proof. To prove the assertion, we have to show that

1. $F_{\mathcal{C}}(\underline{a}(t)) \geq 0$ for $\underline{a}(t) \geq 0$
2. $\sum_{\mathcal{C} \in \Sigma} F_{\mathcal{C}}(\underline{a}(t)) = \sum_{\mathcal{C} \in \Sigma} \bar{\rho}_{\mathcal{C}}$ for a probability vector $\underline{a}(t)$.

1. obviously holds since $\bar{\rho}_{\mathcal{A}} \geq 0$ for all $\mathcal{A} \in \Sigma$ and $\bar{a}_{\mathcal{Z}}(t) \geq 0$ for all $\mathcal{Z} \in \Sigma$ according to the assumption. Furthermore,

$$\sum_{\mathcal{C} \in \Sigma} F_{\mathcal{C}}(\underline{a}(t)) = \sum_{\mathcal{C} \in \Sigma} \sum_{\mathcal{A} \succeq \mathcal{C}} \bar{\rho}_{\mathcal{A}} \prod_{A \in \mathcal{A}} \sum_{\substack{\mathcal{Z} \in \Sigma: \\ \mathcal{Z} \vec{\cap} A = \mathcal{C} \vec{\cap} A}} \bar{a}_{\mathcal{Z}}(t) = \sum_{\mathcal{A} \in \Sigma} \bar{\rho}_{\mathcal{A}} \sum_{\mathcal{C} \preceq \mathcal{A}} \prod_{A \in \mathcal{A}} \sum_{\substack{\mathcal{Z} \in \Sigma: \\ \mathcal{Z} \vec{\cap} A = \mathcal{C} \vec{\cap} A}} \bar{a}_{\mathcal{Z}}(t) = \sum_{\mathcal{A} \in \Sigma} \bar{\rho}_{\mathcal{A}},$$

since for a fixed $\mathcal{A} \in \Sigma(S)$ holds:

$$\sum_{\mathcal{C} \preceq \mathcal{A}} \prod_{A \in \mathcal{A}} \sum_{\substack{\mathcal{Z} \in \Sigma: \\ \mathcal{Z} \vec{\cap} A = \mathcal{C} \vec{\cap} A}} \bar{a}_{\mathcal{Z}}(t) = \prod_{A \in \mathcal{A}} \sum_{\mathcal{D} \preceq I \in \Sigma(A)} \sum_{\substack{\mathcal{Z} \in \Sigma: \\ \mathcal{Z} \vec{\cap} A = \mathcal{D}}} \bar{a}_{\mathcal{Z}}(t) = \prod_{A \in \mathcal{A}} \sum_{\mathcal{Z} \in \Sigma(S)} \bar{a}_{\mathcal{Z}}(t) = 1,$$

where $\Sigma(A)$ denotes the set of all possible partitions of the sites that belong to $A \in \mathcal{A}$. This proves 2. \square

Next, let us have a look at the recombination dynamics of the general model, in particular in comparison with the corresponding single-crossover dynamics discussed in Chapter 3. Again, we start with three sites.

5.2.1 Three Sites

We consider the recombination model (5.3) for three sites $S = \{0, 1, 2\}$, with taking into account 5 possible partitions of sites. The differential equations for the coefficients of the solution are (compare (5.6)):

$$\begin{aligned}\dot{\bar{a}}_{(012)}(t) &= -(\bar{\rho}_{(0|12)} + \bar{\rho}_{(01|2)} + \bar{\rho}_{(02|1)} + \bar{\rho}_{(0|1|2)})\bar{a}_{(012)}(t), \\ \dot{\bar{a}}_{(0|12)}(t) &= \bar{\rho}_{(0|12)}\bar{a}_{(012)}(t) - (\bar{\rho}_{(01|2)} + \bar{\rho}_{(02|1)} + \bar{\rho}_{(0|1|2)})\bar{a}_{(0|12)}(t), \\ \dot{\bar{a}}_{(01|2)}(t) &= \bar{\rho}_{(01|2)}\bar{a}_{(012)}(t) - (\bar{\rho}_{(0|12)} + \bar{\rho}_{(02|1)} + \bar{\rho}_{(0|1|2)})\bar{a}_{(01|2)}(t), \\ \dot{\bar{a}}_{(02|1)}(t) &= \bar{\rho}_{(02|1)}\bar{a}_{(012)}(t) - (\bar{\rho}_{(0|12)} + \bar{\rho}_{(01|2)} + \bar{\rho}_{(0|1|2)})\bar{a}_{(02|1)}(t), \\ \dot{\bar{a}}_{(0|1|2)}(t) &= \bar{\rho}_{(0|1|2)}\bar{a}_{(012)}(t) + (\bar{\rho}_{(01|2)} + \bar{\rho}_{(02|1)} + \bar{\rho}_{(0|1|2)})\bar{a}_{(0|12)}(t) \\ &\quad + (\bar{\rho}_{(0|12)} + \bar{\rho}_{(02|1)} + \bar{\rho}_{(0|1|2)})\bar{a}_{(01|2)}(t) + (\bar{\rho}_{(0|12)} + \bar{\rho}_{(01|2)} + \bar{\rho}_{(0|1|2)})\bar{a}_{(02|1)}(t).\end{aligned}$$

They are thus linear differential equations with the following solution ($\bar{a}_{\mathcal{A}}(0) = \delta_{\mathcal{A},(012)}$):

$$\begin{aligned}\bar{a}_{(012)}(t) &= \exp(-(\bar{\rho}_{(0|12)} + \bar{\rho}_{(01|2)} + \bar{\rho}_{(02|1)} + \bar{\rho}_{(0|1|2)})t), \\ \bar{a}_{(0|12)}(t) &= (1 - \exp(-\bar{\rho}_{(0|12)}t)) \exp(-(\bar{\rho}_{(01|2)} + \bar{\rho}_{(02|1)} + \bar{\rho}_{(0|1|2)})t), \\ \bar{a}_{(01|2)}(t) &= (1 - \exp(-\bar{\rho}_{(01|2)}t)) \exp(-(\bar{\rho}_{(0|12)} + \bar{\rho}_{(02|1)} + \bar{\rho}_{(0|1|2)})t), \\ \bar{a}_{(02|1)}(t) &= (1 - \exp(-\bar{\rho}_{(02|1)}t)) \exp(-(\bar{\rho}_{(0|12)} + \bar{\rho}_{(01|2)} + \bar{\rho}_{(0|1|2)})t), \\ \bar{a}_{(0|1|2)}(t) &= \exp(-(\bar{\rho}_{(0|12)} + \bar{\rho}_{(01|2)} + \bar{\rho}_{(02|1)} + \bar{\rho}_{(0|1|2)})t) \\ &\quad (2 - \exp(\bar{\rho}_{(01|2)}t) - \exp(\bar{\rho}_{(0|12)}t) - \exp(\bar{\rho}_{(02|1)}t) \\ &\quad + \exp((\bar{\rho}_{(0|12)} + \bar{\rho}_{(01|2)} + \bar{\rho}_{(02|1)} + \bar{\rho}_{(0|1|2)})t)).\end{aligned}$$

It should be noted here that the differential equations for the coefficient functions are not only linear but their solution also suggests the same interpretation as in the single-crossover model. Note that the single-crossover solution for three sites is recovered here for $\bar{\rho}_{(02|1)} = \bar{\rho}_{(0|1|2)} = 0$ (i.e. (02|1) reflects the case of a double crossover while the partition (0|1|2) corresponds to the contrived case that three parents are involved in reproduction). In particular, $\bar{R}_{(0|12)} \hat{=} R_{\frac{1}{2}}$ from the definition of the recombinators via the links, and $\bar{R}_{(01|2)} \hat{=} R_{\frac{3}{2}}$.

LDE operators

In Section 3.2, we identified a particularly simple set of LDE operators that diagonalise the continuous-time single-crossover recombination dynamics. Later on, in Section 3.5, we used these for a linearisation of the more complicated discrete-time recombination dynamics. Recall that the inversion formula for these operators, compare (3.11), is directly obtained due to the property of the Möbius function. This raises the question whether there exists an equivalent set of operators for the general model. To find an appropriate transformation, as a starting point, we use a similar ansatz as before, and define a set of operators via the Möbius function, i.e.

$$\bar{T}_{\mathcal{A}} := \sum_{\mathcal{B} \preceq \mathcal{A}} \mu(\mathcal{B}, \mathcal{A}) \bar{R}_{\mathcal{B}}, \quad \text{for } \mathcal{A} \in \Sigma \quad (5.8)$$

where $\mu(\mathcal{B}, \mathcal{A})$ denotes the Möbius function for partitions. The inverse relation is then given by

$$\bar{R}_{\mathcal{A}} = \sum_{\mathcal{B} \preceq \mathcal{A}} \bar{T}_{\mathcal{B}}.$$

The corresponding Möbius function for the lattice of partitions is the following, for the proof refer to [59].

Proposition 5.6. *Let \mathcal{A}, \mathcal{B} be two partitions of a set with n elements, where $\mathcal{B} \preceq \mathcal{A}$ with $|\mathcal{B}| = k \geq |\mathcal{A}| = m$. Define $r_i :=$ number of blocks of \mathcal{A} that contain exactly i blocks of \mathcal{B} . The Möbius function is then given by*

$$\mu(\mathcal{B}, \mathcal{A}) = (-1)^{k-m} (2!)^{r_3} (3!)^{r_4} \dots ((k-1)!)^{r_k}.$$

For partitions \mathcal{A}, \mathcal{B} with $\mathcal{B} \not\preceq \mathcal{A}$, $\mu(\mathcal{B}, \mathcal{A}) = 0$. □

Remark 5.7. *It can be found in [8] that together with the ordering \preceq , the partially ordered set (Σ, \preceq) of partitions is indeed a (finite) geometric lattice. In particular, the minimal element of the poset is \mathcal{S} while the maximal element is I .*

Let us now apply the operators from (5.8) to the general model with three sites. We then obtain

$$\begin{aligned} \bar{T}_{(0|1|2)} &= \bar{R}_{(0|1|2)}, \\ \bar{T}_{(01|2)} &= \bar{R}_{(01|2)} - \bar{R}_{(0|1|2)}, \\ \bar{T}_{(0|12)} &= \bar{R}_{(0|12)} - \bar{R}_{(0|1|2)}, \\ \bar{T}_{(02|1)} &= \bar{R}_{(02|1)} - \bar{R}_{(0|1|2)}, \\ \bar{T}_{(012)} &= \bar{R}_{(012)} - \bar{R}_{(0|12)} - \bar{R}_{(01|2)} - \bar{R}_{(02|1)} + 2\bar{R}_{(0|1|2)}, \end{aligned}$$

and the operators fulfil the following differential equations:

$$\begin{aligned}
\frac{d}{dt} \bar{T}_{(0|1|2)}(p_t) &= 0, \\
\frac{d}{dt} \bar{T}_{(01|2)}(p_t) &= -(\bar{\rho}_{(0|12)} + \bar{\rho}_{(02|1)} + \bar{\rho}_{(0|1|2)}) \bar{T}_{(01|2)}(p_t), \\
\frac{d}{dt} \bar{T}_{(0|12)}(p_t) &= -(\bar{\rho}_{(01|2)} + \bar{\rho}_{(02|1)} + \bar{\rho}_{(0|1|2)}) \bar{T}_{(0|12)}(p_t), \\
\frac{d}{dt} \bar{T}_{(02|1)}(p_t) &= -(\bar{\rho}_{(01|2)} + \bar{\rho}_{(0|12)} + \bar{\rho}_{(0|1|2)}) \bar{T}_{(02|1)}(p_t), \\
\frac{d}{dt} \bar{T}_{(012)}(p_t) &= -(\bar{\rho}_{(01|2)} + \bar{\rho}_{(0|12)} + \bar{\rho}_{(02|1)} + \bar{\rho}_{(0|1|2)}) \bar{T}_{(012)}(p_t).
\end{aligned}$$

The transformation thus leads to diagonalisation of the dynamics and in comparison with the results for the single-crossover model, no differences are observed. Again, let us skip to four sites.

5.2.2 Four Sites

For four sites $S = \{0, 1, 2, 3\}$, we are dealing with 15 possible partitions of sites. In particular, the differential equations for the coefficients functions (5.6) are in general nonlinear, for example

$$\begin{aligned}
\dot{\bar{a}}_{(01|23)}(t) &= \bar{\rho}_{(01|23)} \left(\bar{a}_{(0123)}(t) + \bar{a}_{(01|23)}(t) + \bar{a}_{(012|3)}(t) + \bar{a}_{(013|2)}(t) + \bar{a}_{(01|2|3)}(t) \right) \\
&\quad \left(\bar{a}_{(0123)}(t) + \bar{a}_{(0|123)}(t) + \bar{a}_{(01|23)}(t) + \bar{a}_{(023|1)}(t) + \bar{a}_{(0|1|23)}(t) \right) - \sum_{\mathcal{A} \in \Sigma} \bar{\rho}_{\mathcal{A}} \bar{a}_{(01|23)}(t).
\end{aligned}$$

Recall that in the single-crossover setting the corresponding differential equations for the coefficient functions are *always* linear, see (3.21). Thus, just as in the *discrete-time* single-crossover model, the equations of the general model even in continuous time become more involved from four sites onwards. If we apply the transformation (5.8) to the four sites-model, similarities to the discrete-time single-crossover model can be

observed as well. In detail, one obtains

$$\begin{aligned}
\frac{d}{dt} \bar{T}_{(0|1|2|3)}(p_t) &= 0, \\
\frac{d}{dt} \bar{T}_{(0|1|23)}(p_t) &= - \left(\sum_{\substack{\mathcal{A} \in \Sigma: \\ \mathcal{A} \vec{\pi}(23)=(2|3)}} \bar{\rho}_{\mathcal{A}} \right) \bar{T}_{(0|1|23)}(p_t), \\
\frac{d}{dt} \bar{T}_{(01|2|3)}(p_t) &= - \left(\sum_{\substack{\mathcal{A} \in \Sigma: \\ \mathcal{A} \vec{\pi}(01)=(0|1)}} \bar{\rho}_{\mathcal{A}} \right) \bar{T}_{(01|2|3)}(p_t), \\
\frac{d}{dt} \bar{T}_{(0|12|3)}(p_t) &= - \left(\sum_{\substack{\mathcal{A} \in \Sigma: \\ \mathcal{A} \vec{\pi}(12)=(1|2)}} \bar{\rho}_{\mathcal{A}} \right) \bar{T}_{(0|12|3)}(p_t), \\
\frac{d}{dt} \bar{T}_{(0|13|2)}(p_t) &= - \left(\sum_{\substack{\mathcal{A} \in \Sigma: \\ \mathcal{A} \vec{\pi}(13)=(1|3)}} \bar{\rho}_{\mathcal{A}} \right) \bar{T}_{(0|13|2)}(p_t), \\
\frac{d}{dt} \bar{T}_{(02|1|3)}(p_t) &= - \left(\sum_{\substack{\mathcal{A} \in \Sigma: \\ \mathcal{A} \vec{\pi}(02)=(0|2)}} \bar{\rho}_{\mathcal{A}} \right) \bar{T}_{(02|1|3)}(p_t), \\
\frac{d}{dt} \bar{T}_{(03|1|2)}(p_t) &= - \left(\sum_{\substack{\mathcal{A} \in \Sigma: \\ \mathcal{A} \vec{\pi}(03)=(0|3)}} \bar{\rho}_{\mathcal{A}} \right) \bar{T}_{(03|1|2)}(p_t), \\
\frac{d}{dt} \bar{T}_{(01|23)}(p_t) &= - \left(\sum_{\substack{\mathcal{A} \in \Sigma: \\ \mathcal{A} \vec{\pi}(01)=(0|1)}} \bar{\rho}_{\mathcal{A}} + \sum_{\substack{\mathcal{B} \in \Sigma: \\ \mathcal{B} \vec{\pi}(23)=(2|3)}} \bar{\rho}_{\mathcal{B}} \right) \bar{T}_{(01|23)}(p_t), \\
\frac{d}{dt} \bar{T}_{(02|13)}(p_t) &= - \left(\sum_{\substack{\mathcal{A} \in \Sigma: \\ \mathcal{A} \vec{\pi}(02)=(0|2)}} \bar{\rho}_{\mathcal{A}} + \sum_{\substack{\mathcal{B} \in \Sigma: \\ \mathcal{B} \vec{\pi}(13)=(1|3)}} \bar{\rho}_{\mathcal{B}} \right) \bar{T}_{(02|13)}(p_t), \\
\frac{d}{dt} \bar{T}_{(03|12)}(p_t) &= - \left(\sum_{\substack{\mathcal{A} \in \Sigma: \\ \mathcal{A} \vec{\pi}(03)=(0|3)}} \bar{\rho}_{\mathcal{A}} + \sum_{\substack{\mathcal{B} \in \Sigma: \\ \mathcal{B} \vec{\pi}(12)=(1|2)}} \bar{\rho}_{\mathcal{B}} \right) \bar{T}_{(03|12)}(p_t), \\
\frac{d}{dt} \bar{T}_{(0|123)}(p_t) &= - \left(\sum_{\mathcal{A} \neq (0|123)} \bar{\rho}_{\mathcal{A}} \right) \bar{T}_{(0|123)}(p_t), \\
\frac{d}{dt} \bar{T}_{(012|3)}(p_t) &= - \left(\sum_{\mathcal{A} \neq (012|3)} \bar{\rho}_{\mathcal{A}} \right) \bar{T}_{(012|3)}(p_t), \\
\frac{d}{dt} \bar{T}_{(013|2)}(p_t) &= - \left(\sum_{\mathcal{A} \neq (013|2)} \bar{\rho}_{\mathcal{A}} \right) \bar{T}_{(013|2)}(p_t), \\
\frac{d}{dt} \bar{T}_{(023|1)}(p_t) &= - \left(\sum_{\mathcal{A} \neq (023|1)} \bar{\rho}_{\mathcal{A}} \right) \bar{T}_{(023|1)}(p_t), \\
\frac{d}{dt} \bar{T}_{(0123)}(p_t) &= - \left(\sum_{I \neq \mathcal{A} \in \Sigma} \bar{\rho}_{\mathcal{A}} \right) \bar{T}_{(0123)}(p_t) + \left(\sum_{\substack{\mathcal{A} \in \Sigma: \\ \mathcal{A} \vec{\pi}(01)=(0|1), \\ \mathcal{A} \vec{\pi}(23)=(2|3)}} \bar{\rho}_{\mathcal{A}} \right) \bar{T}_{(01|23)}(p_t) \\
&\quad + \left(\sum_{\substack{\mathcal{A} \in \Sigma: \\ \mathcal{A} \vec{\pi}(02)=(0|2), \\ \mathcal{A} \vec{\pi}(13)=(1|3)}} \bar{\rho}_{\mathcal{A}} \right) \bar{T}_{(02|13)}(p_t) + \left(\sum_{\substack{\mathcal{A} \in \Sigma: \\ \mathcal{A} \vec{\pi}(03)=(0|3), \\ \mathcal{A} \vec{\pi}(12)=(1|2)}} \bar{\rho}_{\mathcal{A}} \right) \bar{T}_{(03|12)}(p_t).
\end{aligned} \tag{5.9}$$

Just as we have seen with four sites in the discrete-time setting, the diagonalisation property of the transformation (5.8) is lost from four sites onwards while a linearisation of the dynamics is still achieved. This confirms that the single-crossover recombination model is indeed a very special case. While in the single-crossover model the setting with continuous time makes things much easier compared to the setting with discrete time, for the general recombination model in continuous time, the arising dynamics show notably analogy with the single-crossover discrete-time dynamics (i.e. the arising difficulties/dependencies here). Hence, this suggests that the simplifying structure of continuous time is lost when considering the general recombination model. To further analyse this, let us have a look at some exemplary coefficient functions for the four sites model. Solving the equations from (5.9), one finds

$$\bar{a}_{(0|123)}(t) = \exp\left(-\sum_{I \neq \mathcal{A} \in \Sigma} \bar{\rho}_{\mathcal{A}} t\right),$$

i.e. this coefficient function is in accordance with previous results (in continuous as well as in discrete time). Continuing with the partition (0|123) one obtains

$$\bar{a}_{(0|123)}(t) = \exp\left(-\sum_{\mathcal{A} \neq (0|123)} \bar{\rho}_{\mathcal{A}} t\right) (1 - \exp(-\bar{\rho}_{(0|123)} t)), \quad (5.10)$$

thus, again, no differences to the analogous solution in continuous time are observed. This is due to the fact that one part of the partition only consists of one site (compare the explanation for the single-crossover model that follows the proof of Theorem 3.7) as becomes clear when turning to the next coefficient function:

$$\begin{aligned} \bar{a}_{(01|23)}(t) &= \frac{\bar{\rho}_{(01|23)}}{\bar{\rho}_{(01|23)} - \sum_{\substack{\mathcal{A} \in \Sigma: \\ \mathcal{A} \vec{\pi}(01)=(0|1), \\ \mathcal{A} \vec{\pi}(23)=(2|3)}} \bar{\rho}_{\mathcal{A}}} \left(\exp\left(-\sum_{\mathcal{A}: \mathcal{A} \neq (01|23)} \bar{\rho}_{\mathcal{A}} t\right) \times \right. \\ &\quad \left. \exp\left(-\sum_{\substack{\mathcal{A} \in \Sigma: \\ \mathcal{A} \vec{\pi}(01)=(0|1), \\ \mathcal{A} \vec{\pi}(23)=(2|3)}} \bar{\rho}_{\mathcal{A}} t\right) - \exp\left(-\sum_{\mathcal{A} \in \Sigma} \bar{\rho}_{\mathcal{A}} t\right) \right) \\ &= \frac{\bar{\rho}_{(01|23)}}{\bar{\rho}_{(01|23)} - \sum_{\substack{\mathcal{A} \in \Sigma: \\ \mathcal{A} \vec{\pi}(01)=(0|1), \\ \mathcal{A} \vec{\pi}(23)=(2|3)}} \bar{\rho}_{\mathcal{A}}} \left(\exp\left(-\left(\sum_{\substack{\mathcal{A} \in \Sigma: \\ \mathcal{A} \vec{\pi}(01)=(0|1)}} \bar{\rho}_{\mathcal{A}} t + \sum_{\substack{\mathcal{A} \in \Sigma: \\ \mathcal{A} \vec{\pi}(23)=(2|3)}} \bar{\rho}_{\mathcal{A}} t\right)\right) \right. \\ &\quad \left. - \exp\left(-\sum_{\mathcal{A} \in \Sigma} \bar{\rho}_{\mathcal{A}} t\right) \right), \end{aligned} \quad (5.11)$$

where indeed the simplifying product structure is lost as soon as we allow for more than only single-crossover events. Moreover, the structure of the solution (5.11) resembles the structure of the solution for the coefficient function $a_{\frac{3}{2}}(t)$ from the discrete-time

model for four sites. This reads

$$a_{\frac{3}{2}}(t) = \frac{\rho_{\frac{3}{2}}}{\lambda_{\frac{3}{2}} - \lambda_{\emptyset}} (\lambda_{\frac{3}{2}}^t - \lambda_{\emptyset}^t).$$

This structural similarity is also observed for further coefficient function, e.g.

$$\begin{aligned} \bar{a}_{(0|1|23)}(t) &= \exp\left(-\sum_{\substack{\mathcal{A} \in \Sigma: \\ \mathcal{A} \vec{\pi}(23)=(2|3)}} \bar{\rho}_{\mathcal{A}} t\right) - \exp\left(-\sum_{\substack{\mathcal{A} \in \Sigma: \\ \mathcal{A} \vec{\pi}(123) \neq (123)}} \bar{\rho}_{\mathcal{A}} t\right) - \exp\left(-\sum_{\substack{\mathcal{A} \in \Sigma: \\ \mathcal{A} \vec{\pi}(023) \neq (023)}} \bar{\rho}_{\mathcal{A}} t\right) \\ &\quad - \frac{\bar{\rho}_{(01|23)}}{\bar{\rho}_{(01|23)} - \sum_{\substack{\mathcal{A} \in \Sigma: \\ \mathcal{A} \vec{\pi}(01)=(0|1), \mathcal{A} \vec{\pi}(23)=(2|3)}} \bar{\rho}_{\mathcal{A}}} \left(\exp\left(-\sum_{\mathcal{A}: \mathcal{A} \neq (01|23)} \bar{\rho}_{\mathcal{A}} t\right) \times \right. \\ &\quad \left. \exp\left(-\sum_{\substack{\mathcal{A} \in \Sigma: \\ \mathcal{A} \vec{\pi}(01)=(0|1), \mathcal{A} \vec{\pi}(23)=(2|3)}} \bar{\rho}_{\mathcal{A}} t\right) - \exp\left(-\sum_{\mathcal{A} \in \Sigma} \bar{\rho}_{\mathcal{A}} t\right) \right) + \exp\left(-\sum_{\mathcal{A} \in \Sigma} \bar{\rho}_{\mathcal{A}} t\right), \end{aligned} \quad (5.12)$$

when compared to

$$a_{\{\frac{1}{2}, \frac{3}{2}\}}(t) = \lambda_{\{\frac{1}{2}, \frac{3}{2}\}}^t - \lambda_{\frac{1}{2}}^t - \frac{\rho_{\frac{3}{2}}}{\lambda_{\frac{3}{2}} - \lambda_{\emptyset}} (\lambda_{\frac{3}{2}}^t - \lambda_{\emptyset}^t).$$

All these similarities of the general recombination model (in continuous time) with the single-crossover model in discrete-time suggest that the general model might be treated with similar methods that we have developed in Section 3.5.

5.2.3 Product structure

Here, we shortly present some results for the general recombination model that are analogous to the subsystem structure revealed for the discrete-time single-crossover model in Section 3.4. First of all, we find for the recombinators (5.2):

Proposition 5.8. *Let \mathcal{C} be a partition of S . Then for each coarsening \mathcal{B}' of \mathcal{C} , $\mathcal{C} \preceq \mathcal{B}'$, with $\mathcal{B}' = \{B, \bar{B}\}$, i.e. $|\mathcal{B}'| = 2$, and $\omega \in \mathcal{P}(X)$, one finds*

$$\bar{R}_{\mathcal{C}}^{(S)}(\omega) = \left(\bar{R}_{\mathcal{C} \vec{\pi} B}^{(B)}(\pi_B \cdot \omega) \right) \otimes \left(\bar{R}_{\mathcal{C} \vec{\pi} \bar{B}}^{(\bar{B})}(\pi_{\bar{B}} \cdot \omega) \right). \quad (5.13)$$

Proof. Following Proposition 3.2 and the definition of the recombinators from (5.2), we have

$$\begin{aligned} \bar{R}_{\mathcal{C}}^{(S)}(\omega) &= \bar{R}_{\mathcal{B}'}^{(S)}(\bar{R}_{\mathcal{C}}^{(S)}(\omega)) = \left(\pi_B \cdot \bar{R}_{\mathcal{C}}^{(S)}(\omega) \right) \otimes \left(\pi_{\bar{B}} \cdot \bar{R}_{\mathcal{C}}^{(S)}(\omega) \right) \\ &= \left(\bar{R}_{\mathcal{C} \vec{\pi} B}^{(B)}(\pi_B \cdot \omega) \right) \otimes \left(\bar{R}_{\mathcal{C} \vec{\pi} \bar{B}}^{(\bar{B})}(\pi_{\bar{B}} \cdot \omega) \right). \end{aligned}$$

□

Here, as before, the upper index specifies the corresponding subsystem (specified through the respective sites and part of a partition, respectively) the recombinators are acting on. Analogously, the notation will be used for the transformation operators as well. This obviously works for *any* coarsening \mathcal{B}' of \mathcal{C} in an analogous way. Proposition 5.8 directly carries over to the transformation operators (5.8):

Proposition 5.9. *On $\mathcal{P}(X)$, the transformation operators (5.8) satisfy*

$$\bar{T}_{\mathcal{A}}(\omega) = \left(\bar{T}_{\mathcal{A}\vec{\cap}B}^{(B)}(\pi_B \cdot \omega) \right) \otimes \left(\bar{T}_{\mathcal{A}\vec{\cap}\bar{B}}^{(\bar{B})}(\pi_{\bar{B}} \cdot \omega) \right)$$

for all $\mathcal{B}' = \{B, \bar{B}\} \in \Sigma$ and $\mathcal{A} \in \Sigma$ with $\mathcal{A} \preceq \mathcal{B}'$.

Proof. We have

$$\begin{aligned} \bar{T}_{\mathcal{A}}(\omega) &= \sum_{\mathcal{C} \preceq \mathcal{A}} \mu(\mathcal{C}, \mathcal{A}) \bar{R}_{\mathcal{C}}(\omega) = \sum_{\mathcal{C} \preceq \mathcal{A}} \mu(\mathcal{C}, \mathcal{A}) \left(\bar{R}_{\mathcal{C}\vec{\cap}B}^{(B)}(\pi_B \cdot \omega) \otimes \bar{R}_{\mathcal{C}\vec{\cap}\bar{B}}^{(\bar{B})}(\pi_{\bar{B}} \cdot \omega) \right) \\ &= \sum_{\mathcal{C}_1 \preceq (\mathcal{A}\vec{\cap}B)} \mu(\mathcal{C}_1, (\mathcal{A}\vec{\cap}B)) \sum_{\mathcal{C}_2 \preceq (\mathcal{A}\vec{\cap}\bar{B})} \mu(\mathcal{C}_2, (\mathcal{A}\vec{\cap}\bar{B})) \left(\bar{R}_{\mathcal{C}_1}^{(B)}(\pi_B \cdot \omega) \otimes \bar{R}_{\mathcal{C}_2}^{(\bar{B})}(\pi_{\bar{B}} \cdot \omega) \right) \\ &= \left(\sum_{\mathcal{C}_1 \preceq (\mathcal{A}\vec{\cap}B)} \mu(\mathcal{C}_1, (\mathcal{A}\vec{\cap}B)) \bar{R}_{\mathcal{C}_1}^{(B)}(\pi_B \cdot \omega) \right) \otimes \left(\sum_{\mathcal{C}_2 \preceq (\mathcal{A}\vec{\cap}\bar{B})} \mu(\mathcal{C}_2, (\mathcal{A}\vec{\cap}\bar{B})) \bar{R}_{\mathcal{C}_2}^{(\bar{B})}(\pi_{\bar{B}} \cdot \omega) \right) \\ &= \left(\bar{T}_{\mathcal{A}\vec{\cap}B}^{(B)}(\pi_B \cdot \omega) \right) \otimes \left(\bar{T}_{\mathcal{A}\vec{\cap}\bar{B}}^{(\bar{B})}(\pi_{\bar{B}} \cdot \omega) \right), \end{aligned}$$

where we use relation (5.13) in the second step and in the third step that the Möbius function is multiplicative, see [1]. \square

Inductively, for any partition $\mathcal{A} = (A_1 | \dots | A_k) \in \Sigma$ and $\omega \in \mathcal{P}(X)$, this proposition then leads to

$$\bar{T}_{\mathcal{A}}^{(S)}(\omega) = \bar{T}_I^{(A_1)}(\pi_{A_1} \cdot \omega) \otimes \dots \otimes \bar{T}_I^{(A_k)}(\pi_{A_k} \cdot \omega)$$

since obviously $\mathcal{A}\vec{\cap}A_i = I \in \Sigma(A_i)$ for all blocks of the partition \mathcal{A} , where now $I \in \Sigma(A_i)$ denotes the coarsest partition of the respective blocks A_i . Thus, the effect of the operator $\bar{T}_{\mathcal{A}}^{(S)}$ of (5.8) on the full system (specified through the complete set of sites S) is given by that of \bar{T}_I on the corresponding parts of the partition of \mathcal{A} . Clearly, this is in accordance with the results for the single-crossover model in discrete time, compare (3.27). Denoting the forward flow of the differential equation (5.3) with φ_t , we thus have $p_t = \varphi_t(p_0)$ and for the differential equations for the operator (5.8) we obtain:

$$\begin{aligned} \frac{d}{dt} \bar{T}_{\mathcal{A}}^{(S)}(\varphi_t(p_0)) &= \frac{d}{dt} \bar{T}_{\mathcal{A}}^{(S)}(p_t) = \frac{d}{dt} \left(\bigotimes_{i=1}^k \bar{T}_I^{(A_i)}(\pi_{A_i} \cdot p_t) \right) \\ &= \sum_{i=1}^k \bar{T}_I^{(A_1)}(\pi_{A_1} \cdot p_t) \otimes \dots \otimes \left(\frac{d}{dt} \bar{T}_I^{(A_i)}(\pi_{A_i} \cdot p_t) \right) \otimes \dots \otimes \bar{T}_I^{(A_k)}(\pi_{A_k} \cdot p_t). \end{aligned}$$

Thus, we are again left to evaluate $\frac{d}{dt} \bar{T}_I(\varphi_t(p_0))$, just as in Section 3.4, to determine the differential equations for all transformation operators. To do so, we first calculate

$$\begin{aligned}
\frac{d}{dt} \bar{T}_I(\varphi_t(p_0)) &= \frac{d}{dt} \sum_{\mathcal{H} \in \Sigma} \mu(\mathcal{H}, I) \bar{R}_{\mathcal{H}}(\varphi_t(p_0)) \\
&= \frac{d}{dt} \left(\sum_{\mathcal{H} \in \Sigma} \mu(\mathcal{H}, I) \varphi_t(\bar{R}_{\mathcal{H}}(p_0)) + \sum_{\mathcal{H} \in \Sigma} \mu(\mathcal{H}, I) [\bar{R}_{\mathcal{H}}, \varphi_t](p_0) \right) \\
&= \sum_{\mathcal{H} \in \Sigma} \mu(\mathcal{H}, I) \frac{d}{dt} \varphi_t(\bar{R}_{\mathcal{H}}(p_0)) + \frac{d}{dt} \sum_{\mathcal{H} \in \Sigma} \mu(\mathcal{H}, I) [\bar{R}_{\mathcal{H}}, \varphi_t](p_0) \\
&= \sum_{\mathcal{H} \in \Sigma} \mu(\mathcal{H}, I) \sum_{I \neq \mathcal{V} \in \Sigma} \bar{\rho}_{\mathcal{V}} (\bar{R}_{\mathcal{H} \wedge \mathcal{V}} - \bar{R}_{\mathcal{H}})(p_t) + \frac{d}{dt} \sum_{\mathcal{H} \in \Sigma} \mu(\mathcal{H}, I) [\bar{R}_{\mathcal{H}}, \varphi_t](p_0).
\end{aligned} \tag{5.14}$$

Before continuing, we need the following corollary that can be found in [59]:

Corollary 5.10 (Weisner). *Let L be a finite lattice with maximal element 1. Let $a < 1$ in L . Then, for any b in L ,*

$$\sum_{x: x \wedge a = b} \mu(x, 1) = 0. \tag{5.15}$$

□

For our particular lattice of partitions, Corollary 5.10 corresponds to the following:

Corollary 5.11. *Let $\mathcal{V} \in \Sigma \neq I$. Then, for any $\mathcal{A} \in \Sigma$,*

$$\sum_{\mathcal{H}: \mathcal{H} \wedge \mathcal{V} = \mathcal{A}} \mu(\mathcal{H}, I) = 0.$$

□

With Corollary 5.11, part of the first term from (5.14) reduces to

$$\begin{aligned}
\sum_{\mathcal{H} \in \Sigma} \mu(\mathcal{H}, I) \sum_{I \neq \mathcal{V} \in \Sigma} \bar{\rho}_{\mathcal{V}} \bar{R}_{\mathcal{H} \wedge \mathcal{V}}(p_t) &= \sum_{I \neq \mathcal{V} \in \Sigma} \bar{\rho}_{\mathcal{V}} \sum_{\mathcal{H} \in \Sigma} \mu(\mathcal{H}, I) \bar{R}_{\mathcal{H} \wedge \mathcal{V}}(p_t) \\
&= \sum_{I \neq \mathcal{V} \in \Sigma} \bar{\rho}_{\mathcal{V}} \sum_{\mathcal{A} \in \Sigma} \bar{R}_{\mathcal{A}}(p_t) \sum_{\substack{\mathcal{H} \in \Sigma: \\ \mathcal{H} \wedge \mathcal{V} = \mathcal{A}}} \mu(\mathcal{H}, I) = 0,
\end{aligned}$$

so that we finally obtain

Corollary 5.12. *The differential equation for $\bar{T}_I(\varphi_t(p_0)) = \bar{T}_I(p_t)$ is given as*

$$\frac{d}{dt} \bar{T}_I(p_t) = - \sum_{I \neq \mathcal{V} \in \Sigma} \bar{\rho}_{\mathcal{V}} \bar{T}_I(p_t) + \frac{d}{dt} \sum_{\mathcal{H} \in \Sigma} \mu(\mathcal{H}, I) [\bar{R}_{\mathcal{H}}, \varphi_t](p_0).$$

□

When comparing this result to Proposition 3.15 of Section 3.5, the similarities with the discrete-time model should become obvious once more. The determination of $\frac{d}{dt} \bar{T}_I(p_t)$ again boils down to evaluating the respective commutator with the final goal to construct an appropriate (i.e. diagonalising) transformation. Taking into account all analogies with the discrete-time recombination model we have revealed so far, further proceedings should follow along the same lines as in Section 3.5.

We finish this section with stating the differential equations of $\bar{T}_I(\varphi_t(p_0))$ for five and six sites to give an impression about the results. For five sites, we obtain

$$\frac{d}{dt} \bar{T}_{(01234)}(p_t) = - \left(\sum_{I \neq \mathcal{V} \in \Sigma} \bar{\rho}_{\mathcal{V}} \right) \bar{T}_{(01234)}(p_t) + \sum_{\substack{\mathcal{A}=(A_1|A_2) \in \Sigma \\ |A_i| \geq 2}} \bar{T}_{\mathcal{A}}(p_t) \left(\sum_{\substack{\mathcal{B} \in \Sigma: \mathcal{B} \cap A_1 \neq I \in \Sigma(A_1) \\ \mathcal{B} \cap A_2 \neq I \in \Sigma(A_2)}} \bar{\rho}_{\mathcal{B}} \right),$$

and for six sites

$$\begin{aligned} \frac{d}{dt} \bar{T}_{(012345)}(p_t) = & - \left(\sum_{I \neq \mathcal{V} \in \Sigma} \bar{\rho}_{\mathcal{V}} \right) \bar{T}_{(012345)}(p_t) + \sum_{\substack{\mathcal{A}=(A_1|A_2) \in \Sigma \\ |A_i| \geq 2}} \bar{T}_{\mathcal{A}}(p_t) \left(\sum_{\substack{\mathcal{B} \in \Sigma: \mathcal{B} \cap A_1 \neq I \\ \mathcal{B} \cap A_2 \neq I}} \bar{\rho}_{\mathcal{B}} \right) \\ & - \sum_{\substack{\mathcal{A}=(A_1|A_2|A_3) \in \Sigma \\ |A_i| \geq 2}} \bar{T}_{\mathcal{A}}(p_t) \left(\sum_{\substack{\mathcal{B} \in \Sigma: \mathcal{B} \cap A_1 \neq I \\ \mathcal{B} \cap A_2 \neq I, \mathcal{B} \cap A_3 \neq I}} \bar{\rho}_{\mathcal{B}} \right). \end{aligned}$$

5.3 Trees in the general recombination model

After we have recovered crucial similarities in the dynamics of the general recombination model with the discrete-time single-crossover model, it suggests itself to study the solution for the general model in terms of tree structures. Recall that the tree structure in Chapter 4 is based upon the concept of segments (or subsystems). The corresponding segments for the general model are always the blocks of a particular partition. Hence, note the following:

Remark 5.13. *In the discrete-time single-crossover model, the probability that there is no further recombination within one time step in a particular segment defined via the contiguous set of links $J \subseteq L$ is given as $\lambda_{\emptyset}^{(J)} = (1 - \sum_{\alpha \in J} \rho_{\alpha})$. In the continuous-time general model, the analogous rate that there is no recombination within the part $B \in \mathcal{B}$ of any partition \mathcal{B} for any time k , is given by $\exp(-\sum_{\substack{\mathcal{A} \in \Sigma: \\ \mathcal{A} \cap B \neq I \in \Sigma(B)}} \bar{\rho}_{\mathcal{A}} k)$.*

We will examine the tree-like structure for the general recombination model with four sites. To do so, let us only consider ‘natural’ recombination events for simplification, i.e. events that partition the sites into exactly two blocks. Thus, $\bar{\rho}_{\mathcal{A}} = 0$ for all $\mathcal{A} \in \Sigma$ with $|\mathcal{A}| \neq 2$. As a consequence, recombination remains to be a binary operation so

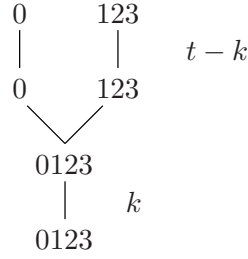


Figure 5.2: The only tree that corresponds to the coefficient function $\bar{a}_{(0|123)}(t)$. After some time k the separation event $(0|123)$ happens. For the remaining time $t - k$ both segments remain unchanged.

that we can expect binary trees. Starting with the coefficient function $\bar{a}_{(0|123)}(t)$, one can indeed state its solution (5.10) as

$$\begin{aligned} \bar{a}_{(0|123)}(t) &= \int_{k=0}^t \exp\left(-\sum_{\substack{\mathcal{A} \in \Sigma \\ |\mathcal{A}|=2}} \bar{\rho}_{\mathcal{A}} k\right) \bar{\rho}_{(0|123)} \exp\left(-\sum_{\substack{\mathcal{A} \in \Sigma \\ |\mathcal{A}|=2, \mathcal{A} \vec{\pi}(123) \neq (123)}} \bar{\rho}_{\mathcal{A}}(t-k)\right) dk \\ &= \exp\left(-\sum_{\substack{|\mathcal{A}|=2 \\ \mathcal{A} \vec{\pi}(123) \neq (123)}} \bar{\rho}_{\mathcal{A}} t\right) (1 - \exp(-\bar{\rho}_{(0|123)} t)). \end{aligned}$$

It should be clear that this can be explained with a continuous-time tree producing process just as in Section 4.2, where the only corresponding tree topology is given in Figure 5.2.

Analogously, the solution for the coefficient function $\bar{a}_{(01|23)}(t)$, compare (5.11), can be explained:

$$\begin{aligned} \bar{a}_{(01|23)}(t) &= \int_{k=0}^t \exp\left(-\sum_{\substack{\mathcal{A} \in \Sigma \\ |\mathcal{A}|=2}} \bar{\rho}_{\mathcal{A}} k\right) \bar{\rho}_{(01|23)} \exp\left(-\sum_{\substack{|\mathcal{A}|=2 \\ \mathcal{A} \vec{\pi}(01)=(0|1)}} \bar{\rho}_{\mathcal{A}}(t-k)\right) \exp\left(-\sum_{\substack{|\mathcal{A}|=2 \\ \mathcal{A} \vec{\pi}(23)=(2|3)}} \bar{\rho}_{\mathcal{A}}(t-k)\right) dk \\ &= \frac{\bar{\rho}_{(01|23)}}{\bar{\rho}_{(01|23)} - \sum_{\substack{\mathcal{A} \in \Sigma: \\ \mathcal{A} \vec{\pi}(01)=(0|1), \\ \mathcal{A} \vec{\pi}(23)=(2|3)}} \bar{\rho}_{\mathcal{A}}} \left(\exp\left(-\left(\sum_{\substack{\mathcal{A} \in \Sigma: \\ \mathcal{A} \vec{\pi}(01)=(0|1)}} \bar{\rho}_{\mathcal{A}} t + \sum_{\substack{\mathcal{A} \in \Sigma: \\ \mathcal{A} \vec{\pi}(23)=(2|3)}} \bar{\rho}_{\mathcal{A}} t\right)\right) - \exp\left(-\sum_{\mathcal{A} \in \Sigma} \bar{\rho}_{\mathcal{A}} t\right) \right) \\ &= \frac{\bar{\rho}_{(01|23)}}{\bar{\rho}_{(01|23)} - \bar{\rho}_{(02|13)} - \bar{\rho}_{(03|12)}} \times \\ &\quad \left(\exp\left(-\sum_{\substack{|\mathcal{A}|=2 \\ \mathcal{A} \neq (01|23)}} \bar{\rho}_{\mathcal{A}} t\right) \exp\left(-(\bar{\rho}_{(02|13)} + \bar{\rho}_{(03|12)})t\right) - \exp\left(-\sum_{\substack{\mathcal{A} \in \Sigma \\ |\mathcal{A}|=2}} \bar{\rho}_{\mathcal{A}} t\right) \right). \end{aligned}$$

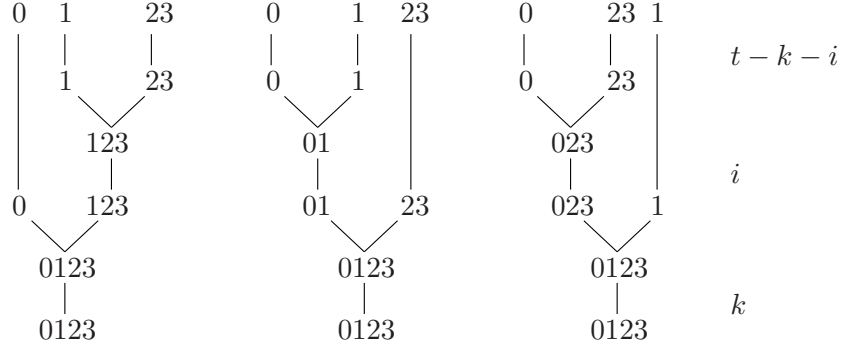


Figure 5.3: Three different histories that correspond to the partition (0|1|23). In particular, the second and the third tree have the same topology and can be only distinguished from making the corresponding partitions explicit.

When considering the coefficient function $\bar{a}_{(0|1|23)}(t)$ as in (5.12), one finds three different trees that correspond to the solution, see Figure 5.3. Here, one main difference to the single-crossover dynamics becomes obvious. In the single-crossover case, each tree topology can be uniquely described by its corresponding links as internal nodes of the tree since this implies the respective partition of sites due to the ordered structure. But since we are no longer dealing with only ordered partitions in the general model, we do not have an implicit order of the partitions anymore. In particular, the same tree topology (in the geometric sense) may refer to different partitions. This can be seen with the trees two and three of Figure 5.3. Consequently, each internal node has to state the whole information of the current parts of the partition. Finally, (5.12) can be indeed stated as

$$\begin{aligned}
 \bar{a}_{(0|1|23)}(t) &= \int_{k=0}^t \int_{i=0}^{t-k} \left[\exp\left(-\sum_{|\mathcal{A}|=2} \bar{\rho}_{\mathcal{A}} k\right) \bar{\rho}_{(0|123)} \exp\left(-\sum_{\mathcal{A} \vec{\pi}(123) \neq (123)} \bar{\rho}_{\mathcal{A}} i\right) \right. \\
 &\quad \left. \left(\sum_{\mathcal{A} \vec{\pi}(123)=(1|23)} \bar{\rho}_{\mathcal{A}} \right) \exp\left(-\sum_{\mathcal{A} \vec{\pi}(23) \neq (23)} \bar{\rho}_{\mathcal{A}} (t-k-i)\right) \right] di dk \\
 &+ \int_{k=0}^t \int_{i=0}^{t-k} \left[\exp\left(-\sum_{|\mathcal{A}|=2} \bar{\rho}_{\mathcal{A}} k\right) \bar{\rho}_{(01|23)} \exp\left(-\sum_{\mathcal{A} \vec{\pi}(01) \neq (01)} \bar{\rho}_{\mathcal{A}} i\right) \right. \\
 &\quad \left. \left(\sum_{\mathcal{A} \vec{\pi}(01)=(0|1)} \bar{\rho}_{\mathcal{A}} \right) \exp\left(-\sum_{\mathcal{A} \vec{\pi}(23) \neq (23)} \bar{\rho}_{\mathcal{A}} (t-k)\right) \right] di dk \\
 &+ \int_{k=0}^t \int_{i=0}^{t-k} \left[\exp\left(-\sum_{|\mathcal{A}|=2} \bar{\rho}_{\mathcal{A}} k\right) \bar{\rho}_{(023|1)} \exp\left(-\sum_{\mathcal{A} \vec{\pi}(023) \neq (023)} \bar{\rho}_{\mathcal{A}} i\right) \right. \\
 &\quad \left. \left(\sum_{\mathcal{A} \vec{\pi}(023)=(0|23)} \bar{\rho}_{\mathcal{A}} \right) \exp\left(-\sum_{\mathcal{A} \vec{\pi}(23) \neq (23)} \bar{\rho}_{\mathcal{A}} (t-k-i)\right) \right] di dk =
 \end{aligned}$$

$$\begin{aligned}
&= \exp\left(-\sum_{\mathcal{A}\vec{\pi}(23)=(2|3)} \bar{\rho}_{\mathcal{A}}t\right) \left(1 - \exp\left(-\sum_{\mathcal{A}\vec{\pi}(023)=(0|23)} \bar{\rho}_{\mathcal{A}}t\right)\right) \\
&\quad - \exp\left(-\sum_{\mathcal{A}\neq(0|123)} \bar{\rho}_{\mathcal{A}}t\right) \left(1 - \exp(-\bar{\rho}_{(0|123)}t)\right) \\
&\quad - \exp\left(-\sum_{\mathcal{A}\neq(023|1)} \bar{\rho}_{\mathcal{A}}t\right) \left(1 - \exp(-\bar{\rho}_{(023|1)}t)\right) \\
&\quad - \frac{\bar{\rho}_{(01|23)}}{\bar{\rho}_{(01|23)} - \sum_{\substack{\mathcal{A}\in\Sigma: \\ \mathcal{A}\vec{\pi}(01)=(0|1), \\ \mathcal{A}\vec{\pi}(23)=(2|3)}} \bar{\rho}_{\mathcal{A}}} \exp\left(-\sum_{\mathcal{A}:\mathcal{A}\neq(01|23)} \bar{\rho}_{\mathcal{A}}t\right) \times \\
&\quad \exp\left(-\sum_{\substack{\mathcal{A}\in\Sigma: \\ \mathcal{A}\vec{\pi}(01)=(0|1), \\ \mathcal{A}\vec{\pi}(23)=(2|3)}} \bar{\rho}_{\mathcal{A}}t\right) \left(1 - \exp\left(-(\bar{\rho}_{(01|23)} - \sum_{\substack{\mathcal{A}\in\Sigma: \\ \mathcal{A}\vec{\pi}(01)=(0|1), \\ \mathcal{A}\vec{\pi}(23)=(2|3)}} \bar{\rho}_{\mathcal{A}})t\right)\right) \\
&= \exp\left(-(\bar{\rho}_{(012|3)} + \bar{\rho}_{(02|13)} + \bar{\rho}_{(03|12)} + \bar{\rho}_{(013|2)})t\right) \times \\
&\quad \left(1 - \exp\left(-(\bar{\rho}_{(0|123)} + \bar{\rho}_{(01|23)} + \bar{\rho}_{(023|1)})t\right)\right) \\
&\quad - \exp\left(-\sum_{\mathcal{A}\neq(0|123)} \bar{\rho}_{\mathcal{A}}t\right) \left(1 - \exp(-\bar{\rho}_{(0|123)}t)\right) - \exp\left(-\sum_{\mathcal{A}\neq(023|1)} \bar{\rho}_{\mathcal{A}}t\right) \left(1 - \exp(-\bar{\rho}_{(023|1)}t)\right) \\
&\quad - \frac{\bar{\rho}_{(01|23)}}{\bar{\rho}_{(01|23)} - \bar{\rho}_{(02|13)} - \bar{\rho}_{(03|12)}} \exp\left(-\sum_{\mathcal{A}:\mathcal{A}\neq(01|23)} \bar{\rho}_{\mathcal{A}}t\right) \times \\
&\quad \exp\left(-(\bar{\rho}_{(02|13)} + \bar{\rho}_{(03|12)})t\right) \left(1 - \exp\left(-(\bar{\rho}_{(01|23)} - \bar{\rho}_{(02|13)} - \bar{\rho}_{(03|12)})t\right)\right),
\end{aligned}$$

where again each (double) integral corresponds to one tree of Figure 5.3.

These examples should show that the model allowing for general recombination events (in continuous time) can be in principle solved with the same methods as the model with the restriction to single-crossovers. While the usage of links is sufficient (and indeed very convenient) to describe recombination in the single-crossover model, the involvement of the underlying partitions in the general model is unavoidable. But anyways, thanks to the extensive studies of the discrete-time single-crossover recombination dynamics, the extension of the problem to general recombination events seems to be rather a problem of notation than of mathematics.

Remark 5.14. *In the above examples, we restricted ourselves to ‘real’ recombination events and the ancestral process thus referred to binary trees. If we also allow for recombination events that include more than two parents, we have to consider all possible arising trees that are not necessarily binary, e.g. the partition $(0|1|23)$ can be also explained by the non-binary tree of Figure 5.4 completing the three histories from Figure 5.3. The arising probability of this tree (with respect to a corresponding segmentation*

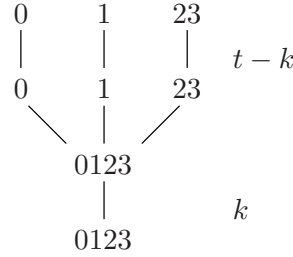


Figure 5.4: History of the partition $(0|1|23)$ due to a non-binary recombination event.

process) can be then stated as

$$\int_{k=0}^t \exp\left(-\sum_{\mathcal{A} \in \Sigma} \bar{\rho}_{\mathcal{A}} k\right) \bar{\rho}_{(0|1|23)} \exp\left(-\sum_{\mathcal{A}: \vec{\pi}(23) \neq (23)} \bar{\rho}_{\mathcal{A}} (t-k)\right) dk$$

$$= \frac{\bar{\rho}_{(0|1|23)}}{\sum_{\mathcal{A}: \vec{\pi}(23) = (23)} \bar{\rho}_{\mathcal{A}}} \exp\left(-\sum_{\mathcal{A}: \vec{\pi}(23) = (23)} \bar{\rho}_{\mathcal{A}} t\right) \left(1 - \exp\left(-\sum_{\mathcal{A}: \vec{\pi}(23) \neq (23)} \bar{\rho}_{\mathcal{A}} t\right)\right).$$

With regard to a general recombination model in *discrete* time, we can so far say that the way to a solution will not differ from the approach to deal with the model in continuous time. Instead of the exponential functions, one has to deal with terms such like the lambda-coefficients from (3.45), now defined on particular parts of respective partitions. While the usage of continuous time in the single-crossover model turned out to simplify the dynamics to an unexpected extent (compared to discrete time), differences in complexity between both approaches seem to vanish when allowing for more general recombination events.

5.4 Genetic algebras for the general recombination model

As mentioned in the introduction, the algebraic structure of genetic inheritance suggests to investigate population genetics models in terms of algebras. Algebraic structures that arise in genetics are also of purely mathematical interest since these algebras generally do not belong to any of the well-known classes of algebras and their study leads to new and interesting mathematical results [69]. In this section, we will briefly explain how recombination dynamics can be embedded into this framework of algebras. This should inspire further analysis in this field - if only for reasons of mathematical interest.

We define an algebra as follows:

Definition 5.15 (Algebra). *An algebra \mathcal{A} is an n -dimensional vector space over a field \mathcal{K} together with a \mathcal{K} -bilinear binary operation, called multiplication, from $\mathcal{A} \times \mathcal{A}$ to \mathcal{A} :*

$$p_1 \times p_2 \mapsto p_1 p_2 \in \mathcal{A} \quad \text{for all } p_1, p_2 \in \mathcal{A}.$$

For algebras that arise in population genetics, the basis of an algebra \mathcal{A} generally corresponds to all possible population types (for example a finite number of gametes) while any $p \in \mathcal{A}$ displays a population state. The multiplication operation specifies the ‘rule’ of inheritance, i.e. $p \mapsto p^2$ describes the evolutionary map from population p to its daughter population p^2 .

Since we are considering the recombination process on the level of gametes, we will need the *gametic algebra* that was already stated in the introduction, see also [56, 69]: Considering gametes a_1, \dots, a_n in a random mating population as basis elements in an n -dimensional real vector space, multiplication is defined by

$$a_i a_j = \sum_{k=1}^n \gamma_{ijk} a_k,$$

such that

- $0 \leq \gamma_{ijk} \leq 1$.
- $\sum_{k=1}^n \gamma_{ijk} = 1$.
- $\gamma_{ijk} = \gamma_{jik}$.

Here, each element $p := \sum_{i=1}^n \alpha_i a_i$, $0 \leq \alpha_i \leq 1$, $\sum_{i=1}^n \alpha_i = 1$, corresponds to an actual population of gametes, in which α_i denotes the frequency of gamete a_i . Furthermore, the coefficients γ_{ijk} specify the laws of inheritance. For two populations $p_1 = \sum_{i=1}^n \alpha_i a_i$ and $p_2 = \sum_{j=1}^n \beta_j a_j$, the daughter population is obtained as

$$p_1 p_2 = \left(\sum_{i=1}^n \alpha_i a_i \right) \left(\sum_{j=1}^n \beta_j a_j \right) = \sum_{k=1}^n \left(\sum_{i,j=1}^n \alpha_i \gamma_{ijk} \beta_j \right) a_k.$$

As a very first example, let us have a look at the diallelic case for two loci with recombination:

Example 5.16. Let us consider two loci that can be occupied by alleles A, a and B, b , respectively.

With respect to the basis that consists of all occurring gametes $a_1 = AB$, $a_2 = Ab$, $a_3 = aB$ and $a_4 = ab$ together with the recombination parameter θ (that is the probability that a zygote $a_1 a_4$ undergoes a transition into $a_2 a_3$, or conversely), the resulting gametic algebra has the following multiplication table:

	a_1	a_2	a_3	a_4
a_1	a_1	$\frac{1}{2}(a_1 + a_2)$	$\frac{1}{2}(a_1 + a_3)$	$\frac{1}{2}(a_1 + a_4) - \frac{1}{2}\theta d$
a_2		a_2	$\frac{1}{2}(a_2 + a_3) + \frac{1}{2}\theta d$	$\frac{1}{2}(a_2 + a_4)$
a_3			a_3	$\frac{1}{2}(a_3 + a_4)$
a_4				a_4

where $d := a_1 - a_2 - a_3 + a_4$

(arrays below the diagonal are omitted due to symmetry).

Algebras which arise in genetics are in general *commutative* but *non-associative* as should be clear from a biological point of view. The most general definition of an algebra with applications in population genetics is an *algebra with genetic realisation* [56, 69]:

Definition 5.17 (Algebra with genetic realisation). *Let \mathcal{A} be an algebra over \mathbb{R} with basis $\{a_1, \dots, a_n\}$ and multiplication table*

$$a_i a_j = \sum_{k=1}^n \gamma_{ijk} a_k,$$

such that $0 \leq \gamma_{ijk} \leq 1$ for all i, j, k , and $\sum_{k=1}^n \gamma_{ijk} = 1$ for $i, j = 1, \dots, n$. Then \mathcal{A} is called algebra with genetic realisation and the basis is called natural basis for \mathcal{A} .

Obviously, the gametic algebra from above is an algebra with genetic realisation. Since the class of algebras with genetic realisation is too large to infer class-specific results [56], a further specialisation of the above definition was needed. The first one to state an appropriate definition of an *Genetic Algebra* was Schafer [60] in 1949. His definition was later reformulated in a more coherent way by Gonshor [26] in 1971:

Definition 5.18 (Genetic algebra, Gonshor). *Let \mathcal{A} be a commutative finite-dimensional algebra. Then \mathcal{A} is called genetic algebra if there exists a basis $\{c_0, \dots, c_n\}$ with multiplication table*

$$c_i c_j = \sum_{k=0}^n \lambda_{ijk} c_k \quad \text{for all } i, j = 0, \dots, n,$$

with multiplication constants that fulfil

- $\lambda_{000} = 1$.
- $\lambda_{0jk} = 0$ for $k < j$.
- $\lambda_{ijk} = 0$ for $k \leq \max(i, j)$ and $i, j > 0$.

$\{c_0, \dots, c_n\}$ is called *canonical basis* (or *Gonshor basis*) of \mathcal{A} and the constants $\lambda_{000} = 1$, $\lambda_{011}, \dots, \lambda_{0nn}$ are called the *train roots* of \mathcal{A} .

Wörz-Busekros [69] worked out in detail that each gametic algebra with recombination is a genetic algebra after Gonshor's definition. For the two-loci example from above, this can be easily seen:

Example 5.19. We continue with the diallelic two-loci model from Example 5.16. To show that this is indeed a genetic algebra after Gonshor's definition, the basis is transformed via $c_0 = a_1$, $c_1 = a_1 - a_2$, $c_2 = a_1 - a_3$ and $c_3 = a_1 - a_2 - a_3 + a_4$. One then obtains the following multiplication table:

	c_0	c_1	c_2	c_3
c_0	c_0	$\frac{1}{2}c_1$	$\frac{1}{2}c_2$	$\frac{1}{2}(1-\theta)c_3$
c_1		0	$\frac{1}{2}\theta c_3$	0
c_2			0	0
c_3				0

The non-vanishing coefficients are $\lambda_{000} = 1$, $\lambda_{011} = \frac{1}{2}$, $\lambda_{022} = \frac{1}{2}$, $\lambda_{033} = \frac{1}{2}(1-\theta)$ (all train roots) and $\lambda_{123} = \frac{1}{2}\theta$. Therefore, this gametic algebra is a genetic algebra.

5.4.1 Linearisation

As before, when studying the process of recombination, the arising nonlinearities exhibit the main problem of dealing with the corresponding dynamics. Our ansatz in Chapter 3 - 5 (for the single-crossover as well as the general recombination model), overcomes this nonlinearity with a transformation to a linear system so that it can be treated with matrix methods. That this is generally possible for systems like the ones described previously, is a result that was actually proved with the theory of genetic algebras. In 1930, Haldane [48, 52] described a procedure - named *Haldane linearisation* - which, in some cases, enabled the quadratic evolutionary operator to be represented as a linear operator (on a higher-dimensional space). Holgate [32] proved that this linearisation works for any mating system that forms a genetic algebra. Consequently, it exists a transformation for the gametic algebra with recombination that embeds the original vector space into an higher-dimensional vector space, where the dynamics can be represented linearly.

Example 5.20. Let us continue with the situations from Examples 5.16 and 5.19. for the gametic algebra with Gonshor basis $\{c_0, c_1, c_2, c_3\}$. The population of gametes is described by $p = c_0 + \alpha_1 c_1 + \alpha_2 c_2 + \alpha_3 c_3$ (for simplification the term corresponding to c_0 is set to 1), $\alpha_i \in \mathbb{R}$. According to the multiplication scheme in Example 5.19, one then obtains

$$\begin{aligned} p^2 &= c_0^2 + 2\alpha_1 c_0 c_1 + 2\alpha_2 c_0 c_2 + 2\alpha_3 c_0 c_3 + 2\alpha_1 \alpha_2 c_1 c_2 \\ &= c_0 + \alpha_1 c_1 + \alpha_2 c_2 + ((1-\theta)\alpha_3 + \theta\alpha_1 \alpha_2) c_3. \end{aligned}$$

Introducing a new variable $\alpha_4 := \alpha_1 \alpha_2$, the dynamics for the mapping $p \mapsto p^2$ can now be represented linearly:

$$\begin{aligned} \alpha_1 &\mapsto \alpha_1, \\ \alpha_2 &\mapsto \alpha_2, \\ \alpha_3 &\mapsto (1-\theta)\alpha_3 + \theta\alpha_4, \\ \alpha_4 &\mapsto \alpha_4, \end{aligned}$$

i.e. the corresponding matrix for mapping (in the order: $\alpha_1, \alpha_2, \alpha_4, \alpha_3$) is given as

$$\begin{pmatrix} 1 & 0 & 0 & 0 \\ 0 & 1 & 0 & 0 \\ 0 & 0 & 1 & 0 \\ 0 & 0 & \theta & (1 - \theta) \end{pmatrix}.$$

5.4.2 Haldane linearisation for the recombination dynamics

With the aim to observe a general pattern for the Haldane linearisation of the recombination dynamics, we construct the transformation for further cases (with regard to the number of sites and corresponding alleles), allowing for any possible recombination event [35].

2 sites, m and n alleles

In this case, we have $m \cdot n$ gametes that form the (natural) basis of the genetic algebra: $a_1 = [1, 1], a_2 = [1, 2], \dots, a_{mn} = [m, n]$. Again, $0 \leq \theta \leq 1$ describes the probability for a crossover between the two sites, and multiplication is specified by the following rule:

$$[i, j] \times [k, l] = \frac{1}{2}([i, j] + [k, l]) + \frac{1}{2}\theta(-([i, j] + [k, l]) + [i, l] + [k, j])$$

for all $1 \leq i, k \leq m, 1 \leq j, l \leq n$.

We then apply the following transformation to obtain a new basis:

$$\begin{aligned} w_1 &= [1, 1] = a_1, \\ w_j &= [1, 1] - [1, j] = a_1 - a_j \quad \text{for } j = 2, \dots, n, \\ w_{kn+1} &= [1, 1] - [k+1, 1] = a_1 - a_{kn+1} \quad \text{for } k = 1, \dots, m-1, \\ w_{kn+j+1} &= [1, 1] - [1, j+1] - [k+1, 1] + [k+1, j+1], \\ &= a_1 - a_{j+1} - a_{kn+1} + a_{kn+j+1} \quad k = 1, \dots, m-1, j = 1, \dots, n-1. \end{aligned}$$

This transformation can be also described by the following transformation matrix (in lexicographical order):

$$\underbrace{\begin{pmatrix} 1 & 0 & 0 & \cdots & 0 \\ 1 & -1 & 0 & \cdots & 0 \\ 1 & 0 & -1 & \cdots & 0 \\ \vdots & \vdots & \vdots & \vdots & \vdots \\ 1 & 0 & 0 & \cdots & -1 \end{pmatrix}}_{m \times m} \otimes \underbrace{\begin{pmatrix} 1 & 0 & 0 & \cdots & 0 \\ 1 & -1 & 0 & \cdots & 0 \\ 1 & 0 & -1 & \cdots & 0 \\ \vdots & \vdots & \vdots & \vdots & \vdots \\ \vdots & \vdots & \vdots & \vdots & \vdots \\ 1 & 0 & 0 & \cdots & -1 \end{pmatrix}}_{n \times n}.$$

$(mn) \times (mn)$

Here, \otimes denotes the tensor product for matrices, also known as *Kronecker product* [27]. Multiplication via the new basis is now specified by

$$\begin{aligned} w_1 \times w_1 &= w_1, \\ w_1 \times w_j &= \frac{1}{2}w_j \quad \text{for } j = 2, \dots, n, \\ w_1 \times w_{kn+1} &= \frac{1}{2}w_{kn+1} \quad \text{for } k = 1, \dots, m-1, \\ w_1 \times w_{kn+j+1} &= \frac{1}{2}\theta w_{kn+j+1} \quad \text{for } k = 1, \dots, m-1 \text{ and } j = 1, \dots, n-1, \end{aligned}$$

while all other matings yield 0. Thus, the basis $\{w_1, \dots, w_{mn}\}$ is indeed a Gonshor basis. The population in terms of the Gonshor basis is then given by

$$p = w_1 + \alpha_2 w_2 + \dots + \alpha_{mn} w_{mn} \quad \text{with } \alpha_i \in \mathbb{R}.$$

With regard to p^2 , resulting from the above multiplication, the dynamics of the $mn-1$ coefficients $\alpha_2, \dots, \alpha_{mn}$ is a nonlinear one. The mapping of the coefficients is given as follows:

$$\begin{aligned} \alpha_j &\mapsto \alpha_j \quad \text{for } j = 1, \dots, n \text{ and } j = n+1, 2n+1, \dots, (m-1)n+1 \quad (5.16) \\ \alpha_{kn+j+1} &\mapsto (1-\theta)\alpha_{kn+j+1} + \theta\alpha_{j+1}\alpha_{kn+1} \quad k = 1, \dots, m-1, j = 1, \dots, n-1 \quad (5.17) \end{aligned}$$

The dynamics can be linearised by taking into account $(m-1)(n-1)$ additional parameters, namely

$$\beta_{j,k} = \alpha_{j+1} \cdot \alpha_{kn+1} \quad \text{for } k = 1, \dots, m-1 \text{ and } j = 1, \dots, n-1,$$

such that these additional parameters are mapped to themselves.

The dynamics can then be described by a $(2mn - m - n) \times (2mn - m - n)$ -matrix (after ordering the parameters in a respective way):

$$\mathbb{1}_{(m-1)+(n-1)} \oplus \left(\mathbb{1}_{(m-1)(n-1)} \otimes \begin{pmatrix} 1-\theta & \theta \\ 0 & 1 \end{pmatrix} \right),$$

where \oplus denotes the *Kronecker sum* of two matrices [27].

For the transformation to the Gonshor basis, we chose the type $a_1 = [1, 1]$ as allocated character (since $w_1 = a_1$). If a_1 mates with non- a_1 types that either have allele 1 at site 1 or allele 1 at site 2, recombination does not produce anything new. This is true for altogether $(m-1) + (n-1)$ types, and thus explains the identity matrix of size $(m-1) + (n-1)$ (compare (5.16)); for all other $(m-1)(n-1)$ types recombination with a_1 results in mixed gametes. The respective explanation for the decisive block of the second matrix together with (5.17) should then be obvious.

3 sites: n_1, n_2, n_3 alleles

Considering the model with three sites, we have to include three different recombination probabilities for the three possible partitions of the sites $\{1, 2, 3\}$ into two parts: Partition (1|23) (probability θ_1), partition (12|3) (probability θ_2) and the partition (13|2) which corresponds to a double-crossover event (probability γ).

As a start, we again consider the natural basis consisting of all possible gametes: $a_1 = [1, 1, 1]$, $a_2 = [1, 1, 2], \dots, a_{n_1 n_2 n_3} = [n_1, n_2, n_3]$, where multiplication is given by

$$\begin{aligned} [a, b, c] \times [d, e, f] &= \frac{1}{2}([a, b, c] + [d, e, f]) + \frac{1}{2}\theta_1(-[a, b, c] - [d, e, f] + [a, e, f] + [d, b, c]) \\ &\quad + \frac{1}{2}\theta_2(-[a, b, c] - [d, e, f] + [a, b, f] + [d, e, c]) \\ &\quad + \frac{1}{2}\gamma(-[a, b, c] - [d, e, f] + [a, e, c] + [d, b, f]). \end{aligned}$$

As before, we search for a corresponding Gonshor basis via

$$\begin{aligned} w_{1,1,1} &= [1, 1, 1], \\ w_{1,1,k} &= [1, 1, 1] - [1, 1, k] \quad \text{for } k = 2, \dots, n_3, \\ w_{1,j,1} &= [1, 1, 1] - [1, j, 1] \quad \text{for } j = 2, \dots, n_2, \\ w_{i,1,1} &= [1, 1, 1] - [i, 1, 1] \quad \text{for } i = 2, \dots, n_1, \\ w_{i,j,1} &= [1, 1, 1] - [1, j, 1] - [i, 1, 1] + [i, j, 1] \quad \text{for } i = 2, \dots, n_1 \text{ and } j = 2, \dots, n_2, \\ w_{i,1,k} &= [1, 1, 1] - [i, 1, 1] - [1, 1, k] + [i, 1, k] \quad \text{for } i = 2, \dots, n_1 \text{ and } k = 2, \dots, n_3, \\ w_{1,j,k} &= [1, 1, 1] - [1, j, 1] - [1, 1, k] + [1, j, k] \quad \text{for } j = 2, \dots, n_2 \text{ and } k = 2, \dots, n_3, \\ w_{i,j,k} &= [1, 1, 1] - [1, 1, k] - [1, j, 1] - [i, 1, 1] + [1, j, k] + [i, 1, k] + [i, j, 1] - [i, j, k] \\ &\quad \text{for } i = 2, \dots, n_1, j = 2, \dots, n_2 \text{ and } k = 2, \dots, n_3. \end{aligned}$$

With the notation of a transformation matrix this corresponds to

$$\underbrace{\begin{pmatrix} 1 & 0 & 0 & \cdots & 0 \\ 1 & -1 & 0 & \cdots & 0 \\ 1 & 0 & -1 & \cdots & 0 \\ \vdots & \vdots & \vdots & \vdots & \vdots \\ 1 & 0 & 0 & \cdots & -1 \end{pmatrix}}_{n_1 \times n_1} \otimes \underbrace{\begin{pmatrix} 1 & 0 & 0 \cdots & 0 \\ 1 & -1 & 0 \cdots & 0 \\ 1 & 0 & -1 \cdots & 0 \\ \vdots & \vdots & \vdots & \vdots \\ \vdots & \vdots & \vdots & \vdots \\ 1 & 0 & \cdots & -1 \end{pmatrix}}_{n_2 \times n_2} \otimes \underbrace{\begin{pmatrix} 1 & 0 & 0 & \cdots & 0 \\ 1 & -1 & 0 & \cdots & 0 \\ 1 & 0 & -1 & \cdots & 0 \\ \vdots & \vdots & \vdots & \vdots & \vdots \\ 1 & 0 & 0 & \cdots & -1 \end{pmatrix}}_{n_3 \times n_3}.$$

Like in the case with two sites, it is easily verified that the above basis indeed specifies a Gonshor basis. For a population $p = \alpha_{1,1,1}w_{1,1,1} + \alpha_{1,1,2}w_{1,1,2} + \dots + \alpha_{n_1, n_2, n_3}w_{n_1, n_2, n_3}$,

the coefficients $\alpha_{i,j,k} \in \mathbb{R}$ evolve in the following way:

$$\begin{aligned}
\alpha_{1,1,1} &\mapsto \alpha_{1,1,1}, \\
\alpha_{1,1,k} &\mapsto \alpha_{1,1,k} \quad k = 2, \dots, n_3, \\
\alpha_{1,j,1} &\mapsto \alpha_{1,j,1} \quad j = 2, \dots, n_2, \\
\alpha_{i,1,1} &\mapsto \alpha_{i,1,1} \quad i = 2, \dots, n_1, \\
\alpha_{i,j,1} &\mapsto (1 - \theta_1 - \gamma)\alpha_{i,j,1} + (\theta_1 + \gamma)\alpha_{1,j,1} \cdot \alpha_{i,1,1} \quad i = 2, \dots, n_1, j = 2, \dots, n_2, \\
\alpha_{i,1,k} &\mapsto (1 - \theta_1 - \theta_2)\alpha_{i,1,k} + (\theta_1 + \theta_2)\alpha_{1,1,k} \cdot \alpha_{i,1,1} \quad i = 2, \dots, n_1, k = 2, \dots, n_3, \\
\alpha_{1,j,k} &\mapsto (1 - \theta_2 - \gamma)\alpha_{1,j,k} + (\theta_2 + \gamma)\alpha_{1,1,k} \cdot \alpha_{1,j,1} \quad j = 2, \dots, n_2, k = 2, \dots, n_3, \\
\alpha_{i,j,k} &\mapsto (1 - \theta_1 - \theta_2 - \gamma)\alpha_{i,j,k} + \theta_1 \cdot \alpha_{i,1,1} \cdot \alpha_{1,j,k} + \theta_2 \cdot \alpha_{1,1,k} + \gamma \cdot \alpha_{1,j,1} \cdot \alpha_{i,1,k} \\
&\quad \text{for } i = 2, \dots, n_1, j = 2, \dots, n_2 \text{ and } k = 2, \dots, n_3.
\end{aligned}$$

The dynamics can then be linearised by adding $(n_1 - 1)(n_2 - 1) + (n_1 - 1)(n_3 - 1) + (n_2 - 1)(n_3 - 1) + 4(n_1 - 1)(n_2 - 1)(n_3 - 1)$ additional parameters:

$$\begin{aligned}
\alpha_{1,j,1} \cdot \alpha_{i,1,1} &\mapsto \alpha_{1,j,1} \cdot \alpha_{i,1,1} \quad \text{for } i = 2, \dots, n_1 \text{ and } j = 2, \dots, n_2, \\
\alpha_{1,1,k} \cdot \alpha_{i,1,1} &\mapsto \alpha_{1,1,k} \cdot \alpha_{i,1,1} \quad \text{for } i = 2, \dots, n_1 \text{ and } k = 2, \dots, n_3, \\
\alpha_{1,1,k} \cdot \alpha_{1,j,1} &\mapsto \alpha_{1,1,k} \cdot \alpha_{1,j,1} \quad \text{for } j = 2, \dots, n_2 \text{ and } k = 2, \dots, n_3, \\
\alpha_{i,1,1} \cdot \alpha_{1,j,k} &\mapsto \alpha_{i,1,1}((1 - \theta_2 - \gamma)\alpha_{1,j,k} + \alpha_{1,1,k} \cdot \alpha_{1,j,1}(\theta_2 + \gamma)) \\
&\quad \text{for } i = 2, \dots, n_1, j = 2, \dots, n_2 \text{ and } k = 2, \dots, n_3, \\
\alpha_{1,1,k} \cdot \alpha_{i,j,1} &\mapsto \alpha_{1,1,k}((1 - \theta_1 - \gamma)\alpha_{i,j,1} + \alpha_{1,j,1} \cdot \alpha_{i,1,1}(\theta_1 + \gamma)) \\
&\quad \text{for } i = 2, \dots, n_1, j = 2, \dots, n_2 \text{ and } k = 2, \dots, n_3, \\
\alpha_{1,j,1} \cdot \alpha_{i,1,k} &\mapsto \alpha_{1,j,1}((1 - \theta_1 - \theta_2)\alpha_{i,1,k} + \alpha_{1,1,k} \cdot \alpha_{i,1,1}(\theta_1 + \theta_2)) \\
&\quad \text{for } i = 2, \dots, n_1, j = 2, \dots, n_2 \text{ and } k = 2, \dots, n_3, \\
\alpha_{i,1,1} \cdot \alpha_{1,1,k} \cdot \alpha_{1,j,1} &\mapsto \alpha_{i,1,1} \cdot \alpha_{1,1,k} \cdot \alpha_{1,j,1} \\
&\quad \text{for } i = 2, \dots, n_1, j = 2, \dots, n_2 \text{ and } k = 2, \dots, n_3.
\end{aligned}$$

The resulting linear dynamics is depicted more clearly with the matrix notation:

$$\begin{aligned}
&\mathbb{1}_{(n_1-1)+(n_2-1)+(n_3-1)} \oplus \mathbb{1}_{(n_1-1)(n_2-1)} \otimes \begin{pmatrix} 1 - \theta_1 - \gamma & \theta_1 + \gamma \\ 0 & 1 \end{pmatrix} \\
&\oplus \mathbb{1}_{(n_1-1)(n_3-1)} \otimes \begin{pmatrix} 1 - \theta_1 - \theta_2 & \theta_1 + \theta_2 \\ 0 & 1 \end{pmatrix} \oplus \mathbb{1}_{(n_2-1)(n_3-1)} \otimes \begin{pmatrix} 1 - \theta_2 - \gamma & \theta_2 + \gamma \\ 0 & 1 \end{pmatrix} \oplus \\
&\mathbb{1}_{(n_1-1)(n_2-1)(n_3-1)} \otimes \begin{pmatrix} 1 - \theta_1 - \theta_2 - \gamma & \theta_1 & \theta_2 & \gamma & 0 \\ 0 & 1 - \theta_2 - \gamma & 0 & 0 & \theta_2 + \gamma \\ 0 & 0 & 1 - \theta_1 - \gamma & 0 & \theta_1 + \gamma \\ 0 & 0 & 0 & 1 - \theta_1 - \theta_2 & \theta_1 + \theta_2 \\ 0 & 0 & 0 & 0 & 1 \end{pmatrix}.
\end{aligned}$$

We can see a clear structure in this matrix which describes the dynamics after linearisation. The allocated character is again $a_1 = [1, 1, 1]$ (since $w_1 = a_1$) and recombination

cannot produce a mixed gamete if a_1 mates with non- a_1 -types that have only one site occupied by an allele different from 1. This is the case for $(n_1 - 1) + (n_2 - 1) + (n_3 - 1)$ types (i.e. only allele at site 1 is different from allele 1, only allele at site 2 is different from allele 1 and only allele at site 3 is different from allele 1, respectively) and may therefore explain the first unity matrix. The next block $\mathbb{1}_{(n_1-1)(n_2-1)} \otimes \begin{pmatrix} 1 - \theta_1 - \gamma & \theta_1 + \gamma \\ 0 & 1 \end{pmatrix}$ refers to the sites 1 and 2 in case they are occupied by alleles different from allele 1 while site 3 should be occupied by allele 1. Again, with respect to $a_1 = [1, 1, 1]$ recombination can only produce something new if *both* alleles at the sites 1 and 2 of the mating partner are different from 1. This is the case for $(n_1 - 1)(n_2 - 1)$ types. The probability that a recombination event between the sites 1 and 2 takes place is $\theta_1 + \gamma$. Analogously, this holds with respect to the sites 1 and 3 and with respect to the sites 2 and 3, respectively (explaining the next two blocks). The last block concerns types where all three sites carry alleles different from 1 ($(n_1 - 1)(n_2 - 1)(n_3 - 1)$ types) together with the respective recombination probabilities.

4 sites: n_1, n_2, n_3, n_4 alleles

The four-site case follows along the same lines as the previously discussed cases. With regard to the transformation matrix for three sites, for the transformation to a Gonshor basis in the four-site case, a fourth $n_4 \times n_4$ -matrix of the same kind has to be added. For Haldane linearisation $(n_1 - 1)(n_2 - 1) + \dots + (n_3 - 1)(n_4 - 1) + 4(n_1 - 1)(n_2 - 1)(n_3 - 1) + \dots + 4(n_2 - 1)(n_3 - 1)(n_4 - 1) + 14(n_1 - 1)(n_2 - 1)(n_3 - 1)(n_4 - 1)$ additional parameters are needed.

The resulting linear dynamics is then described by a matrix that has the same structure as the matrices we have seen above. It is built in the same recursive manner, meaning that the first block consists of a unity matrix that refers to types where only one allele is different from allele 1 (if again type $[1, 1, 1, 1]$ is allocated). Then the blocks that refer to types with two sites occupied with alleles different from allele 1 follow (same structure as in the 3 site case) etc., again with the respective recombination probabilities. The new block in this matrix is the last one that refers to $[1, 1, 1, 1]$ mating with types that have all four sites occupied with alleles different from 1. Just as in the detailed discussion of the single-crossover dynamics in discrete time in Chapter 3, for the first time product terms (that refer to two non-trivial segments) as eigenvalues of the linear dynamics can be observed (compare Section 3.3) [35].

What can we infer from this algebraic approach? We show how recombination dynamics is described by genetic algebras, and demonstrate (at least up to four sites) a way to construct the Gonshor basis as well as Haldane linearisation. As can be already seen with three sites, the dimension of the problem increases rapidly. In particular, the number of additional parameters (for the linearisation procedure) depends on the number of alleles. In contrast, our previously described ansatz for the general recombination dynamics, compare Section 5.2, is allele-*independent* and therefore of lower complexity.

Instead, the number of linearisation parameters is restricted by the number of possible partitions of the sites. This shows that the dimensional increase for the algebraic approach is unnecessarily high, i.e. the allele information can be skipped.

The ansatz of genetic algebras considers all allele combinations and the structure of the block matrix, which describes the linearised dynamics, is built in a recursive manner (taking into account all subsets of sites). Thus, as can be already observed with the above examples, the algebraic setting uses a lot of redundant information. For example, see the matrix for three sites: all information is given by the 5×5 matrix of the last block.

Thus, although algebras contribute an interesting approach in population genetics our less formal approach seems - at least for the recombination dynamics - more promising.

Chapter 6

Summary and Discussion

In this work, we have investigated the dynamics of an ‘infinite’ population that evolves due to recombination alone. To this end, we assumed discrete (non-overlapping) generations and restricted ourselves to the special case of single crossovers. The dynamics is described by a large system of nonlinear and coupled difference equations that are difficult to treat. Therefore, we rewrote the arising equations with the help of specific recombination operators in a more compact way. This not only helped to explore the recombination dynamics but also allowed for an allele-*independent* formulation of the equations.

Previous results had shown that the corresponding single-crossover dynamics in continuous time admits a closed solution [3]. This astonishing result is in accordance with a ‘hidden’ linearity in the system that is due to the independence of links. The fact that crossovers at different links occur independently manifests itself in the product structure of the coefficient functions of the solution ensuing from the linear action of the nonlinear recombination operators along the solution of the recombination equation. Additionally, as shown in [3], certain transformation operators, which are independent of the recombination parameters, can be found that linearise and diagonalise the dynamics.

Since the overwhelming part of published literature deals with discrete-time models, one aim was to find out whether, and to what extent, these continuous-time results carry over to single-crossover dynamics in discrete time. This was investigated in detail in Chapter 3 where we showed that the discrete-time dynamics is significantly more complex than the continuous-time one.

For up to three sites, the discrete-time dynamics behave similarly to the continuous-time dynamics, but with four or more sites they differ in an important way. The main reason for the arising difficulties lies in the fact that the key feature of the continuous-time model, the independence of links, does not carry over to discrete time. This is due to interference whereby the occurrence of a recombination event in the discrete-time model forbids any further crossovers in the same generation. As a consequence,

the iteration for the coefficient functions $a_G(t)$ is (in contrast to the continuous-time model) *nonlinear* from four sites onwards and therefore does not allow for an explicit solution. Furthermore, whilst in continuous time all recombinators R_G act linearly along solutions of the corresponding dynamics, in discrete time this is only true for certain subsets $G \subseteq L$.

Thus, the diagonalising transformation operators T_G from the continuous-time model are insufficient to diagonalise the discrete-time dynamics. Nevertheless, we could show that these transformation operators at least *linearise* the discrete-time dynamics and we used this result to transform the recombination equations into a solvable system with a two-step procedure: first linearisation via the T_G operators, followed by diagonalisation. Unfortunately, the coefficients of the second step must be constructed via recursions that involve the recombination probabilities. However, once this is done for a given system, it allows for an explicit solution valid for all times.

A similar approach has already been pursued by Dawson [14, 15] (following the idea of Bennett [7]), who also presented an appropriate diagonalising transformation for the more general recombination equation (without the restriction to single crossovers) and which includes parameters that must be determined recursively. Unfortunately, the corresponding derivations are relatively technical and fail to reveal the underlying mathematical structure. It was our aim to improve on this and add structural insight. Furthermore, Dawson restricted his model solely to diallelic loci while our ansatz is allele-independent. The transformation agrees with the one of Dawson [14, 15] when translated into his framework.

After having solved the diagonalisation problem and equipped with the structural insights gained in Chapter 3, we set out in Chapter 4 to find an explicit solution to the dynamics whilst avoiding the need to perform a transformation. We stated a stochastic process of recombination, a specific Wright-Fisher process, that converges to our deterministic model as the population size tends to infinity (*infinite population limit*). We then traced the recombination process backwards in time, i.e. as the time reversal of the Wright-Fisher process. Since we assumed a population in the infinite population limit, we could ignore genetic drift and thus backtracked the history of one type in the present population with respect only to recombination. We showed that each possible history can be explained with a binary tree, which we call the ancestral recombination tree, and thus corresponds to the outcome of a particular stochastic process (the segmentation process) with respect to the recombination model. We then developed a method to state the probability for a certain tree topology under this process. A key factor in this process was to make use of another weaker kind of independence, namely the independence of the segments produced by recombination, which allowed us to state the probability for a tree topology via certain subtrees. Ultimately, each coefficient function could be stated as the sum over the probabilities for all corresponding tree topologies and - for the first time - we could present an explicit solution for the discrete-time recombination dynamics.

Finally, we gave an outlook for the general recombination model in Chapter 5. Here,

the initial studies suggested that the general recombination model can be explored with the same methods that we had developed in Chapter 3 (constructing a diagonalising transformation) and Chapter 4 (using the time-reversal tree producing process to infer an explicit solution). The restriction on single-crossovers always leads to ordered partitions of the sites and thus recombination events (and the recombinator) can be described via links (since this implies the respective partition of sites due to the ordered structure). This simplification is lost for the general recombination model, where the recombinators have to be defined via the possible partitions (and the composite recombinators via refinements of partitions). In spite of these complications, we could show that the overall structure (e.g. independence of segments, arising tree structures) of the solution remains the same, and therefore the extension of the problem seems to be more a problem of notation than of the mathematics itself. We concluded the outlook by adumbrating how to treat recombination dynamics in the framework of genetic algebras. This suggested that the ansatz of genetic algebras seems to be unnecessarily complicated - although the approach still has to be completed and may be useful for extensions of the recombination model (see below).

Concerning further research on recombination dynamics, it would be interesting to explain the simple structure of the continuous-time single-crossover solution via ancestral recombination trees. The corresponding approach is explained in Chapter 5, but the simplicity of the coefficient functions is not immediately evident. Furthermore, the investigation of the general recombination model (building on the results of Chapter 5) has to be finished.

After the dynamics of recombination has been studied in isolation, a logical next step would be to include additional evolutionary forces into the model (e.g. mutation or selection). Ideas on how this might be achieved with our ansatz are given in [3]. Also, the approach of genetic algebras might find application when considering other factors in addition to recombination. This is due to the fact that it is often possible to construct a more ‘complex’ algebra, which models several evolutionary forces, via ‘simpler’ algebras, where each algebra only considers a single factor. The construction of new algebras can be achieved by forming linear combinations, tensor products, duplications and linear mappings of existing algebras [69].

Another interesting area regarding recombination concerns itself with the effects of gene conversion. While (single -) crossover events lead to the reciprocal exchange of the leading and trailing regions, gene conversion results in the non-reciprocal replacement of the region in between the flanking regions (see also Figure 2.2). The ability to distinguish between crossover and gene conversion events is currently of great interest since these factors have different effects on the measures of linkage disequilibrium (LD) [39, 66]. Patterns of LD are in turn important to infer information about sequence variation and population history and are also used for gene mapping. With regard to our (general) recombination model, gene conversion refers to special partitions, i.e. to *non-crossing* partitions of the sites. This would also be interesting from a mathematical point of view since these partitions constitute another mathematical research area in themselves [63].

Acknowledgements

An erster Stelle möchte ich Ellen Baake danken, die es mir überhaupt erst ermöglicht hat, diese Arbeit anzufertigen. Neben ihrer fachlichen Hilfe und ihren Ideen, danke ich ihr besonders für ihre ständige Unterstützung, Motivation und Aufmunterung in allen Phasen meiner Promotionszeit.

Ich danke auch Sven Rahmann für sein Interesse an meiner Arbeit und seine Bereitschaft zur Zweitkorrektur.

Michael Baake danke ich für seine Zusammenarbeit und Hilfe bei weiten Teilen dieser Arbeit.

Allen aktuellen, ehemaligen und assoziierten Kollegen meiner AG Biomathematik danke ich nicht nur für ihre Unterstützung, sondern vor allem auch für die freundschaftliche Atmosphäre auf 'unserem' Flur. Mein besonderer Dank geht dabei an Thimeo Hustedt, mit dem ich nicht nur erfolgreich zusammenarbeiten konnte, sondern der auch meine schlechte Laune immer mit Geduld zu ertragen wusste.

Weiterer Dank geht an alle Teilnehmer des Seminars 'Dynamik der Rekombination' für ihr Interesse an diesem Thema und ihre Ideen.

Ein Dank geht auch an Britta Quisbrok, die einem bei allen organisatorischen Fragen immer mit Rat und Tat zur Seite steht. Für die finanzielle Unterstützung während meiner Promotionszeit bin ich dem *Graduiertenkolleg Bioinformatik* (GK 635) sehr dankbar.

Stefan Börner möchte ich dafür danken, dass er mir immer wieder bei jeglichen 'Computer- und Präsentationsproblemen' ausgeholfen hat.

Gerade im Endspurt dieser Arbeit haben mir viele Freunde hilfreich zur Seite gestanden und mich immer ermuntert. Christina Miller, Judith Mielke und Katharina Heiny möchte ich an dieser Stelle danken. Meinem Englischhelden Aaron Bishell bin ich ebenfalls für seine Geduld, meine sprachlichen Fehler immer wieder auszubessern, zu Dank verpflichtet.

Nicht zuletzt danke ich meinen Eltern für ihre Unterstützung während meiner gesamten Studienzeit.

Bibliography

- [1] Aigner, M.: *Combinatorial Theory*. Springer, Berlin (1979).
- [2] Allen, L. J. S.: *An Introduction to Stochastic Processes with Applications to Biology*. Prentice Hall, Upper Saddle River, New Jersey (2003).
- [3] Baake, M., Baake, E.: An exactly solved model for mutation, recombination and selection. *Can. J. Math.* **55**, 3–41 (2003) and **60**, 264–265 (2008) (Erratum); [arXiv:math.CA/0210422](#).
- [4] Baake, M.: Recombination semigroups on measure spaces. *Monatsh. Math.* **146**, 267–278 (2005) and **150**, 83–84 (2007) (Addendum); [arXiv:math.CA/0506099](#).
- [5] Baake, E., Herms, I.: Single-crossover dynamics: finite versus infinite populations. *Bull. Math. Biol.* **70**, 603–624 (2008).
- [6] Baake, E.: Deterministic and stochastic aspects of single-crossover recombination. *Proceedings of the International Congress of Mathematicians VI*, Hyderabad, India, 3037-3053 (2010).
- [7] Bennett, J. H.: On the theory of random mating. *Ann. Human Genetics* **18**, 311–317 (1954).
- [8] Berge, C.: *Principles of Combinatorics*. Academic Press, New York (1971).
- [9] Bishop, D., Zickler, D.: Early decision: meiotic crossover interference prior to stable strand exchange and synapsis. *Cell* **117**, 9–15 (2004).
- [10] Boyd, R., Richardson, P. J.: *Culture and the Evolutionary Process*. University of Chicago Press, Chicago (1985).
- [11] Bürger, R.: *The Mathematical Theory of Selection, Recombination and Mutation*. Wiley, Chichester (2000).
- [12] Christiansen, F. B.: *Population Genetics of Multiple Loci*. Wiley, Chichester (1999).

-
- [13] Coop, G., Przeworski, M.: An evolutionary view of human recombination. *Nature Rev. Genet.* **8**, 23–34 (2007).
- [14] Dawson, K. J.: The decay of linkage disequilibria under random union of gametes: How to calculate Bennett’s principal components. *Theor. Popul. Biol.* **58**, 1–20 (2000).
- [15] Dawson, K. J.: The evolution of a population under recombination: How to linearise the dynamics. *Lin. Alg. Appl.* **348**, 115–137 (2002).
- [16] Donnelly, P.: *Dual processes in population genetics*. Stochastic spatial processes, Lect. Notes Math. **1212**, 94–105 (1986).
- [17] Etherington, I. M. H.: Genetic algebras. *Proc. Royal Soc. Edinburgh*, **59**, 153–162 (1939).
- [18] Ethier, S. N., Kurtz, T. G.: *Markov Processes - Characterization and Convergence*. Wiley, New York (Reprint 2005).
- [19] Ewens, W. J.: *Mathematical Population Genetics*. 2nd ed., Springer, Berlin (2004).
- [20] Falconer, D. S.: *Introduction to Quantitative Genetics*. 3rd ed., Longmans Green/ John Wiley & Sons, Harlow, Essex, UK/New York (1989).
- [21] Fisher, R. A.: *The Genetical Theory of Natural Selection*. Clarendon Press, Oxford (1930).
- [22] Ford, W., Topp, W.: *Data Structures with Java*. Prentice Hall, Upper Saddle River, New Jersey (2005).
- [23] Fung, J. C. et al.: Imposition of crossover interference through the non-random distribution of synapsis initiation complexes. *Cell* **116**, 795–802 (2004).
- [24] Geiringer, H.: On the probability theory of linkage in Mendelian heredity. *Ann. Math. Stat.* **15**, 25–57 (1944).
- [25] Geiringer, H.: Further remarks on linkage theory in Mendelian heredity. *Ann. Math. Stat.*, **16**, 390–393 (1945).
- [26] Gonshor, H.: Contributions to genetic algebras. *Proc. Edinburgh Math. Soc.* **17**, 289–298 (1971).
- [27] Graham, A.: *Kronecker products and matrix calculus with applications*. Chichester, Horwood (1981).
- [28] Griffiths, R. C., Marjoram, P.: Ancestral inference from samples of DNA sequences with recombination. *J. Comput. Biol.* **3**, 479–502 (1996).

-
- [29] Hämmerlin, G., Hoffmann, K.-H.: *Numerische Mathematik*. 3rd ed., Springer, Berlin (1992).
- [30] Hardy, G.H.: Mendelian proportions in a mixed population. *Science*, **28**, 49–50 (1908).
- [31] Hartl, D.L., Clark, A.G.: *Principles of Population Genetics*. 3rd ed., Sinauer, Sunderland, MA (1997).
- [32] Holgate, P.: Sequences of powers in genetic algebras. *J. London Math. Soc.* **42**, 489–496 (1967).
- [33] Holliday, R.: A mechanism for gene conversion in fungi. *Genet. Res.* **5**, 282–304 (1964).
- [34] Hudson, R.R.: Properties of a neutral allele model with intragenic recombination. *Theor. Popul. Biol.* **23**, 183–201 (1983).
- [35] Hustedt, Th.: *unpublished work together with Th. Hustedt* (2010).
- [36] Jennings, H.S.: The numerical results of diverse systems of breeding, with respect to two pairs of characters, linked or independent, with special relation to the effects of linkage. *Genetics* **2**, 97–154 (1917).
- [37] Jensen-Seaman, M.I. et al.: Comparative recombination rates in the rat, mouse, and human genomes. *Genome Res.* **14**, 528–538 (2004).
- [38] Johnsen, B.: Generating binary trees with uniform probability. *BIT* **31** (1), 15–31 (1991).
- [39] Jones, D., Wakeley, J.: Recombination, gene conversion, and identity-by-descent at three loci. *Theor. Popul. Biol.* **73**, 264–276 (2008).
- [40] Jones, G.H., Franklin, F.C.H.: Meiotic crossing-over: obligation and interference. *Cell* **126**, 246–248 (2006).
- [41] Kauppi, L. et al.: Where the crossovers are: recombination distributions in mammals. *Nature Rev. Genet.* **5**, 413–424 (2004).
- [42] Keeney, S. et al.: Meiosis-specific DNA double-strand breaks are catalyzed by Spo11, a member of a widely conserved protein family. *Cell* **88**, 375–384 (1997).
- [43] Kingman, J.F.C.: On the genealogy of large populations. *J. Appl. Probab.* **19A**, 27–43 (1982).
- [44] Knott, G.D.: A numbering system for binary trees. *J. ACM* **20** (2), 113–115 (1977).

-
- [45] Kong, A. et al.: A high-resolution recombination map of the human genome. *Nature Genetics* **31**, 241–247 (2002).
- [46] Larribe, F., Lessard, S.: Gene mapping via the ancestral recombination graph. *Theor. Popul. Biol.* **62**, 215–229 (2002).
- [47] Lodish, H. et al.: *Molecular Cell Biology*. 6th ed., W.H. Freeman and Company, New York (2008).
- [48] Lyubich, Y.I.: *Mathematical Structures in Population Genetics*. Springer, Berlin (1992).
- [49] Mäkinen, E.: A survey on binary tree codings. *Comput. J.* **34** (5), 438–443 (1991).
- [50] Marston, A.L., Amon, A.: Meiosis: Cell-cycle controls shuffle and deal. *Nature Rev. Mol. Cell. Biol.* **5**, 983–997 (2004).
- [51] Martinez-Perez, E., Colaiacovo, M.P.: Distribution of meiotic recombination events: talking to your neighbors. *Curr. Op. Genet. Dev.* **19**, 105–112 (2009).
- [52] McHale, D., Ringwood, G.A.: Haldane linearisation of baric algebras, *J. London Math. Soc.* **28** (2), 17–26 (1983).
- [53] Moore, G.L. et al.: Modeling and optimization of DNA recombination. *Comput. Chem. Eng.*, **24**, 693–699 (2000).
- [54] Nordborg, M.: Linkage disequilibrium, gene trees, and selfing: An ancestral recombination graph with partial self-fertilization. *Genetics* **154**, 923–929 (2000).
- [55] Popa, E.: *Some remarks on a nonlinear semigroup acting on positive measures*. In: Carja, O., Vrabie, I.I. (Eds.), *Applied Analysis and Differential Equations*, World Scientific, Singapore, 308–319 (2007).
- [56] Reed, M.L.: Algebraic structure of genetic inheritance. *Amer. Math. Soc.* **34**, 107–130 (1997).
- [57] Robbins, R.B.: Some applications of mathematics to breeding problems III. *Genetics* **3**, 375–389 (1918).
- [58] Rosenberg, N.A, Nordborg, M.: Genealogical trees, coalescent theory and the analysis of genetic polymorphisms. *Nature Rev. Genet.* **3**, 380–390 (2002).
- [59] Rota, G.: On the foundations of combinatorial theory
I. Theory of Moebius functions *Z. Wahrscheinlichkeitstheorie* **2**, 340–368 (1964).

-
- [60] Schafer, R. D.: Structure of genetic algebras. *Amer. J. Math.* **71**, 121–135 (1949).
- [61] Schmitt, L. M.: Theory of genetic algorithms. *Theor. Comp. Sc.* **259**, 1–61 (2001).
- [62] Solomon, M., Finkel, R. A.: A note on enumerating binary trees. *J. ACM* **27** (1), 3–5 (1980).
- [63] Speicher, R.: Free probability theory and noncrossing partitions. in 39^e *Séminaire Lotharingien de Combinatoire* Thurnau, Germany (1997).
- [64] The International HapMap Consortium: The International HapMap Project, *Nature*, **426**, 789–796 (2003).
- [65] Wakeley, J.: Recent trends in population genetics: More data! More Math! Simple Models?. *J. Hered.* **95** (5), 397–405 (2004).
- [66] Wall, J. D.: Close look at gene conversion hot spots. *Nat. Genet.* **36** (2), 114–115 (2004).
- [67] von Wangenheim, U., Baake, E., Baake, M.: Single-crossover recombination in discrete time. *J. Math. Biol.* **60**, 727–760 (2010).
- [68] von Wangenheim, U.: *Diskrete Rekombinationsdynamik*. Diplomarbeit, Universität Greifswald (2007).
- [69] Wörz-Busekros, A.: *Algebras in Genetics*, Lecture Notes in Biomathematics. **36**, Springer, Berlin (1980).
- [70] Wright, S.: Evolution in Mendelian populations. *Genetics* **16**, 97–159 (1931).
- [71] Zaks, S.: Lexicographic generation of ordered trees. *Theor. Comp. Sc.* **10**, 63–82 (1980).